University of Illinois at Urbana-Champaign

ACRC

Air Conditioning and Refrigeration Center A National Science Foundation/University Cooperative Research Center

Experimental Measurement and Modeling of Oil Holdup

J. A. Crompton, T. A. Newell, and J. C. Chato

ACRC TR-226 May 2004

For additional information:

Air Conditioning and Refrigeration Center
University of Illinois
Mechanical & Industrial Engineering Dept.
1206 West Green Street
Urbana, IL 61801

(217) 333-3115

Prepared as part of ACRC Project #150
Experimental Measurement and Modeling of Oil Holdup
T. A. Newell, and J. C. Chato, Principal Investigators

The Air Conditioning and Refrigeration Center was founded in 1988 with a grant from the estate of Richard W. Kritzer, the founder of Peerless of America Inc. A State of Illinois Technology Challenge Grant helped build the laboratory facilities. The ACRC receives continuing support from the Richard W. Kritzer Endowment and the National Science Foundation. The following organizations have also become sponsors of the Center.

Alcan Aluminum Corporation
Amana Refrigeration, Inc.
Arçelik A. S.
Behr GmbH and Co.
Carrier Corporation
Copeland Corporation
Daikin Industries, Ltd.
Delphi Thermal and Interior
Embraco S. A.
Fujitsu General Limited
General Motors Corporation
Hill PHOENIX
Honeywell, Inc.
Hydro Aluminum Adrian, Inc.
Ingersoll-Rand Company
Lennox International, Inc.
LG Electronics, Inc.
Modine Manufacturing Co.
Parker Hannifin Corporation
Peerless of America, Inc.
Samsung Electronics Co., Ltd.
Sanyo Electric Co., Ltd.
Tecumseh Products Company
Trane
Visteon Automotive Systems
Wieland-Werke, AG
Wolverine Tube, Inc.

For additional information:

Air Conditioning & Refrigeration Center
Mechanical & Industrial Engineering Dept.
University of Illinois
1206 West Green Street
Urbana, IL 61801

217 333 3115

Abstract

Often in air conditioning and refrigeration vapor compression systems the working fluid is mixed with lubricating oil, which flows through the system as it operates. The effects of this oil in the system include the possible degradation of heat transfer, increased pressure drop, insufficient lubrication for the compressor and the possibility of flooding the compressor suction ports with oil should the compressor valve fail. In order to quantitatively evaluate these effects on the system, a better understanding of the flow of oil through various operating conditions is required. The purpose of this investigation is the measurement of oil retention in small diameter round copper tubes with various internal geometries. Test sections include an internally smooth, an axially microfinned and a helically microfinned tube, all with an outer diameter of 9.53 mm (3/8"). Mass fluxes of 75 to 300 kg/m^{2}s are tested, with an emphasis on 75 and 150 kg/m^{2}s, and qualities of 0% to 100% are reached. The refrigerant/oil mixtures examined include R134a with a polyol ester, R134a with a polyalkylene glycol, R134a with an alkylbenzene, R22 with an alkylbenzene and R410A with a polyol ester. Additionally, it is important to examine the void fraction and flow visualization of the mixtures to determine if the oil has an effect in these areas. Finally, two models have been developed for oil holdup prediction. The first is based on the test section's liquid volume fraction and is used at mid to low-range qualities, while the second, with the Blasius turbulent flow formula as a basis, is used to predict holdup at high qualities.

Table of Contents

List of Figures

Page

List of Tables

Nomenclature

A	Area (m^2)
c_o	Oil Concentration (%)
$\dot{C}_o$	Oil to Total Mass Flow Rate Ratio
D	Diameter (m)
f	Friction Factor
F	Force (N)
Ft	Froude Rate
g	Gravitational Acceleration
G	Mass Flux (kg/m^2s)
h	Film Thickness (m)
L	Length (m)
m_c	Evacuated Clean Test Section Mass (g)
m_e	Evacuated Test Section Mass (g)
m_f	Full Test Section Mass (g)
m_o	Oil Mass Holdup (g)
m_r	Refrigerant Mass in Test Section (g)
$\dot{m}$	Mass Flow Rate (kg/s)
$\mathcal{M}$	Viscous Film Model Multiplier
P_{sat}	Saturation Pressure (kPa)
Re_D	Reynolds Number
S	Slip Ratio
T	Temperature (°C)
T_{bub}	Bubble Point Temperature (°C)
V	Velocity (m/s)
$\forall_{ts}$	Test Section Vapor Volume (m^3)
Vol_l	Liquid Refrigerant Specific Volume (m^3/kg)
Vol_{ts}	Test Section Specific Volume (m^3/kg)
Vol_v	Vapor Refrigerant Specific Volume (m^3/kg)
w_{oil}	Oil Mass Fraction
x	Quality
x_o	Oil Based Quality
$\dot{x}$	Vapor to Total Mass Flow Rate Ratio
X_{tt}	Lockhart-Martinelli Parameter
α	Void Fraction
μ	Dynamic Viscosity (kg/m-s)
ν	Kinematic Viscosity (m^2/s)
ρ	Density (kg/m^3)
τ_w	Wall Shear Stress (kPa)

Common Subscripts

cs	Cross Sectional
i	Inner
l	Liquid
m	Refrigerant-Oil Mixture
o	Oil
r	Refrigerant
s	Surface
tot	Total
v	Vapor
x	at a Given Quality

Chapter 1. Introduction

1.1 Objectives of this Study

This study aims to collect quantitative data on oil holdup that can be used to develop prediction models and provide a better understanding of the effects oil has on other refrigeration and air conditioning system parameters.

Oil entrained in the system flow can degrade heat transfer, increase pressure drop, leave the compressor with insufficient lubrication and possibly lead to a flood of oil in the compressor's suction ports. Before a study is done to quantitatively define how the oil affects these parameters, an understanding of how the oil travels through a basic system is required. This study provides the basis for further research by developing a set of oil holdup results in various refrigerant oil mixtures for adiabatic conditions.

Additionally, void fraction is investigated in comparison to previously established correlations to determine if these correlations continue to make accurate predictions with the presence of oil.

Finally, a brief flow visualization study is performed to determine what types of effects oil may have on a flow, in particular, whether the oil creates highly unusual visible behavior that might cause established flow regime models to become inaccurate with the presence of oil.

1.2 Methodology

All experimental data is acquired using an existing two-phase refrigerant loop in the Air Conditioning and Refrigeration Center at the University of Illinois at Urbana-Champaign. Details not addressed in this section can be found in Dobson [1], Graham [2], Kopke [3], Piggott [4] and Wilson [5].

1.2.1 Experimental Facility

A schematic of the refrigerant loop used to perform the analysis is given in Figure 1.1. A receiver tank separating liquid from vapor refrigerant supplies liquid to the loop, and sits in a water bath that is heated with electric heaters. Liquid is forced into the system by the pressure generated with the hot water bath and travels through a shell-in-tube heat exchanger that uses cold building water to ensure subcooled refrigerant enters the pump. The magnetically coupled pump circulates the refrigerant through the loop and controls the mass flow rate. The flow rate is measured using a Micro-Motion® Coriolis flow meter, and liquid is sent through the electric preheater.

The preheater section consists of 7.5 meters of 9.53 mm outer diameter copper tube, configured in a serpentine pattern with a total of seven passes, shown in Figure 1.2. This tube section is flattened to an outer height of 6.35 mm and sandwiched between two 6.35 mm thick (1.15 m x 0.36 m) aluminum plates. Attached on the outside of these plates are a total of four Vulcan® electric strip heaters, each with a 1.5 kW rating. The power supply in the laboratory, however, limits each heater to a 1.0 kW capacity. This configuration provides enhanced heat transfer, results shown in Wilson [5], as well as prevention of failure due to wall dry out causing burnout of the electric resistance heater strips previously used. Wilson determined for smooth tubes an optimal tube height of 2.57 mm (original tube of 8.9 mm diameter) for best heat transfer results. Flattening the tube to any height above this value increases the enhancement factor, while flattening past this value has a detrimental effect. Additionally, much higher qualities, including superheated vapor, are achievable with this setup.

After the quality is set with the preheater, the two-phase mixture flows through the test section or flow visualization section, through a water-cooled flat plate heat exchanger and back into the receiver tank, where the liquid is again separated from any remaining vapor.

1.2.2 Test Section Geometry

1.2.2.1 Oil Holdup Test Section

Three test sections are fashioned for this investigation, all using 9.53 mm outer diameter copper tubing with a length of 1.61 m. The first test section is internally smooth, while the second and third are enhanced with axial and 18° helical microfins. The tube wall thickness is 0.3 mm, and the enhanced sections have a fin height of 0.2 mm. Each end of the test section has a Hoke® ball valve and a spring lock connector manufactured by Visteon® to allow for quick disconnect from the loop. Figure 1.3 shows a photograph of the internal geometry of the 18° helically enhanced test section.

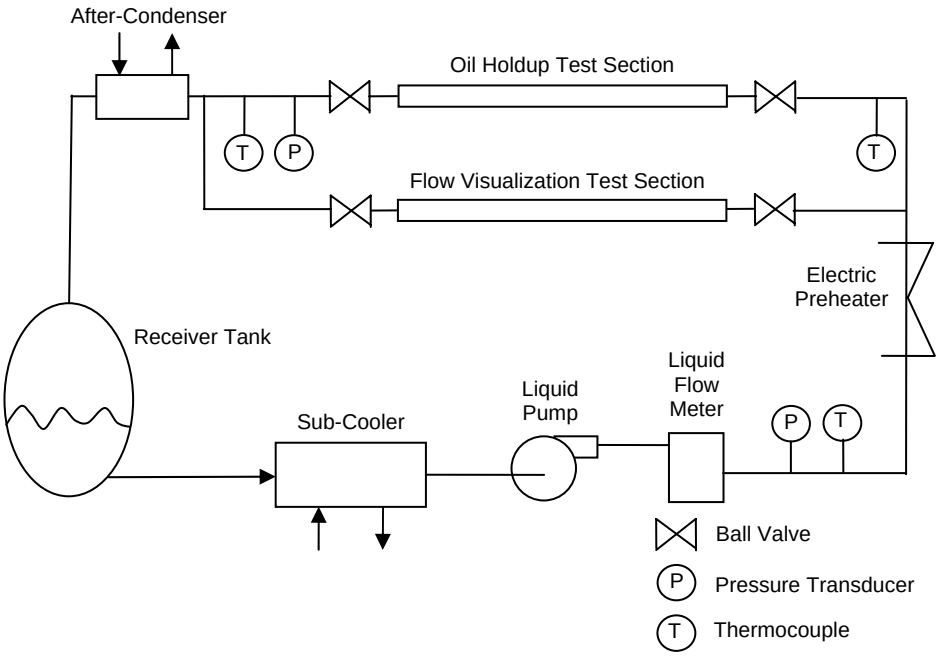

Figure 1.1. Schematic of two-phase refrigerant loop

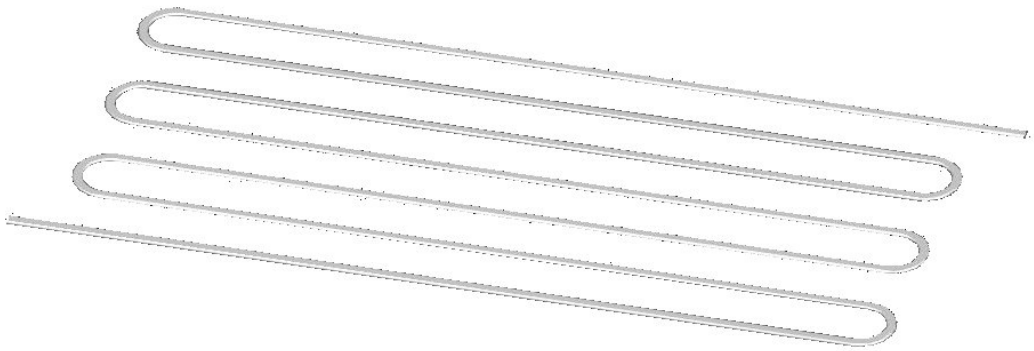

Figure 1.2. Flattened section of tubing through preheater

Figure 1.3. Internal geometry of helically microfinned tubing

1.2.2.2 Flow Visualization Section

The flow visualization test section is simply a 30 cm length of Pyrex glass tubing with a 9.53 mm outer diameter and 2 mm wall thickness. This section is attached using nylon ferrules in compression fittings, and due to the fragile transition between glass and copper, is protected by a 1 cm thick piece of Plexiglas (PMMA).

1.2.3 Test Conditions

This investigation is comprised of five data sets taken at comparable operating conditions. The refrigerant-oil mixtures considered include R134a/polyol ester (POE), R134a/polyalkylene glycol (PAG), R134a/alkylbenzene, R22/alkylbenzene and R410A/polyol ester. The constraints consistent through all data sets are a saturation temperature of 35°C and adiabatic running conditions. Table 1.1 details the remaining parameters tested for each mixture, where the oil concentration refers to the oil circulation rate determined by taking a sample from a liquid feed line.

Table 1.1. Various test conditions for each data set

Mixture	Mass Flux (kg/m^2s)	Quality (%)	Oil Concentration (%)
R134a/POE	75 150	10-95	0.2-0.4 2.0-4.0
R134a/PAG	75 150 ~200	50-100	0.0-15.0
R134a/alkylbenzene	75 150 300	30-100	0.0-3.5
R22/alkylbenzene	75 150 300	0 50-100	0.0-4.0
R410A/POE	75 150	0-100	0.0-4.3

1.2.4 Experimental Methods and Procedure

1.2.4.1 Oil Holdup and Void Fraction

The test section volumes needed to calculate void fraction are found experimentally. Thermocouples are attached to the exterior of the test section, which is then evacuated and charged with pure R134a, R22 or nitrogen

vapor through a fitting equipped with a pressure tap and gauge. The pressure and temperature of the test section are recorded and the section is then weighed without the fitting. After a final evacuation, weight measurement and test repetition, Engineering Equation Solver (EES) is used to calculate the average gas volume, which is then assigned as the test section volume.

The technique for measuring void fraction and oil holdup begins with setting the loop at the desired mass flux and quality conditions and maintaining steady state. The valves on each end of the test section are closed simultaneously to trap the mixture as a bypass line is opened. The section is removed from the loop and a weight measurement of the full test section (refrigerant plus oil) is recorded (m_f). The refrigerant in the section is vented out through one valve, and any oil that may leak out is collected on a towel covering the end and accounted for. After venting, the section is evacuated and weighed (m_e). Next, the test section is rinsed by running pure liquid refrigerant from a recovery tank at room temperature through the section and into a recovery tank in an ice bath. A final evacuation and weight measurement (m_c) is performed.

This experimental procedure is followed by calculations of oil holdup and void fraction. The oil holdup mass is given as

$$m_o = m_e - m_c \tag{1.1}$$

The specific volume of the test section is defined as

$$Vol_{ts} = \frac{\forall_{ts}}{m_r}, \tag{1.2}$$

where $\forall_{ts}$ is the vapor volume of the section and $m_r = m_f - m_e$ is the mass of the refrigerant in the test section. The property calls used in EES, shown in Equations 1.3 to 1.5, obtain the test section quality as a function of saturation temperature and specific volume, the specific volume at 100% quality for the given saturation temperature and the specific volume at zero quality for the given saturation temperature, respectively.

$$x = \text{QUALITY(R134a, T=T\_sat, v=}Vol_{ts}\text{)} \tag{1.3}$$

$$Vol_v = \text{VOLUME(R134a, T=T\_sat, x=1)} \tag{1.4}$$

$$Vol_l = \text{VOLUME(R134a, T=T\_sat, x=0)} \tag{1.5}$$

Finally, Equation 1.6 is solved simultaneously with the property calls to find experimental void fraction, α.

$$x = \left[\left(\frac{1-\alpha}{\alpha}\right)\cdot\frac{Vol_v}{Vol_l} + 1\right]^{-1} \tag{1.6}$$

1.2.4.2 Slip Ratio

The slip ratio is defined as the ratio of refrigerant vapor velocity to liquid velocity. This factor is examined because it addresses the physics between the two phases, which is of great importance when attempting to explain how oil travels in two-phase flow. The relationship between slip ratio (S) and void fraction is most generally defined as

$$\alpha = \frac{1}{1 + \frac{1-x}{x}\left(\frac{\rho_v}{\rho_l}\right)S} \tag{1.7}$$

The experimental slip ratio is determined by using the experimental void fraction, quality and refrigerant properties. An ideal oil holdup limit is also investigated by assuming a slip ratio of 1, or homogeneous flow.

1.2.4.3 Flow Visualization

As the refrigerant-oil mixture flows through the flow visualization section observations are made and the image is recorded on digital videotape. A strobe light, set at a frequency near 5000Hz to create a freeze frame image of the flow, is reflected off a white background and through the section into the camera. This setup is illustrated in Figure 1.4. The digital video is analyzed using video editing software and individual images are extracted.

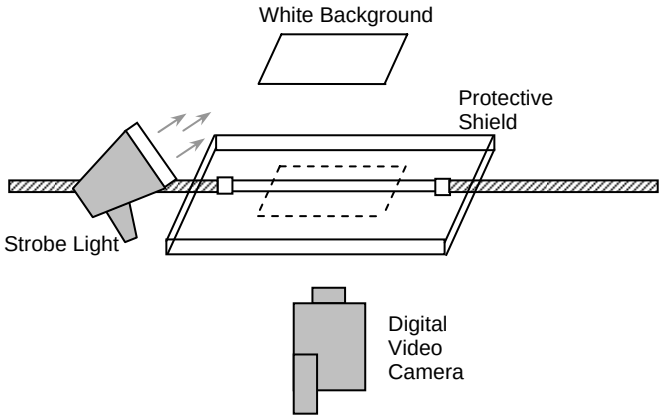

Figure 1.4. Setup for the flow visualization acquisition

1.3 Organization of this Document

The present study is divided into three main sections. The first, Chapter 2, is based on Piggott [4] in which the data collection procedure is developed and acquisition begins with an R134a/POE mixture. Chapter 3 continues by addressing the four remaining mixtures: R134a/PAG, R134a/alkylbenzene, R22/alkylbenzene and R410A/POE. In each of these chapters a review of necessary literature is made, results of oil holdup, void fraction and flow visualization for each mixture are presented and conclusions are offered. Chapter 4 reviews modeling literature and presents two oil holdup prediction models presently intended to be used together for the most accurate predictions across the entire quality spectrum. Finally, Chapter 5 will summarize results and address the course of future research projected to build upon this study.

1.4 List of References

[1] Dobson, M.K., J.C. Chato, J.P. Wattelet, J.A. Gaibel, M. Ponchner, P.J. Kenney, R.L. Shimon, T.C. Villaneuva, N.L. Rhines, K.A. Sweeney, D.G. Allen, and T.T. Hershberger, "Heat Transfer and Flow Regimes During Condensation in Horizontal Tubes", *ACRC TR-57* (also PhD dissertation by M.K. Dobson), Air Conditioning and Refrigeration Center, University of Illinois at Urbana-Champaign IL, 1994.

[2] Graham, D.M., H.R. Kopke, M.J. Wilson, D.A. Yashar, J.C. Chato, and T.A. Newell, "An Investigation of Void Fraction in the Annular/Stratified Flow Regions in Smooth, Horizontal Tubes", *ACRC TR-144*, Air Conditioning and Refrigeration Center, University of Illinois at Urbana-Champaign IL, 1998(b).

[3] Kopke, H.R., T.A. Newell, and J.C. Chato, "Experimental Investigation of Void Fraction during Refrigerant Mixtures in Horizontal Tubes", *ACRC TR-142* (also MS thesis by H.R. Kopke), Air Conditioning and Refrigeration Center, University of Illinois at Urbana-Champaign, 1998.

[4] Piggott III, W.T., T.A. Newell, and J.C. Chato, "Investigation of an R134a Refrigerant/Iso 32 Polyol Ester Oil Mixture in Condensation", *ACRC TR-192* (also MS thesis by W.T. Piggott), Air Conditioning and Refrigeration Center, University of Illinois at Urbana-Champaign IL, 2001.

[5] Wilson, M.J., T.A. Newell, and J.C. Chato, "A Study of Two-Phase Refrigerant Behavior in Flattened Tubes", *ACRC CR-35* (also PhD dissertation by M.J. Wilson), Air Conditioning and Refrigeration Center, University of Illinois at Urbana-Champaign IL, 2001.

Chapter 2. R134a and Polyol Ester

2.1 Introduction

The purpose of this part of the study, originally performed by Piggott [11], begins with identifying the proper procedure for collecting oil holdup data and determining the repeatability of this procedure. Once this is established, void fraction and oil holdup can be studied. The methodology given in Chapter 1 is defined as the proper procedure for collecting data. Defining the procedure and studying an R134a/POE mixture is presented in Piggott [11] and this chapter reviews the experimental results. This study is also the basis for the work following in Chapter 3 using the same procedure to analyze four additional refrigerant-oil mixtures. The two oil concentration ranges tested, 0.2-0.4% and 2.0-4.0% are both detailed in Piggott [11]. The lower range, however, did not produce sufficient evidence to identify clear trends. Therefore, the presentation of results in this chapter will only detail the 2.0-4.0% oil concentration range unless a comparison is being made between the two concentration ranges.

2.2 Literature Review

2.2.1 Void Fraction

Although significant studies have been performed with respect to void fraction, this review details the literature used specifically for the application of the current data. For an extensive literature review see Kopke [9].

The Lockhart-Martinelli parameter, developed in 1949, Lockhart [10], was originally used to correlate pressure drop between four flow regimes defined by the turbulent or laminar behavior of the refrigerant vapor and liquid phases. It was later found that the parameter was also adequate for correlating void fraction in these flow regimes. The parameter for turbulent vapor and liquid, used in most correlations, is defined as

$$X_{tt} = \left(\frac{1-x}{x}\right)^{0.9}\left(\frac{\rho_v}{\rho_l}\right)^{0.5}\left(\frac{\mu_l}{\mu_v}\right)^{0.1} \tag{2.1}$$

Hurlburt and Newell [8] defined the Froude rate parameter, a ratio relating vapor kinetic energy to gravitational effects on the liquid, as

$$Ft = \left(\frac{x^3 G^2}{\rho_v g D_i (1-x)}\right)^{0.5} \tag{2.2}$$

Using this parameter, Graham [5] developed a void fraction model through an empirical study. Graham's model defines the void fraction for two regions, distinguished only by Froude rate values. The model, shown below, fit the experimental data to within ±10%.

$$\alpha = 1 - \exp\left\{-1 - \left[0.3\ln(Ft)\right] - \left[0.0328\ln^2(Ft)\right]\right\} \qquad Ft>0.01032 \tag{2.3}$$

$$\alpha = 0 \qquad Ft\leq 0.01032 \tag{2.4}$$

Further work lead Graham [6] to develop another void fraction model based on the Wallis [14] model, but taking into account the effect of mass flux variations. This model is recommended for smooth tubes only.

$$\alpha = \left(1 + X_{tt} + \frac{1}{Ft}\right)^{-0.321} \tag{2.5}$$

Finally, Yashar [17] followed Graham's study modifying the model to be applicable to enhanced tubes most specifically in condensation. The findings produced the following model, and together with Equation 2.5 are referred to as the ACRC void fraction model.

$$\alpha = \left(1 + X_{tt} + \frac{1}{Ft}\right)^{-0.375} \tag{2.6}$$

It should be noted that the quality used in this procedure is a theoretical quality assuming no oil. In other words, it is the quality attained with a given heat input to pure refrigerant. With the introduction of oil, some of the heat is absorbed by the oil and leaves a portion of refrigerant in liquid form. For the first study on an R134a/POE mixture, the quality referenced is this theoretical value. For the remaining data (R134a/PAG, R134a/alkylbenzene, R22/alkylbenzene and R410A/POE) in Chapter 3 the quality referenced will be the corrected rather than theoretical value, which will be defined at that point.

2.2.2 Refrigerant-Oil Mixtures

The fluid properties for refrigerant-oil mixtures are represented by various models. Three being considered during this study include a linear model assuming ideal mixing and two mixture correlations. Another possible correlation is a model using pure refrigerant properties with an applied correction factor like that used in Tichy [13], but this correlation will not be presented with the results of this study. The results shown will include the experimental data compared to the ACRC void fraction model using pure refrigerant properties and the following three property models.

The linear model is presented in Reid [12], and provides correlations for density, specific heat and thermal conductivity along with the viscosity relationship shown below.

$$\mu = x_r \mu_r + (1 - x_r)\mu_o \tag{2.7}$$

Baustian [2] used the following correlation for determining mixture viscosity.

$$\mu = \left(x_r \mu_r^{1/3} + x_o \mu_o^{1/3}\right)^3 \tag{2.8}$$

Finally, although Cawte [3] used the model in evaporation, the following is presented in this study for comparison to experimental and pure refrigerant property data.

$$\mu = \mu_r \exp\left[x_r \left(\frac{\mu_o}{\mu_r}\right)^{0.3}\right] \tag{2.9}$$

2.3 Experimental Results

2.3.1 Void Fraction

The void fraction results, calculated as described in Chapter 1, can be shown in a variety of settings. Included in the investigation are the effects of quality, mass flux, tube type and oil concentration on the void fraction values.

Figures 2.1 and 2.2 introduce the experimental void fraction with respect to quality. Figure 2.1 separates the data by mass flux, while Figure 2.2 separates the data by tube type.

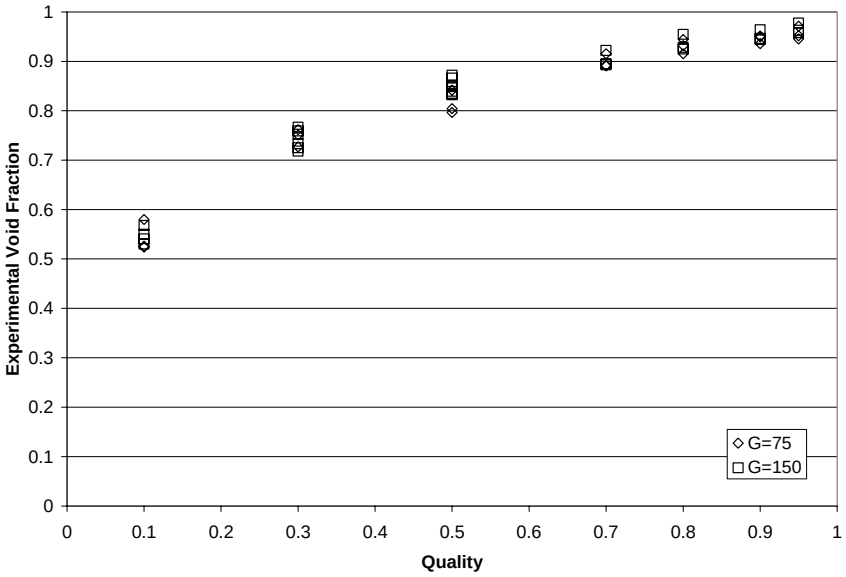

Figure 2.1. Experimental void fraction as a function of quality, separated by mass flux for the R134a/POE mixture at 2.0-4.0% oil concentration

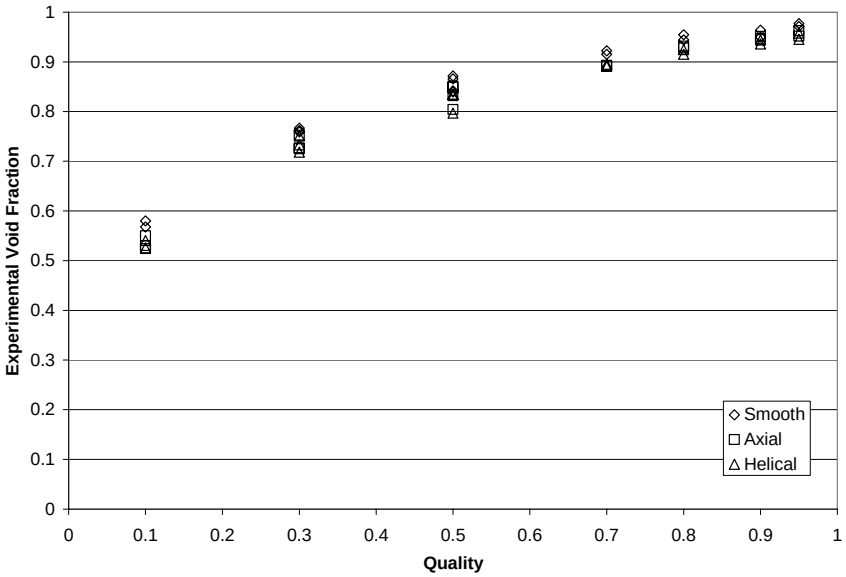

Figure 2.2. Experimental void fraction as a function of quality, separated by tube type for the R134a/POE mixture at 2.0-4.0% oil concentration

Because mass flux is defined as the ratio of vapor refrigerant mass flow rate to total refrigerant mass flow rate and void fraction is defined as the ratio of vapor refrigerant volume to total refrigerant volume, it is expected there will be a corresponding trend between the two. This is confirmed in Figures 2.1 and 2.2 where as quality increases experimental void fraction increases as well.

The data separated by mass flux does not show a clear division between void fraction results for the different flux values. Unlike the results found in Graham [5] and Kopke [9], a lower mass flux does not necessarily predict a lower void fraction for this investigation.

For the data separated by tube type, though the points are not vastly divided, it is clear that the smooth test section shows a higher void fraction than those of either of the enhanced tubes. This observation agrees with earlier work of Graham [5], Kopke [9], Wilson [16] and Yashar [17].

Finally, though the lower oil concentration range, 0.2-0.4%, is not represented with data for this study, Piggott [11] found there to be no significant effect of oil concentration on void fraction. This agrees with the results of Gupta [7], who performed similar tests under evaporation conditions.

The experimental void fraction results, computed as described in Chapter 1, are also compared to results using the ACRC model with various refrigerant-oil mixture properties. Methods for determining the mixture properties included in this comparison are a linear method used by Reid [12], the Baustian [2] model and the Cawte [3] model, all of which are detailed in the literature review of this chapter. These property values are then used to determine the Lockhart-Martinelli parameter. Additionally, the experimental results are compared to results using pure refrigerant properties.

Results for the smooth test section at all oil concentrations tested are shown in Figure 2.3. The enhanced test sections produced very similar results, with representative figures in Appendix A. The error lines for these figures signify ±10%.

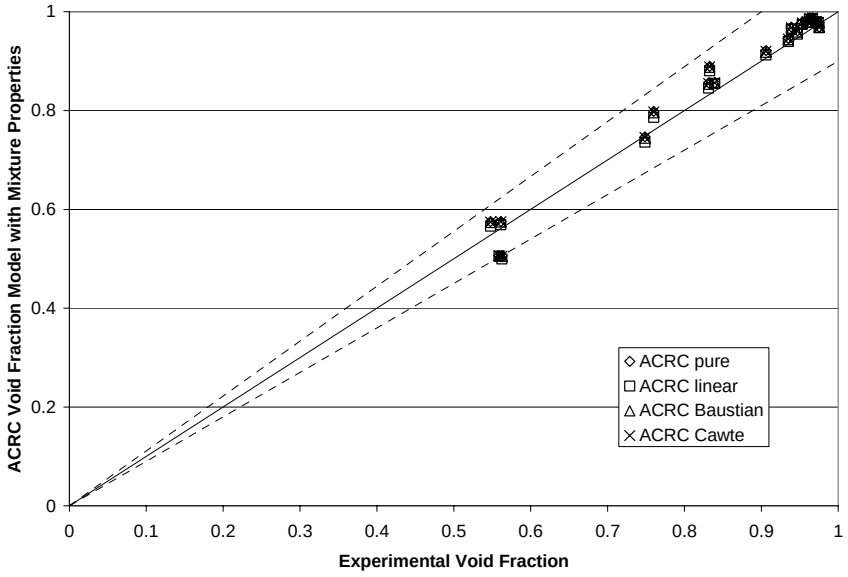

Figure 2.3. Experimental void fraction data for the smooth test section plotted versus void fraction determined using refrigerant-oil mixture properties in the ACRC model

2.3.2 Oil Holdup

The oil holdup data collected using the procedure described in Chapter 1 is presented in Figures 2.4-2.5. There is a significant trend in the data with respect to quality, where holdup decreases with increasing quality beginning with all liquid, reaches a minimum and increases again until 100% quality (theoretically without the presence of oil).

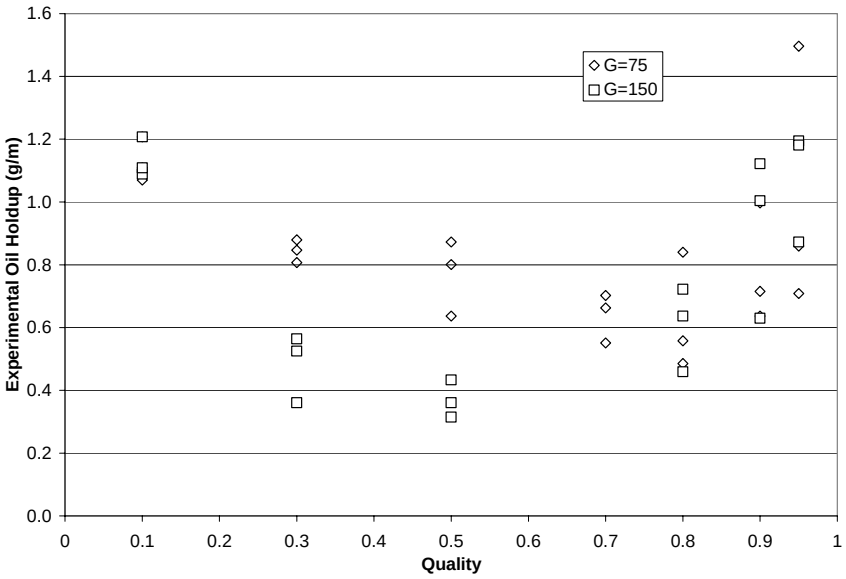

Figure 2.4. Experimental oil holdup with quality separated by mass flux for an R134a/POE mixture with 2.0-4.0% oil concentration

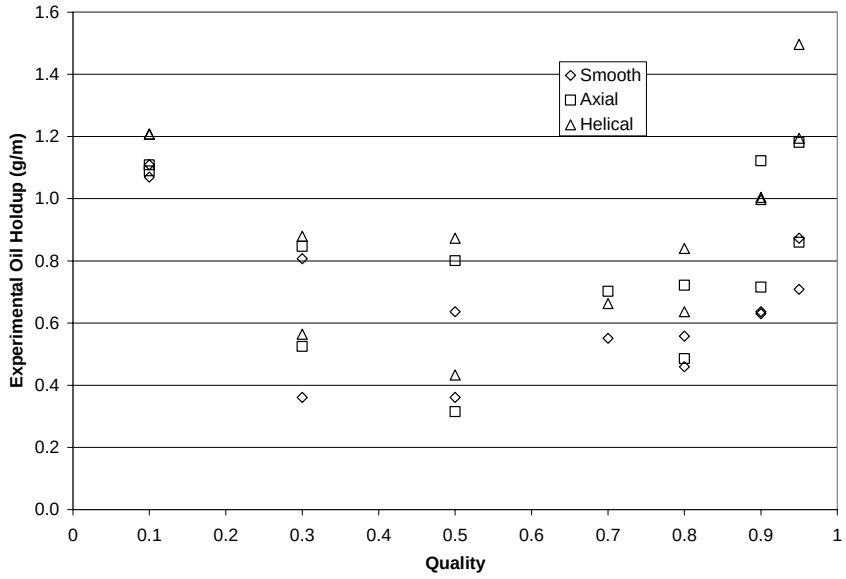

Figure 2.5. Experimental oil holdup with quality separated by tube type for an R134a/POE mixture with 2.0-4.0% oil concentration

Also evident from this data is the influence of both mass flux and tube type at different locations with respect to quality. At mid-range qualities a lower mass flux indicates a lower oil holdup. Additionally, the enhanced tubes, particularly the tube with helical microfins, show higher oil holdup along the entire quality range, with the most prominent influence at high qualities.

Between the low and high oil concentration ranges the oil holdup followed a logical trend. In the low range, very little oil was retained in the test section, while much more was held up in the higher concentration range. The oil holdup for the lower concentrations can be considered negligible. Also, within the 2.0-4.0% concentration

range, the data is further segmented and shows increasing holdup with the increasing concentrations. This can be seen in Figure 2.6.

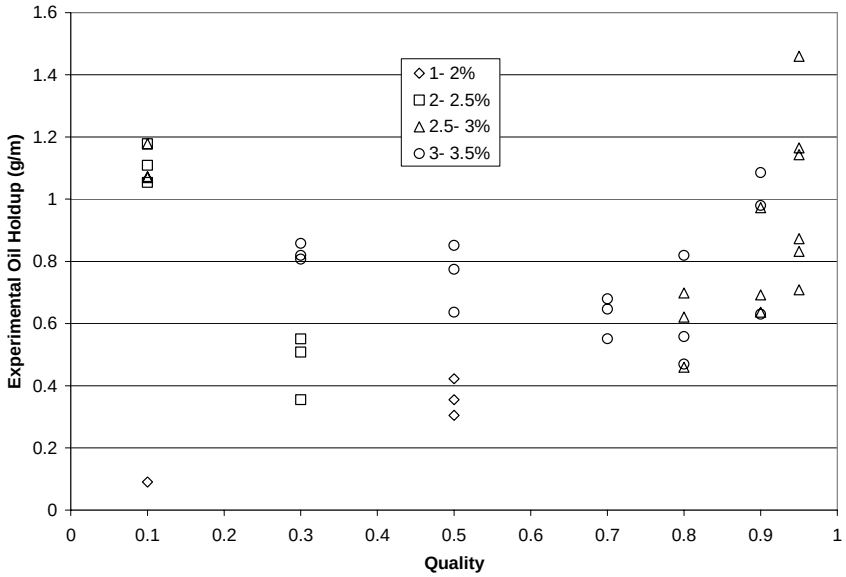

Figure 2.6. Experimental oil holdup showing the effect of oil concentration for an R134a/POE mixture with 2.0-4.0% oil concentration

2.3.3 Slip Ratio

Slip ratios for this data set are calculated as described in Chapter 1 and plotted against quality. It can be seen that the slip ratio has a slightly increasing trend from zero to about 80% quality, and takes a sharp turn to increase quickly from 80 to 100% quality. This is shown in Figures 2.7 and 2.8, which separate the data by mass flux and tube type.

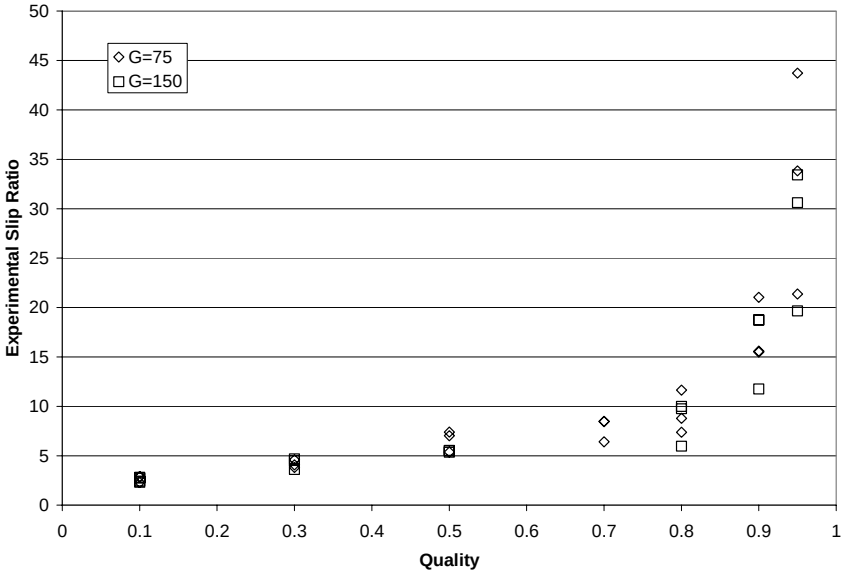

Figure 2.7. Experimental slip ratio with respect to quality, separated by mass flux for an R134a/POE mixture with 2.0-4.0% oil concentration

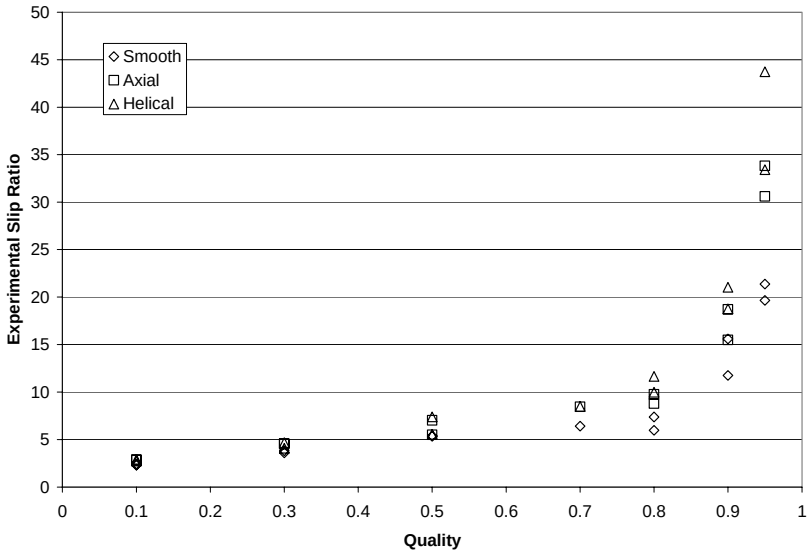

Figure 2.8. Experimental slip ratio with respect to quality, separated by tube type for an R134a/POE mixture with 2.0-4.0% oil concentration

The effect of mass flux and tube type on the experimental slip ratios is slight, but still detectable. A higher mass flux tends to show a small decrease in slip ratio. Additionally, the enhanced tubes show an increase in slip ratio, where the microfins may be slowing the liquid phase thus increasing the difference between vapor and liquid velocities. Both of these effects are indistinguishable below about 40% quality, which also makes sense because at these qualities the liquid phase dominates the flow and the phase velocities will differ less regardless of mass flux or tube type.

Figure 2.9 shows the experimental slip ratio for the lower oil concentration range tested, 0.2-0.4%, and when compared to the higher oil concentrations shows oil to have no impact on slip ratio. These results are consistent between mass flux and tube type variations, as well as between various concentration segments within the larger ranges.

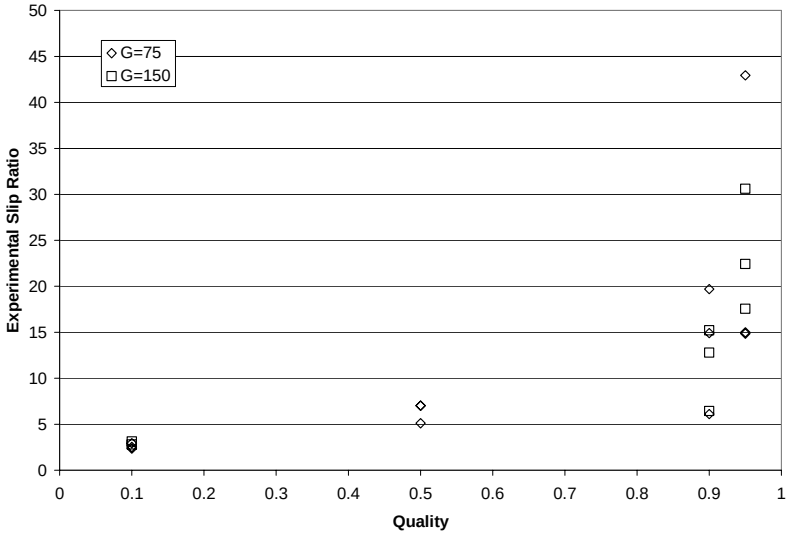

Figure 2.9. Experimental slip ratio with respect to quality, separated by mass flux (kg/m^2s) for an R135a/POE mixture with 0.2-0.4% oil concentration

2.3.4 Flow Visualization

Lockhart and Martinelli [10] found a relationship between two-phase pressure drop and superficial gas velocity. Further investigation by Alves [1] lead to the conclusion that consideration of flow regimes (corresponding to various liquid and vapor superficial velocities) is necessary when determining pressure drop.

This study performs a simple observation of flow patterns to determine whether or not the introduction of oil to the system may have a significant effect on the visible flow regimes. The following photographs were collected using the procedure described in Chapter 1. The shaded regions on the edges of the tube are simply light refractions through the glass. Some figures may appear to have a three dimensional interface between the liquid and vapor phases. This is most evident in stratified flow regimes where the interface has various shades of gray. Figure 2.10.*a* is labeled appropriately for identifying these regions. This figure is also the only photograph with visible oil, seemingly spiraling around the tube as it travels relatively slowly at a mass flux of 50 kg/m^{2}s. All other photographs indicate common flow patterns with no visible effect of oil. Note the quality referenced is a theoretical quality, not accounting for the presence of oil.

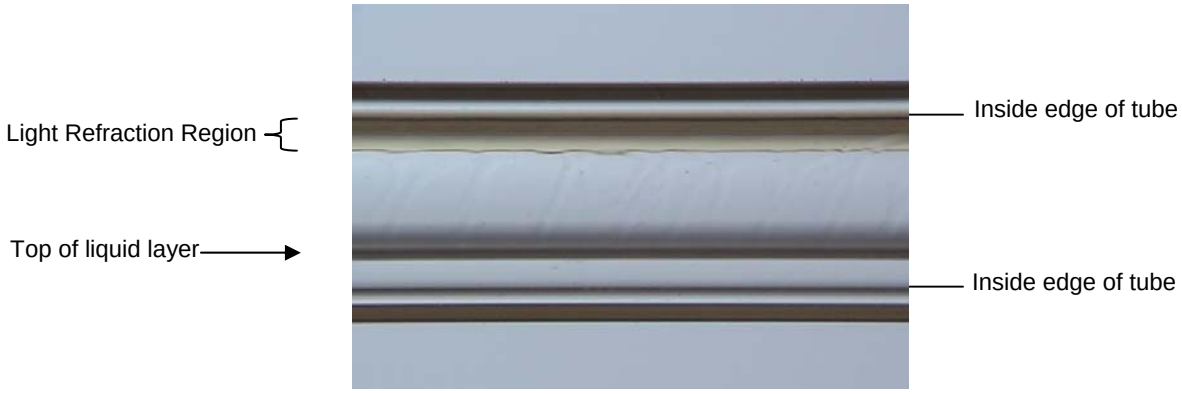

a) 50 kg/m^{2}s mass flux, 50% quality

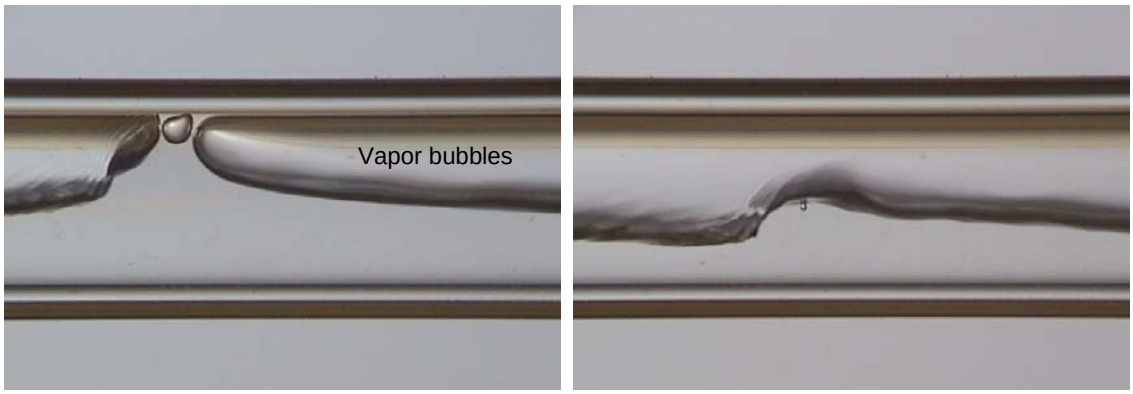

b) 125 kg/m^{2}s mass flux, 10% quality *c) 125 kg/m^{2}s mass flux, 20% quality*

Figure 2.10. Flow visualization photographs *(a)-(n)* of an R134a/POE mixture at various mass fluxes and qualities

d) 125 kg/m^{2}s mass flux, 50% quality

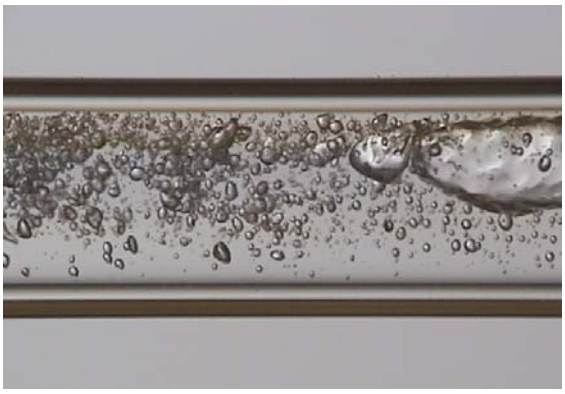

e) 125 kg/m^{2}s mass flux, 50% quality

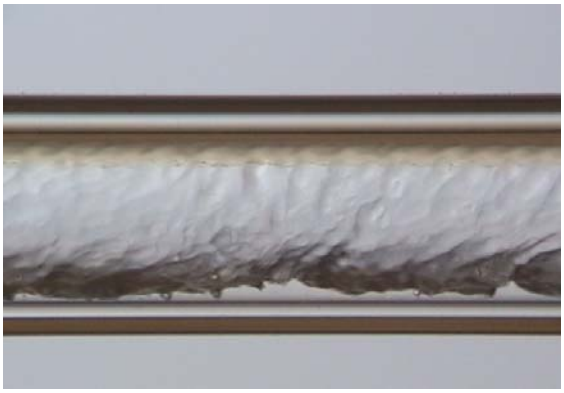

f) 125 kg/m^{2}s mass flux, 75% quality

g) 125 kg/m^{2}s mass flux, 95% quality

h) 250 kg/m^{2}s mass flux, 10% quality

i) 250 kg/m^{2}s mass flux, 10% quality

Figure 2.10, *continued*. Flow visualization photographs *(a)-(n)* of an R134a/POE mixture at various mass fluxes and qualities

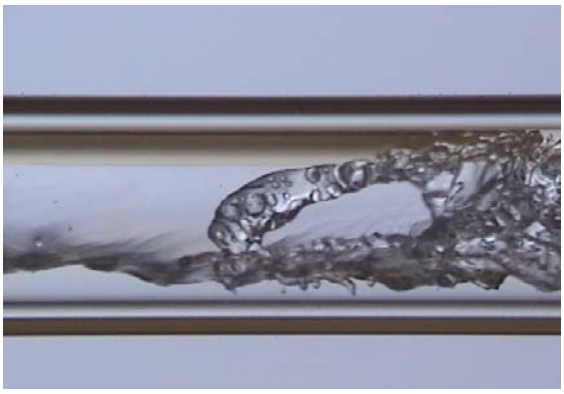

j) 250 kg/m^{2}s mass flux, 20% quality

k) 250 kg/m^{2}s mass flux, 20% quality

l) 250 kg/m^{2}s mass flux, 50% quality

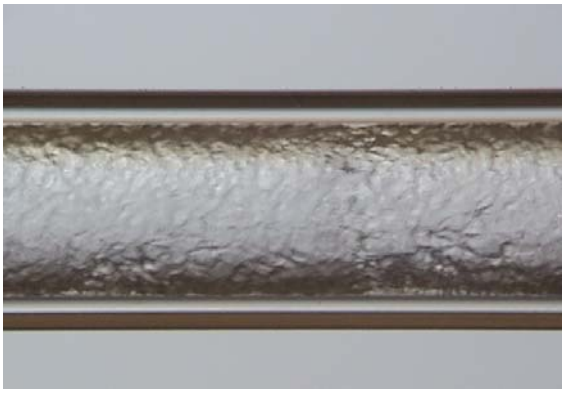

m) 250 kg/m^{2}s mass flux, 75% quality

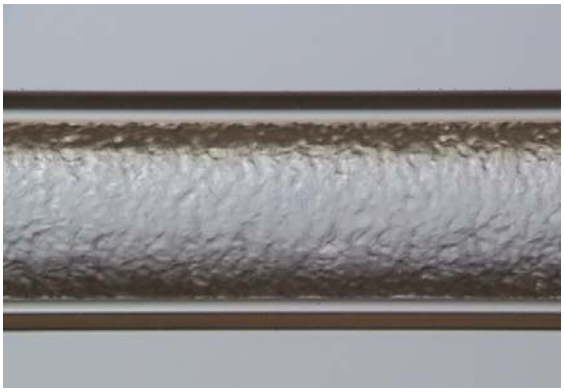

n) 250 kg/m^{2}s mass flux, 95% quality

Figure 2.10, *continued*. Flow visualization photographs *(a)-(n)* of an R134a/POE mixture at various mass fluxes and qualities

The photographs indicate behavior closer to pure refrigerant with small and random disturbances in the liquid at high qualities. One should be cautioned, however, that the behavior observed may not exist exactly this way in the test sections and rest of the system because the surface wetting capabilities of each lubricant are dependent on the type of surface it is interacting with. The flow visualization test section is smooth glass, whereas the rest of the system is copper with and without enhanced geometry.

2.4 Error and Uncertainty Analysis

An uncertainty analysis is performed on the experimental measurements and data reduction calculations using Engineering Equation Solver. The Uncertainty Propagation feature finds the uncertainty of a calculation given the relative or absolute uncertainties of the variables. The oil holdup measurements throughout this investigation have been found to have an uncertainty of ±0.052g, which is a maximum percent error of 10.8% at an oil holdup of 0.48g. The average percent error over all oil holdup measurements is 4.9%. Also, the largest uncertainty for the void fraction calculations is ±0.0326 at the void fraction value of 0.5236, which results in a maximum percent error of 6.22%. The average percent error for all void fraction calculations is 2.1%. Full analysis results are found in Appendix A.

2.5 Conclusions

2.5.1 Void Fraction

The void fraction results, as expected, increase with increasing quality. Mass flux does not seem to have an influence on void fraction, whereas results show a slight dependence on tube type. An increase in void fraction is visible with the smooth test section. Oil concentrations also do not influence void fraction results. The only results that do not agree with previous work are those of void fraction separated by mass flux. Graham [5] and Kopke [9] found higher mass fluxes producing higher void fractions.

The void fraction results calculated using the procedure described in Chapter 1 are compared to the ACRC void fraction model using pure refrigerant properties and three sets of mixture properties detailed in the literature review. These results show agreement to within ±10% for all tube types and all oil concentrations. This implies, for the current study, correction for the liquid void fraction due to the addition of oil provides little improvement to the model. It also indicates oil to have insignificant influence on refrigerant charge prediction.

2.5.2 Oil Holdup

Evident from the oil holdup data is the sensitivity of holdup to quality, mass flux, tube type and oil concentration. The following trends are observed:

1) At mid-range qualities, the oil holdup reaches a minimum. Stretching of the liquid layer by the vapor's increased velocity is the primary effect causing the reduction of oil holdup.
2) As higher qualities are reached, oil holdup increases as the viscosity of the oil begins to dominate the liquid fraction's flow. A significant oil holdup increase is observed as quality moves beyond 90%, indicating the beginning of oil logging.
3) Some effects due to mass flux are observed with lower mass fluxes (75 kg/m^{2}s) displaying higher levels of oil holdup
4) Minimal effects of tube surface (smooth versus enhanced) on oil holdup are observed for adiabatic conditions from low to mid-range qualities.
5) Surface structure causes higher oil holdup and oil logging as high quality ranges are reached.
6) At low qualities, the oil in the refrigerant tends toward the limit of zero quality in which the amount of oil is determined by the "flow concentration" of oil in the system.

A prediction model for oil holdup developed with this data is presented in Chapter 4.

2.5.3 Slip Ratio

Slip ratio results also show an expected increase with increasing quality. Mass flux and tube type are found to have a minimal influence on slip ratio, but an influence none the less. This effect, however, is indistinguishable

below about 40% quality. Lower mass fluxes and enhanced tubes show higher slip ratio values. Intuitively this makes sense because lower mass fluxes have a lower shear between the liquid and vapor phases, resulting in more slip and a higher slip ratio. Finally, oil concentration is seen to have no effect on slip ratio results.

2.5.4 Flow Visualization

At low mass fluxes and qualities oil can be seen moving on the flow visualization test section, while not affecting the flow conditions. At higher mass fluxes and qualities, when annular behavior is present, oil is not visible and does not exhibit any visible influence on the flow conditions, which progresses through common flow patterns.

2.6 List of References

[1] Alves, G.E., "Cocurrent liquid-gas flow in a pipe-line contactor," *Chemical Engineering Progress*, Vol. 50, No. 9, pp. 449-456, 1954.

[2] Baustian, J.J., M.B. Pate, and A.E. Bergles, "Properties of Oil-Refrigerant Mixtures with Applications to Oil Concentration Measurement: Part I—Thermophysical and Transport Properties," *ASHRAE Transactions*, Vol. 92, part 1, pp. 55-73, 1986.

[3] Cawte, H., D.A. Sanders, and G.A. Poland, "Effect of Lubricating Oil Contamination on Evaporation in Refrigerants R12 and R22," *International Journal of Energy Research*, Vol. 20, pp. 663-679, 1996.

[4] Dobson, M.K., J.C. Chato, J.P. Wattelet, J.A. Gaibel, M. Ponchner, P.J. Kenney, R.L. Shimon, T.C. Villaneuva, N.L. Rhines, K.A. Sweeney, D.G. Allen, and T.T. Hershberger, "Heat Transfer and Flow Regimes During Condensation in Horizontal Tubes," *ACRC TR-57* (also PhD dissertation by M.K. Dobson), Air Conditioning and Refrigeration Center, University of Illinois, Urbana-Champaign IL, 1994.

[5] Graham, D.M. T.A. Newell and J.C. Chato, "Experimental Investigation of Void Fraction During Refrigerant Condensation," *ACRC TR-135* (also MS thesis by D.M. Graham), Air Conditioning and Refrigeration Center, University of Illinois, Urbana-Champaign IL, 1997.

[6] Graham, D.M., H.R. Kopke, M.J. Wilson, D.A. Yashar, J.C. Chato, and T.A. Newell, "An Investigation of Void Fraction in the Annular/Stratified Flow Regions in Smooth, Horizontal Tubes," *ACRC TR-144*, Air Conditioning and Refrigeration Center, University of Illinois, Urbana-Champaign IL, 1999.

[7] Gupta, S., J.C. Chato and T.A. Newell, "Investigation of the Effect of an R134a/Polyol Ester Mixture on Void Fraction and Pressure Drop in Horizontal Tube Evaporators," *ACRC TR-173* (also MS thesis by S. Gupta), Air Conditioning and Refrigeration Center, University of Illinois, Urbana-Champaign IL, 2000.

[8] Hurlburt, E.T., and T.A. Newell, "Modeling of the Evaporation and Condensation of Zeotropic Refrigerant Mixtures in Horizontal, Annular Flow," *ACRC TR-129* (also PhD dissertation by E.T. Hurlburt), Air Conditioning and Refrigeration Center, University of Illinois, Urbana-Champaign IL, 1997.

[9] Kopke, H.R., T.A. Newell, and J.C. Chato, "Experimental Investigation of Void Fraction during Refrigerant Mixtures in Horizontal Tubes," *ACRC TR-142* (also MS thesis by H.R. Kopke), Air Conditioning and Refrigeration Center, University of Illinois, Urbana-Champaign, 1998.

[10] Lockhart, R.W. and R.C. Martinelli, "Proposed correlation of data for isothermal two-phase, two-component flow in pipes," *Chemical Engineering Progress*, Vol. 45, no. 1, pp. 39-48, 1949.

[11] Piggott III, W.T., T.A. Newell, and J.C. Chato, "Investigation of an R134a Refrigerant/Iso 32 Polyol Ester Oil Mixture in Condensation," *ACRC TR-192* (also MS thesis by W.T. Piggott), Air Conditioning and Refrigeration Center, University of Illinois, Urbana-Champaign IL, 2001.

[12] Reid, Robert C., John M. Prausnitz, and Bruce E. Poling, *The Properties of Gases & Liquids*, Fourth ed., McGraw-Hill, United States, 1987.

[13] Tichy, J.A., N.A. Macken, and W.M.B. Duval, "An Experimental Investigation of Heat Transfer in Forced Convection Condensation of Oil-Refrigerant Mixtures," *ASHRAE Transactions*, Vol. 91, part 1A, pp. 297-303, 1985.

[14] Wallis, G.B., *One Dimensional Two-Phase Flow*, McGraw Hill, New York, pp. 51-54, 1969.

[15] Wilson, M.J., T.A. Newell, and J.C. Chato, "Experimental Investigation of Void Fraction During Horizontal Flow in Larger Diameter Refrigeration Applications," *ACRC TR-140* (also MS thesis by M.J. Wilson), Air Conditioning and Refrigeration Center, University of Illinois, Urbana-Champaign IL, 1998.

[16] Wilson, M.J., T.A. Newell, and J.C. Chato, "A Study of Two-Phase Refrigerant Behavior in Flattened Tubes," *ACRC CR-35* (also PhD dissertation by M.J. Wilson), Air Conditioning and Refrigeration Center, University of Illinois, Urbana-Champaign IL, 2001.

[17] Yashar, D.A., T.A. Newell, and J.C. Chato, "Experimental Investigation of Void Fraction during Horizontal Flow in Smaller Diameter Refrigeration Applications," *ACRC TR-141* (also MS thesis by D.A. Yashar), Air Conditioning and Refrigeration Center, University of Illinois, Urbana-Champaign IL, 1998.

Chapter 3. More Refrigerant-Oil Mixtures

3.1 Introduction

This chapter uses the results from the previous study involving R134a and a polyol ester oil as a basis for further investigation of various refrigerant-oil mixtures. The experimental methods and procedures of that study are utilized to collect void fraction, oil holdup and flow visualization data of R134a/polyalkylene glycol, R134a/alkylbenzene, R22/alkylbenzene and R410A/polyol ester mixtures. The results of this chapter will then be compared to the investigation of Chapter 2, and the combination of results will be used to formulate conclusions of oil holdup prediction modeling, which will be presented in Chapter 4.

3.2 Literature Review

3.2.1 Void Fraction

In addition to the ACRC void fraction model presented in Chapter 2, void fraction values are also calculated using the homogeneous model shown in Equation 3.1 and a slip ratio model developed by Zivi [4].

$$\alpha = \frac{1}{1 + \frac{1-x}{x}\left(\frac{\rho_v}{\rho_l}\right)S} \tag{3.1}$$

The homogeneous model represents liquid and vapor flowing at the same velocity with a slip ratio of unity, while Zivi's model uses the slip ratio model described in Chapter 1 with a slip ratio value defined by

$$S = \left(\frac{\rho_l}{\rho_v}\right)^{\frac{1}{3}} \tag{3.2}$$

The quality used in this model and the rest of the investigation is a corrected quality based on a liquid line oil concentration measurement. The data acquisition program used calculates quality based on enthalpies determined with temperatures and pressures of the system as well as the amount of heat added through the preheaters. Theoretically with only refrigerant, the amount of heat provided to the system would result in a quality of one, however some of the input is being used to heat the oil entrained in the flow, which results in a mixture quality less than one. Equation 3.3 gives the corrected quality based on the oil concentration, c_o, and "measured" quality.

$$x = x_{measured}\left(1 - c_o\right) \tag{3.3}$$

3.2.2 Refrigerant-Oil Mixtures

The investigation of the remaining refrigerant-oil mixtures uses a slightly different calculation for experimental void fraction than detailed in Chapter 1. The effect of oil in the high quality range is of much interest so the liquid specific volume is determined, not by the saturation temperature of liquid refrigerant, but by the inverse of the liquid mixture density. This mixture density is defined as

$$\rho_m = \frac{\rho_l}{1 - \left(1 - w_{oil}\right)\left(1 - \frac{\rho_l}{\rho_o}\right)} \tag{3.4}$$

where ρ_l is the liquid refrigerant density, ρ_o is the oil density and w_{oil} is the oil mass fraction.

All oil properties used in calculations are determined with measured property data acquired by Christopher Seeton [1] in an ongoing ACRC project, and will be published when testing is complete. This data includes density and viscosity measurements at a range of temperatures for the various lubricants, which are fit and allow properties to be calculated as a function of the test section temperature.

3.2.3 Bubble Point Temperature

Thermodynamic properties as well as fluid properties of a mixture are affected by the presence of oil. Though ultimately incorrect, in practice properties such as the saturation temperature are assumed for pure refrigerants when the oil is actually affecting boiling point temperatures, specific heats and enthalpies, which can alter energy balances and quality calculations. Takaishi and Oguchi [2] developed an empirical formula to determine bubble point temperature as a function of saturation pressure and oil concentration.

$$T_{bub} = \frac{A(w_{oil})}{\ln(P_{sat}) - B(w_{oil})} \tag{3.5}$$

Here, P_{sat} is the saturation pressure and w_{oil} is the oil mass fraction in the liquid refrigerant. $A(w_{oil})$ and $B(w_{oil})$ are found using

$$A(w_{oil}) = a_0 + a_1 w_{oil} + a_2 w_{oil}^3 + a_3 w_{oil}^5 + a_4 w_{oil}^7 \tag{3.6}$$

$$B(w_{oil}) = b_0 + b_1 w_{oil} + b_2 w_{oil}^3 + b_3 w_{oil}^5 + b_4 w_{oil}^7, \tag{3.7}$$

where the values of the constants are given in Table 3.1.

Table 3.1. Empirical constants for bubble point temperature calculation

a_0 = -2394.5	b_0 = 8.0736
a_1 = 182.52	b_1 = -0.72212
a_2 = -724.21	b_2 = 2.3914
a_3 = 3868.0	b_3 = -13.779
a_4 = -5268.9	b_4 = 17.066

As suggested by Thome [3], the values for a_0 and b_0 are found using a pure refrigerant vapor pressure equation at the test pressure, rather than the given constants.

3.3 Experimental Results

3.3.1 R134a and Polyalkylene Glycol

Polyalkylene glycol lubricant is miscible with R134a and is used primarily in the automotive industry. As a polyglycol, this formula shows almost no tendency to evaporate making it a suitable choice for high temperature applications. Over the range of testing conditions performed, this lubricant showed an average density of 982 kg/m^3, dynamic viscosity of 0.066 kg/m-s and kinematic viscosity of 6.73 x 10^{-5} m^2/s.

3.3.1.1 Void Fraction

The three void fraction models utilized, the ACRC, homogeneous and Zivi models, are shown versus experimental data in Figure 3.1 with error bands representative of ±10%. As expected, the homogeneous model predicts the highest void fractions because liquid moving at the same velocity as vapor gives the thinnest liquid layer. Additionally, the Zivi model which considers differing liquid and vapor velocities compares more closely to

experimental data than the homogeneous model, but still deviates possibly due to the absence of mass flux influence. Finally, the correlation between the ACRC prediction model and experimental data confirms its accuracy and validity for use in this investigation.

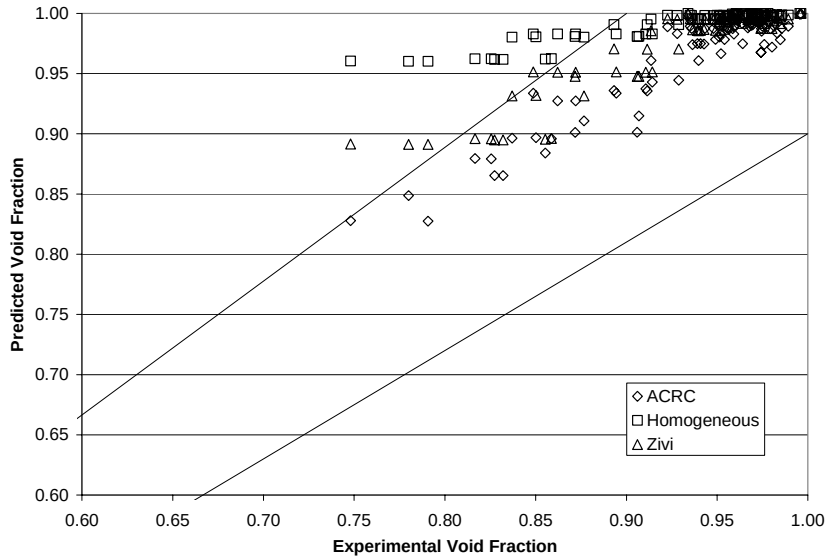

Figure 3.1. Comparison of void fraction models to experimental void fraction for an R134a/PAG mixture with error lines of ±10%

Figure 3.2 shows the experimental void fraction separated by mass flux and Figure 3.3 is separated by tube type. Figure 3.2 does not provide clear evidence of a mass flux effect on void fraction because this effect is primarily in the lower quality range. At the lowest quality tested the effect of mass flux begins to show. Tube type influence is shown clearly in Figure 3.3. The smooth test section provides a higher void fraction. These results agree with results found for the R134a/POE mixture detailed in Chapter 2.

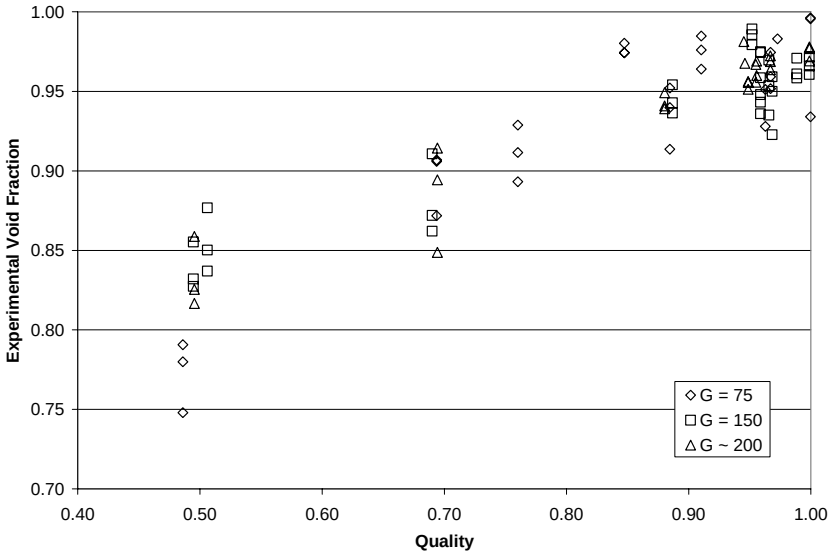

Figure 3.2. Experimental void fraction separated by mass flux (kg/m^2s) for an R134a/PAG mixture

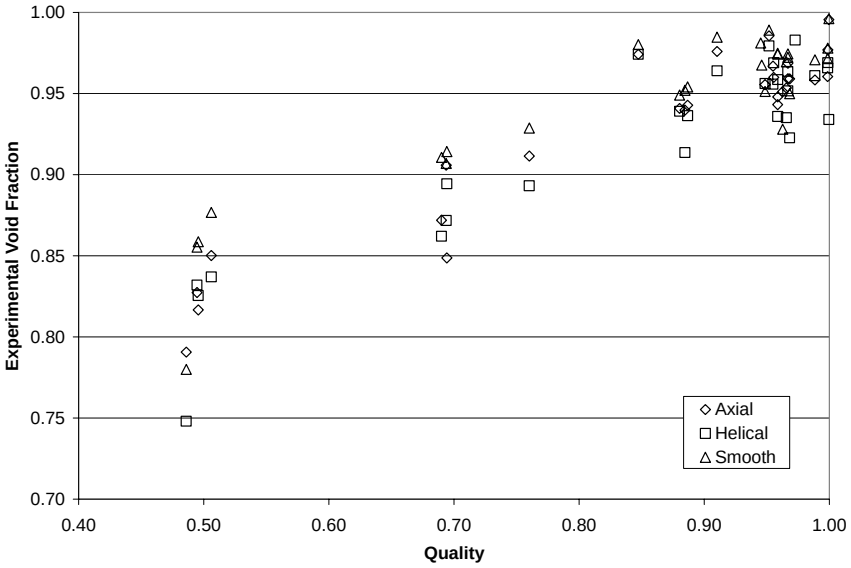

Figure 3.3. Experimental void fraction separated by tube type for an R134a/PAG mixture

3.3.1.2 Oil Holdup

Figure 3.4 shows experimental oil holdup in grams per meter of the R134a/PAG mixture separated by mass flux, and Figure 3.5 separates the data by tube type. Both figures show a slight influence of mass flux and tube type, respectively. Notice a lower mass flux generally gives a higher oil holdup, while the enhanced tubes, particularly the helical section, generally have the higher oil holdup. All data sets are tested at oil concentrations between zero and about 4% except for the R134a/PAG set. The PAG data includes oil concentrations up to 13%, and the effect of this high concentration is shown in Figure 3.6. The higher the oil concentration in the liquid feed line, the more oil is measured in the test section.

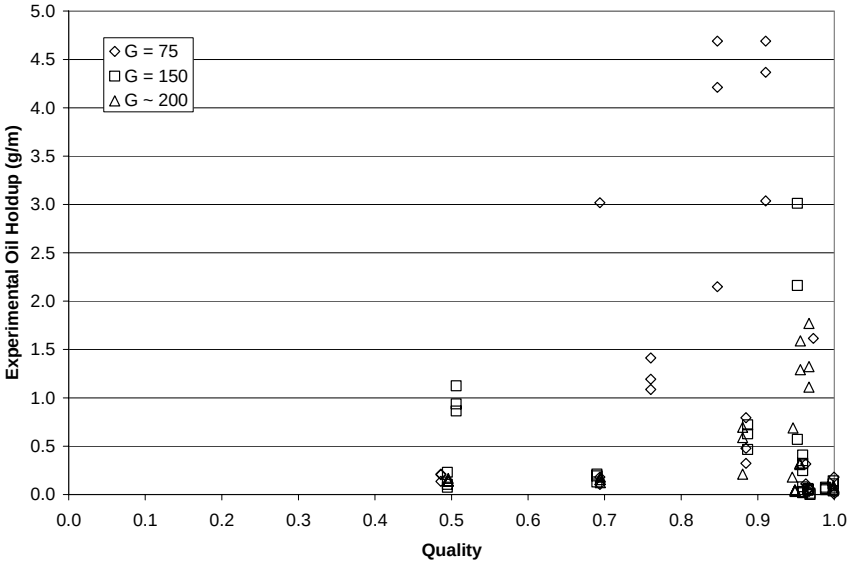

Figure 3.4. Experimental oil holdup for an R134a/PAG mixture separated by mass flux (kg/m^2s)

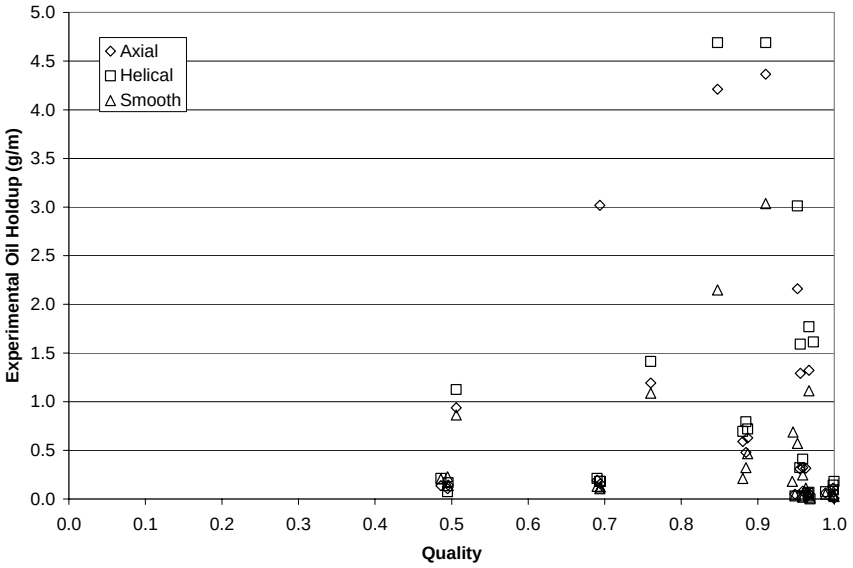

Figure 3.5. Experimental oil holdup for an R134a/PAG mixture separated by tube type

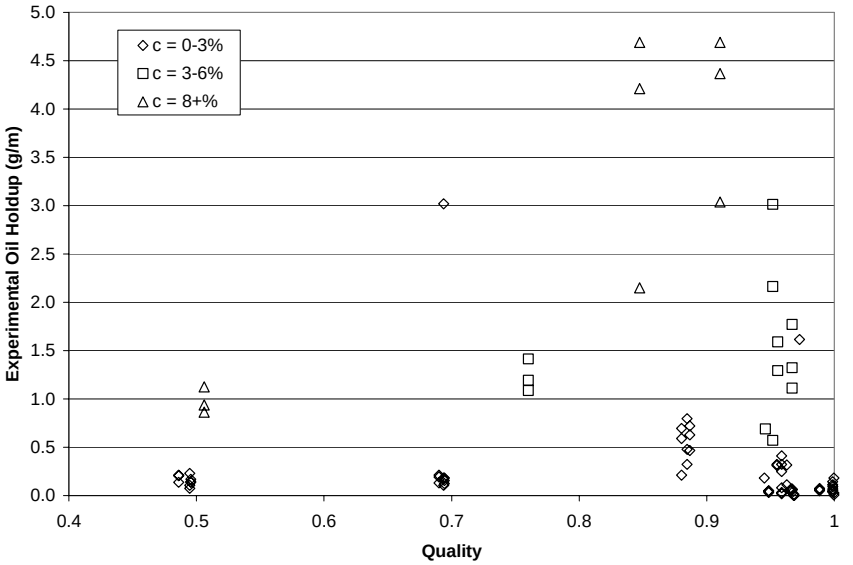

Figure 3.6. Experimental oil holdup for an R134a/PAG mixture separated by oil concentration

3.3.1.3 Slip Ratio

As previously seen with the R134a and Polyol Ester mixture, the slip ratio is expected to increase gradually with increasing quality, and then make a sharp increasing turn to be more sensitive to increases in quality. Figure 3.7 shows experimental slip ratios for the R134a/PAG combination separated by mass flux, while Figure 3.8 shows separation by tube type. From these figures it is evident that the increasing influence of quality is present. Upon closer examination, tube type influences experimental slip ratio as well. Enhanced tubing shows higher slip ratios at high qualities where oil has the same effect on experimental oil holdup. The effect of mass flux on slip ratio is less clear.

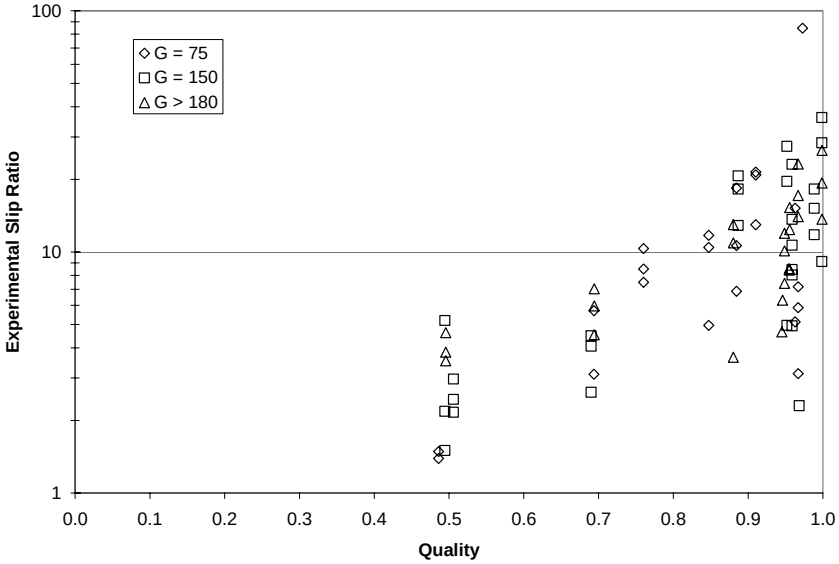

Figure 3.7. Experimental slip ratio on a logarithmic scale with respect to quality, separated by mass flux (kg/m^2s) for an R134a/PAG mixture

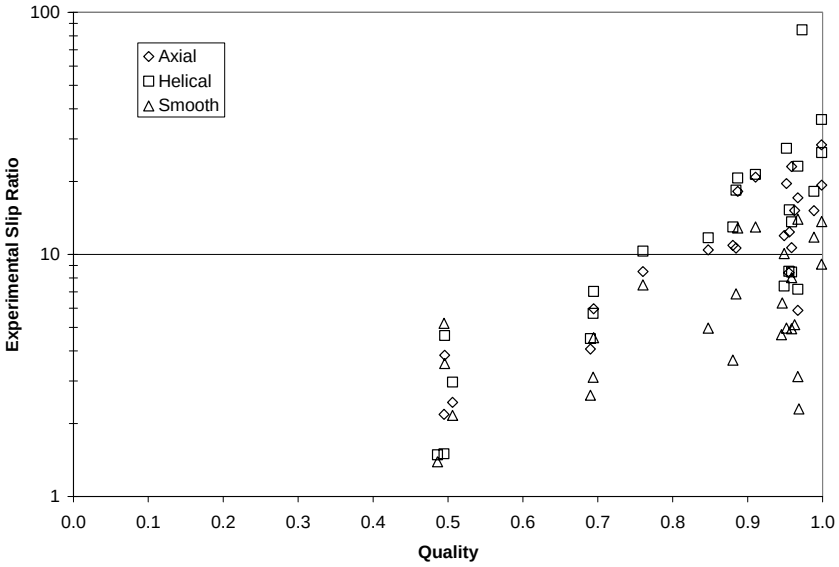

Figure 3.8. Experimental slip ratio on a logarithmic scale with respect to quality, separated by tube type for an R134a/PAG mixture

3.3.1.4 Flow Visualization

As seen with the R134a/POE mixture, a collection of flow visualization photographs is presented in Figure 3.9 for various mass fluxes and qualities. Note the quality referenced is the theoretical quality, not accounting for the presence of oil. Photographs taken at low and mid-range qualities show stratified behavior where oil effects are not evident. At higher qualities, the effect of oil becomes more apparent. These figures, Figure 3.9.*e* for example, show large and more circumferential disturbances rather than small and random disturbances in the liquid layer. This effect is not, however, consistent with all photographs taken at high qualities. For those at high mass fluxes, the effect is not clear, but the remaining visible liquid layer at 100% quality indicates the presence of the oil. Again,

one must realize that the surface wetting capabilities of the lubricant are dependent on the surface it is interacting with. Therefore, the observations in the following figure may not be representative of the behavior within the rest of the system, made of copper with smooth and enhanced geometry rather than smooth glass.

a) 75 kg/m^{2}s mass flux, 50% quality

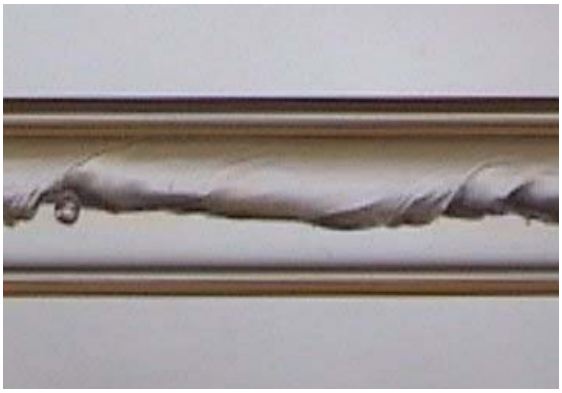

b) 75 kg/m^{2}s mass flux, 50% quality

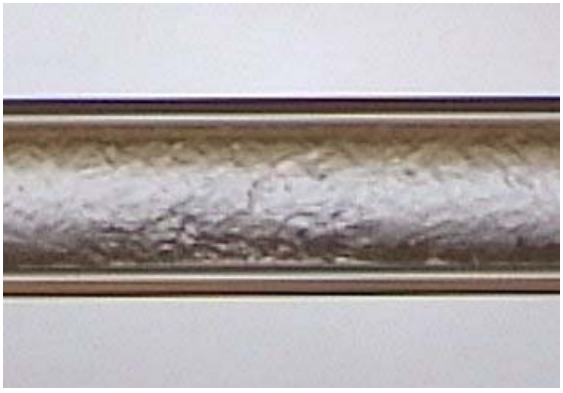

c) 75 kg/m^{2}s mass flux, 70% quality

d) 75 kg/m^{2}s mass flux, 90% quality

e) 75 kg/m^{2}s mass flux, 100% quality

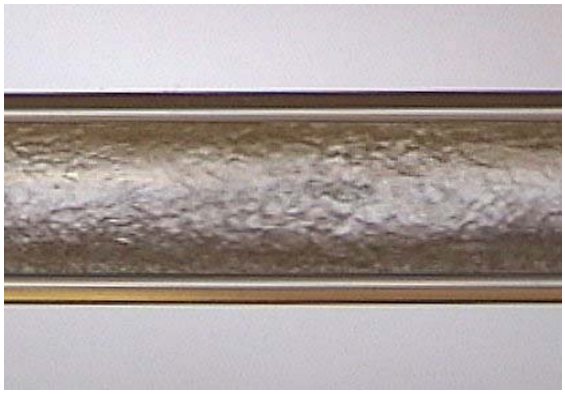

f) 150 kg/m^{2}s mass flux, 50% quality

Figure 3.9. Flow visualization photographs *(a)-(l)* of an R134a/PAG mixture at various mass fluxes and qualities

g) 150 kg/m^{2}s mass flux, 70% quality

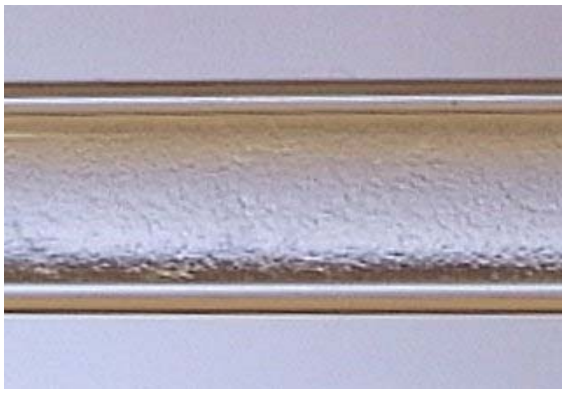

h) 150 kg/m^{2}s mass flux, 100% quality

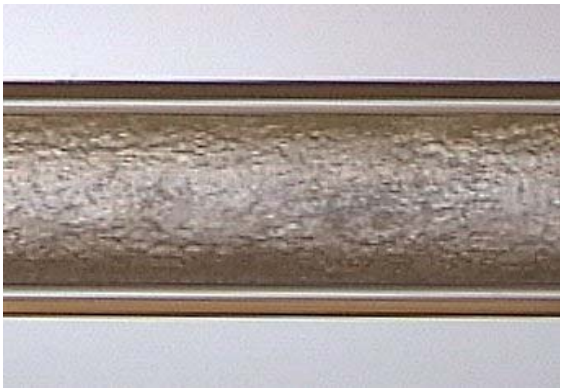

i) 200 kg/m^{2}s mass flux, 50% quality

j) 200 kg/m^{2}s mass flux, 70% quality

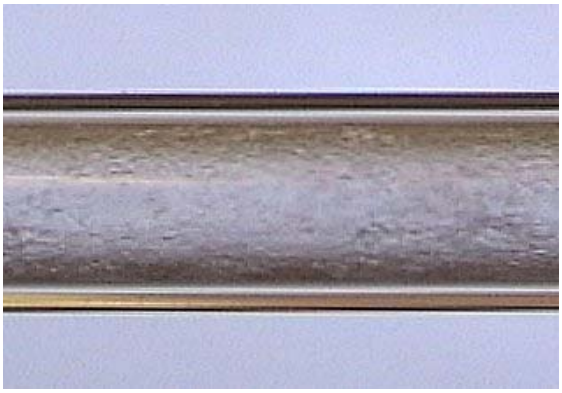

k) 200 kg/m^{2}s mass flux, 90% quality

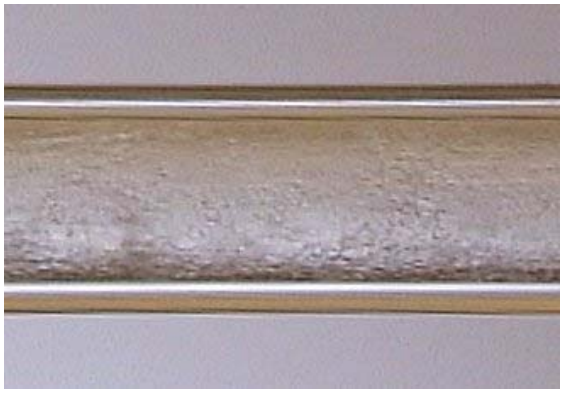

l) 250 kg/m^{2}s mass flux, 100% quality

Figure 3.9, *continued*. Flow visualization photographs *(a)-(l)* of an R134a/PAG mixture at various mass fluxes and qualities

3.3.2 R134a and Alkylbenzene

The alkylbenzene lubricant used for this investigation is determined to have an average density of 858 kg/m^3, dynamic viscosity of 0.0306 kg/m-s and kinematic viscosity of 3.57x10^{-5} m^2/s. Note that this combination of refrigerant and oil is immiscible. This condition resulted in a difficulty in system management pertaining specifically to startup. The apparatus would seemingly start well, but after running briefly mass flux would drop to zero. It was deduced that the less dense oil floating on top of the liquid refrigerant in the receiver tank would plug the inlet tube as the liquid level decreased during the start. To treat this problem, the charge in the system was

increased to prevent the floating oil layer from ever reaching the inlet tube level. One disadvantage of this is that the initial oil concentration inserted into the system does not reflect the amount of oil circulating with the flow. At an estimated 10% oil concentration in the system, very few data points in this set reached 2% oil concentration in the liquid feed line.

3.3.2.1 Void Fraction

The ACRC, homogeneous and Zivi void fraction models are compared with experimental results for the R134a/alkylbenzene mixture. This comparison is shown in Figure 3.10. Again, the homogeneous show the highest void fraction predictions and the ACRC model correlates well with experimental data. The experimental data separated by mass flux and tube type, respectively, follow in Figures 3.11 and 3.12.

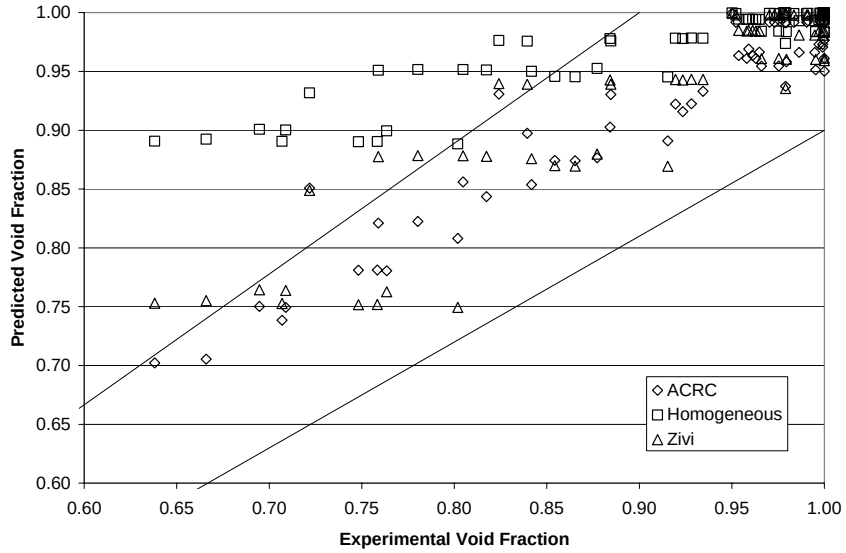

Figure 3.10. Comparison of void fraction models to experimental void fraction for an R134a/alkylbenzene mixture with error lines of ±10%

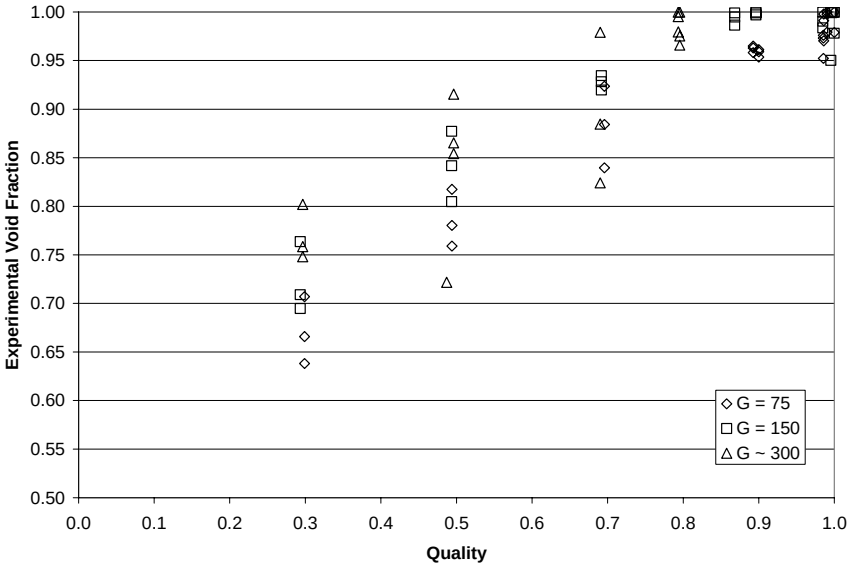

Figure 3.11. Experimental void fraction separated by mass flux (kg/m^{2}s) for an R134a/alkylbenzene mixture

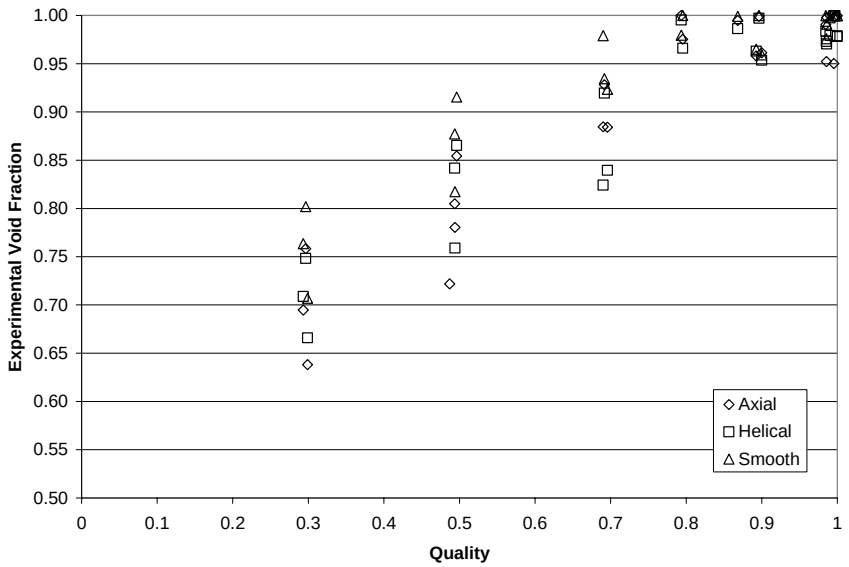

Figure 3.12. Experimental void fraction separated by tube type for an R134a/alkylbenzene mixture

Unlike the R134a/POE and R134a/PAG mixtures, both mass flux and tube type are found to affect void fraction results. This is primarily due to testing lower qualities where the mass flux effects are expected. The figures clearly show higher mass fluxes and the smooth test section giving higher void fraction values.

3.3.2.2 Oil Holdup

Figure 3.13 shows experimental oil holdup in grams per meter of the R134a/alkylbenzene mixture separated by mass flux, and Figure 3.14 separates the data by tube type. Again, mass flux shows a slight influence with lower mass fluxes producing a higher oil holdup. However, the influence of tube type is much more pronounced with helical sections showing significantly more oil retention than either the axial or smooth sections at high qualities.

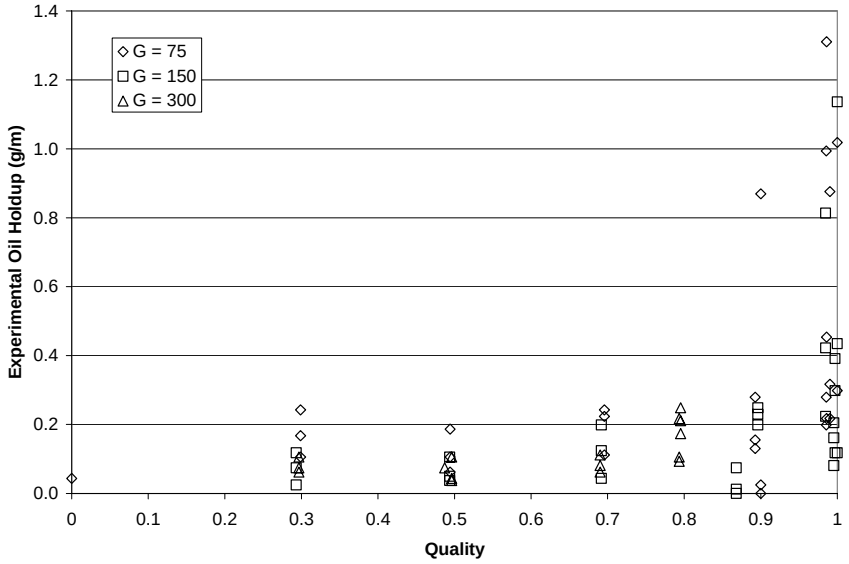

Figure 3.13. Experimental oil holdup for an R134a/alkylbenzene mixture separated by mass flux (kg/m^{2}s)

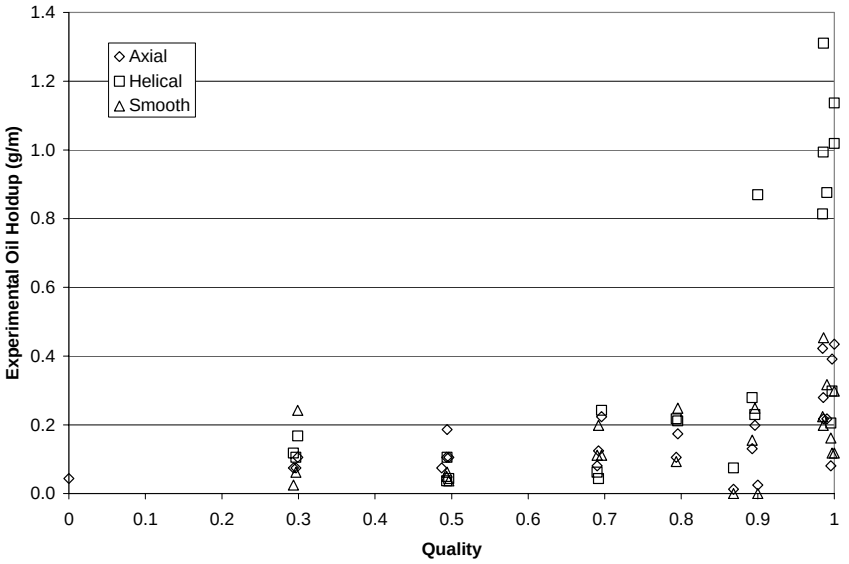

Figure 3.14. Experimental oil holdup for an R134a/alkylbenzene mixture separated by tube type

3.3.2.3 Slip Ratio

Experimental slip ratio values are shown in Figures 3.15 and 3.16, separated by mass flux and tube type, respectively for the R134a/alkylbenzene mixture. This data again shows little sensitivity to mass flux, but does show the increase in slip ratio for the enhanced tubes.

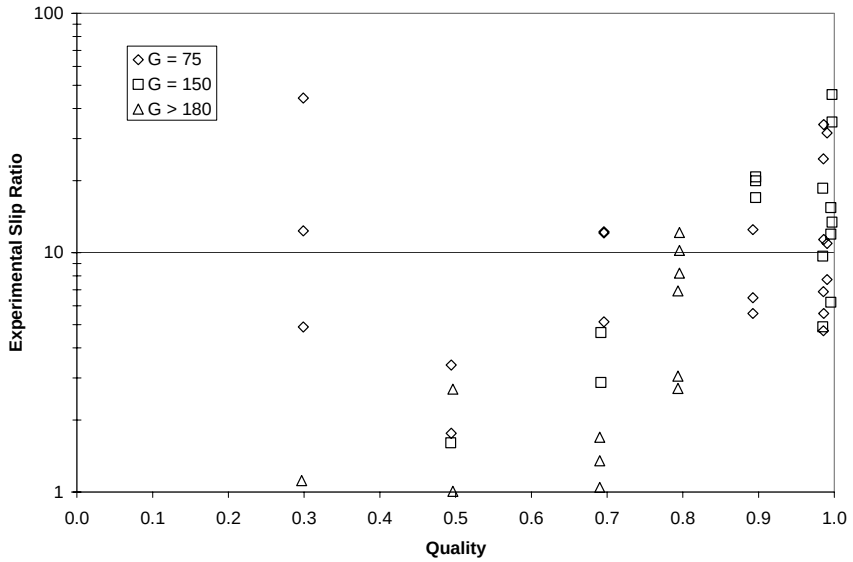

Figure 3.15. Experimental slip ratio on a logarithmic scale with respect to quality, separated by mass flux (kg/m^2s) for an R134a/alkylbenzene mixture

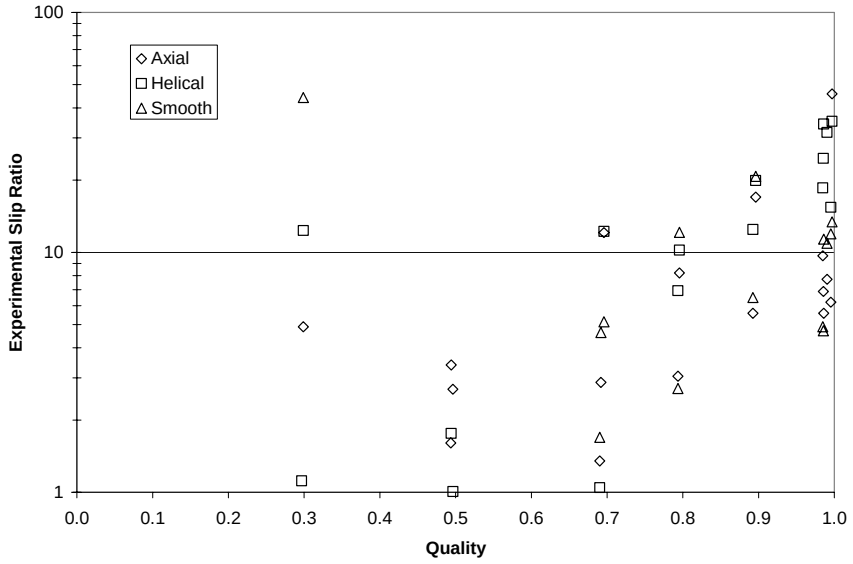

Figure 3.16. Experimental slip ratio on a logarithmic scale with respect to quality, separated by tube type for an R134a/alkylbenzene mixture

3.3.2.4 Flow Visualization

As seen with the previous mixtures, a collection of flow visualization photographs is presented in Figure 3.17 for various mass fluxes and qualities. Notice the first three pictures are of the system off or at very low startup flow, showing the most visible presence of oil. This video was taken near the point of injection just after oil is introduced into the system. The first (*a*) shows a vapor bubble moving due to a pressure gradient in the system, pushing a globule of oil floating on the refrigerant surface as indicated by the marker. The second photograph (*b*) shows a large amount of oil again floating on the surface of the refrigerant, but also spiraling down the sides of the tube due to the low mass flux. And, the third (*c*) shows a wavy oil layer floating on the surface of the refrigerant. After running the apparatus, the large amount of visible oil is flushed into the receiver tank, where most remains during operation.

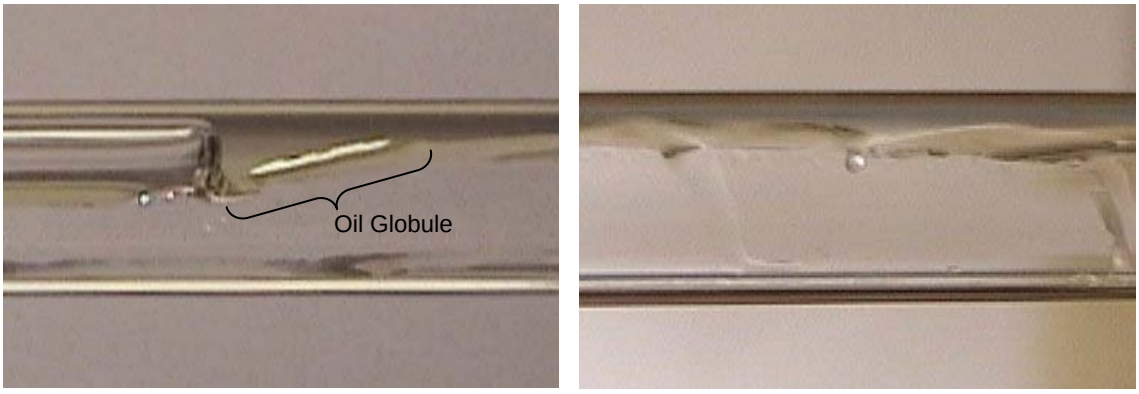

a) zero mass flux, zero quality *b) ~20 kg/m^{2}s mass flux, zero quality*

Figure 3.17. Flow visualization photographs *(a)-(n)* of an R134a/alkylbenzene mixture at various mass fluxes and qualities

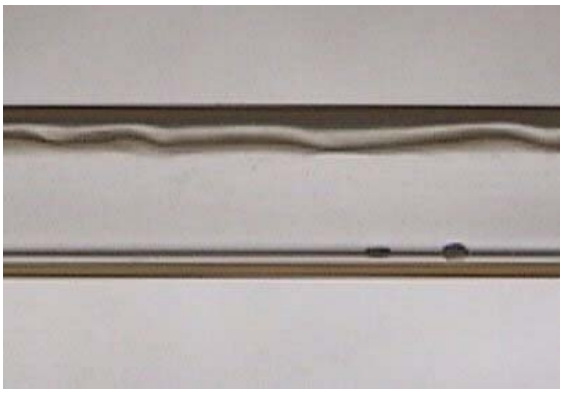

c) ~20 kg/m^{2}s mass flux, zero quality

d) 75 kg/m^{2}s mass flux, 30% quality

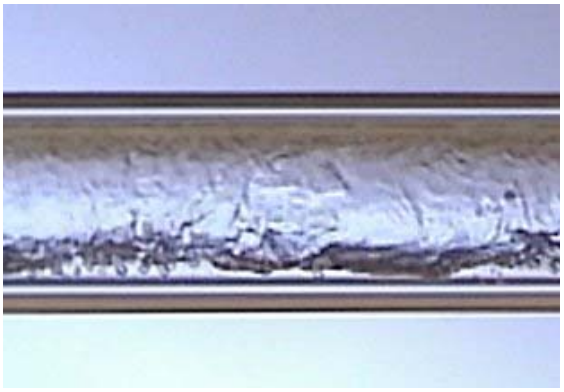

e) 75 kg/m^{2}s mass flux, 50% quality

f) 75 kg/m^{2}s mass flux, 50% quality

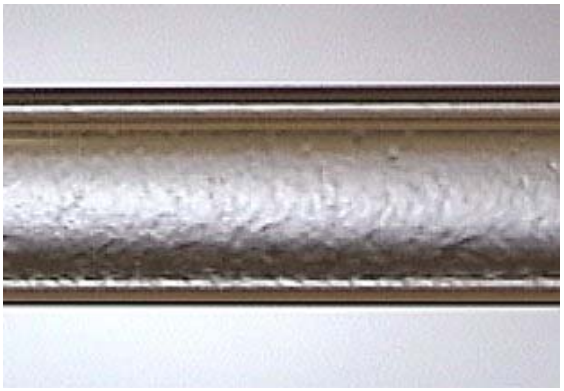

g) 75 kg/m^{2}s mass flux, 90% quality

h) 75 kg/m^{2}s mass flux, 100% quality

Figure 3.17, *continued*. Flow visualization photographs *(a)-(n)* of an R134a/alkylbenzene mixture at various mass fluxes and qualities

i) 150 kg/m2s mass flux, 30% quality

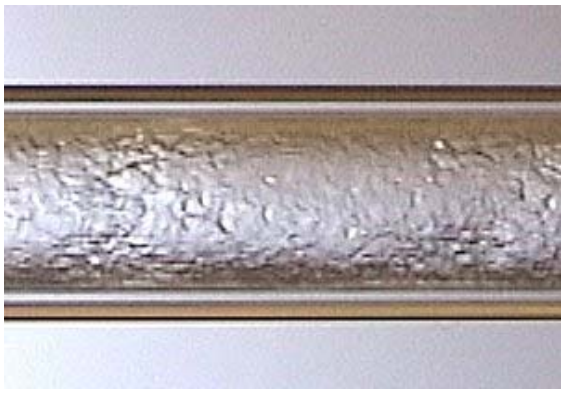

j) 150 kg/m2s mass flux, 50% quality

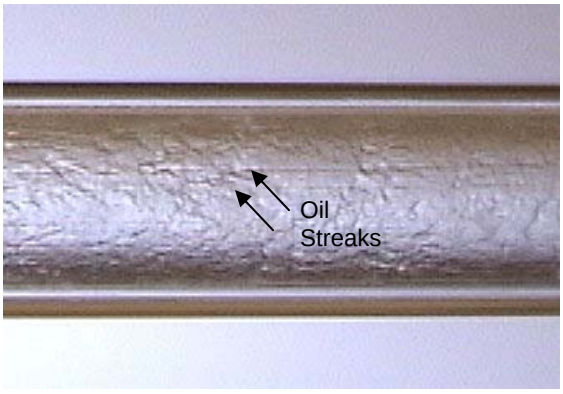

k) 150 kg/m^{2}s mass flux, 70% quality

l) 150 kg/m^{2}s mass flux, 90% quality

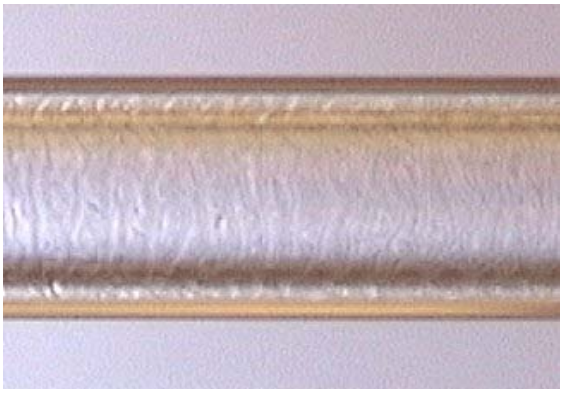

m) 150 kg/m^{2}s mass flux, 100% quality

n) 300 kg/m^{2}s mass flux, 70% quality

Figure 3.17, *continued*. Flow visualization photographs *(a)-(n)* of an R134a/alkylbenzene mixture at various mass fluxes and qualities

The presence of oil in this mixture is visible in two forms. As discussed previously, the larger and circumferential disturbances in the liquid layer at high qualities indicates the presence of oil where the lubricant is tending to laminarize the annular flow. The other form seen above in Figure 3.17.*k* is a series of horizontal streaks along the tube. This may be a transition between the wetting capabilities of the oil where refrigerant or flow parameters are preventing the oil from wetting the tube surface behaving as a liquid film and instead acts non-wetting, forms globules and the flow shears it into the streaks observed.

3.3.3 R22 and Alkylbenzene

The combination of R22 and alkylbenzene lubrication data is acquired in the process of transitioning between the previous mixture (R134a and alkylbenzene) and the final mixture (R410A and POE). Because alkylbenzene is immiscible in R134a and miscible in R22, the latter is used to essentially wash the experimental apparatus dissolving any lubricant that may be stuck in joints or valves. The average density and viscosities of the oil in this mixture parallel the values reported in the previous section also using alkylbenzene.

3.3.3.1 Void Fraction

The ACRC, homogeneous and Zivi void fraction models are compared with experimental results for the R22/alkylbenze mixture. This comparison is shown in Figure 3.18. Again, the homogeneous model shows the highest void fraction predictions and the ACRC model correlates well with experimental data. The experimental data separated by mass flux and tube type, respectively, follow in Figures 3.19 and 3.20.

Though slight, an influence of both mass flux and tube type is seen for this mixture. Higher mass fluxes and the smooth test section show higher void fraction results.

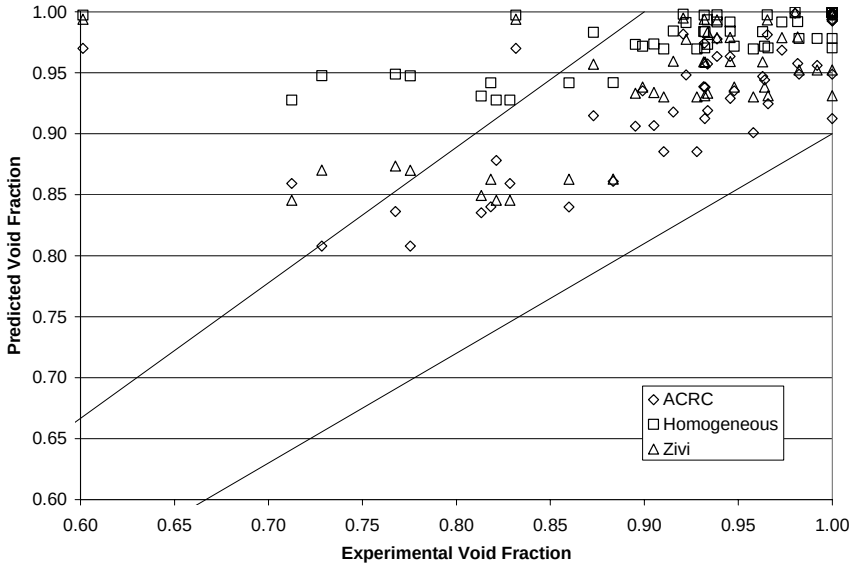

Figure 3.18. Comparison of void fraction models to experimental void fraction for an R22/alkylbenzene mixture with error lines of ±10%

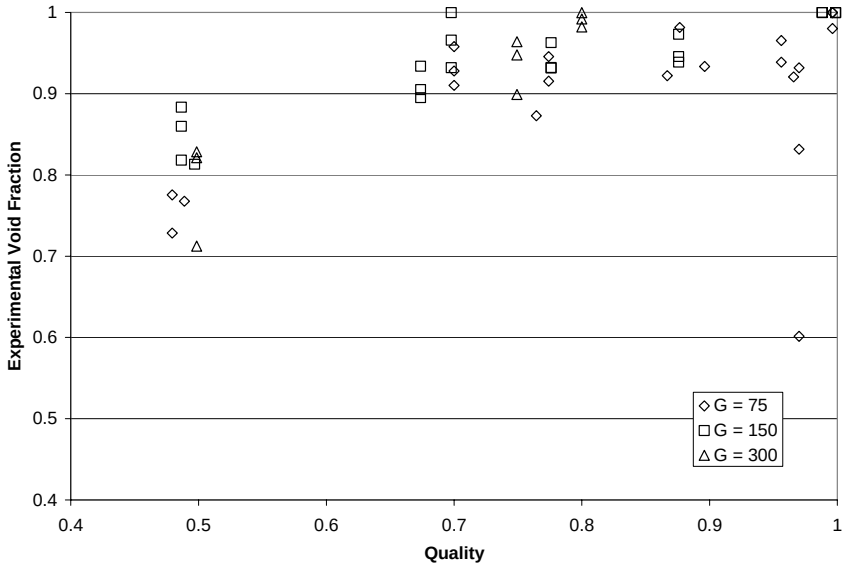

Figure 3.19. Experimental void fraction separated by mass flux (kg/m^{2}s) for an R22/alkylbenzene mixture

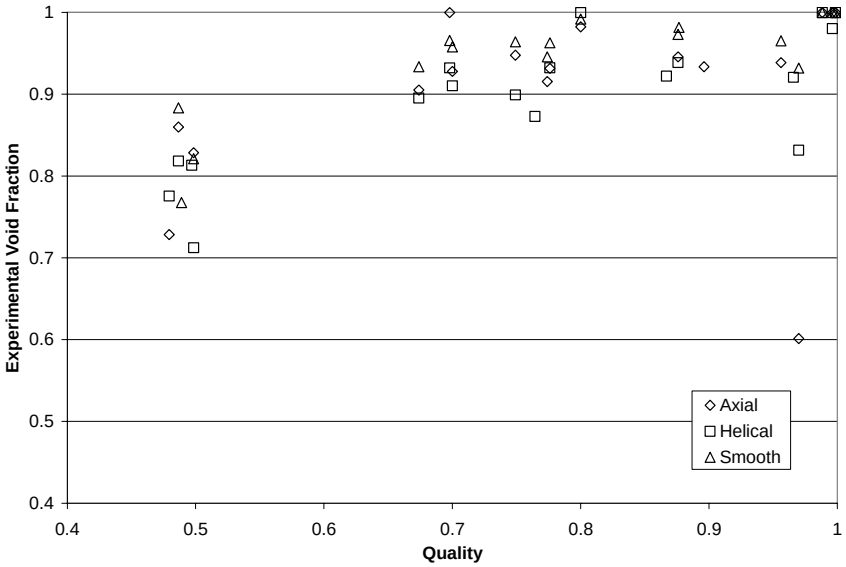

Figure 3.20. Experimental void fraction separated by tube type for an R22/alkylbenzene mixture

3.3.3.2 Oil Holdup

Figure 3.21 shows experimental oil holdup in grams per meter of the R22/alkylbenzene mixture separated by mass flux, and Figure 3.22 separates the data by tube type. The trend continues with lower mass flux showing only a slight influence on oil holdup and a more noticeable influence of the enhanced test sections on oil holdup at high qualities.

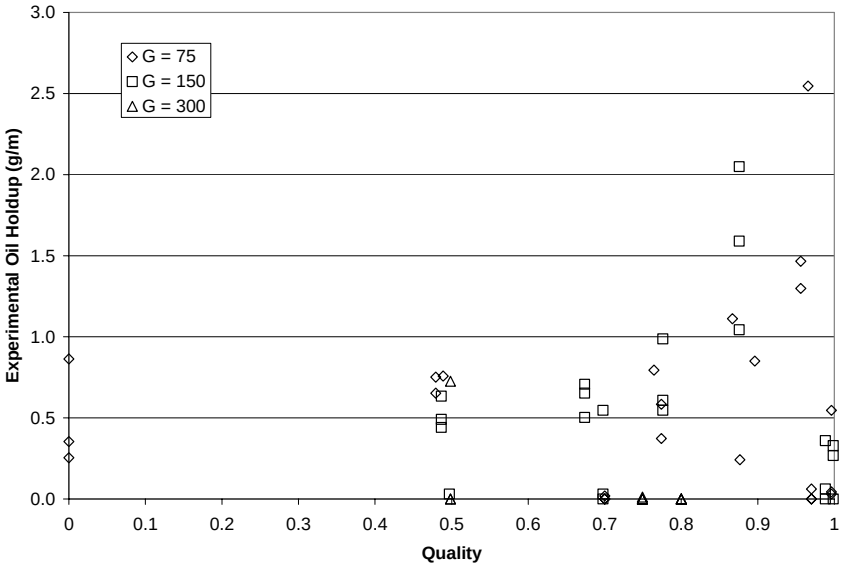

Figure 3.21. Experimental oil holdup for an R22/alkylbenzene mixture separated by mass flux (kg/m^2s)

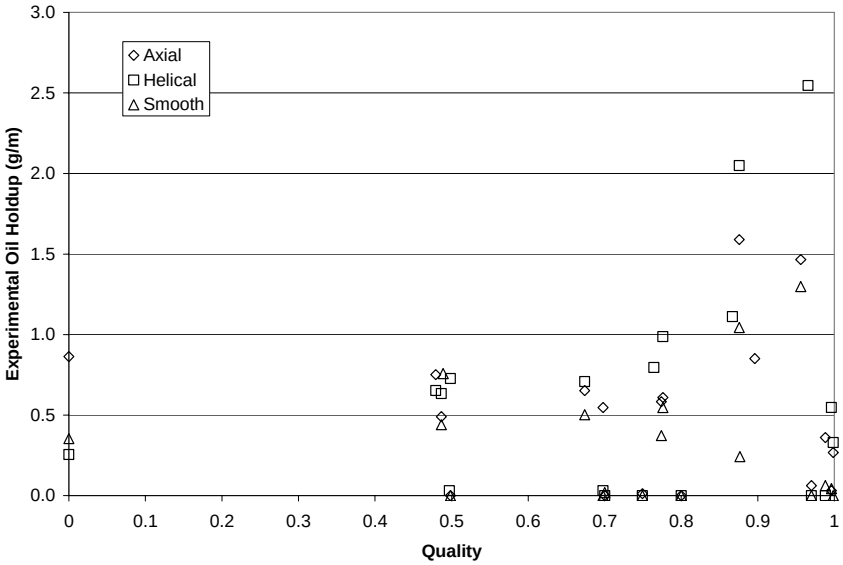

Figure 3.22. Experimental oil holdup for an R22/alkylbenzene mixture separated by tube type

3.3.3.3 Slip Ratio

Experimental slip ratio values are shown in Figures 3.23 and 3.24, separated by mass flux and tube type, respectively for the R22/alkylbenzene mixture. Increased mass flux seems to show a slight increase in slip ratio which differs from the previous results and conclusions of the R134a/POE mixture. This observation, however, is seen only at high qualities. Again, enhanced tubes show an increase in slip ratio particularly at high qualities.

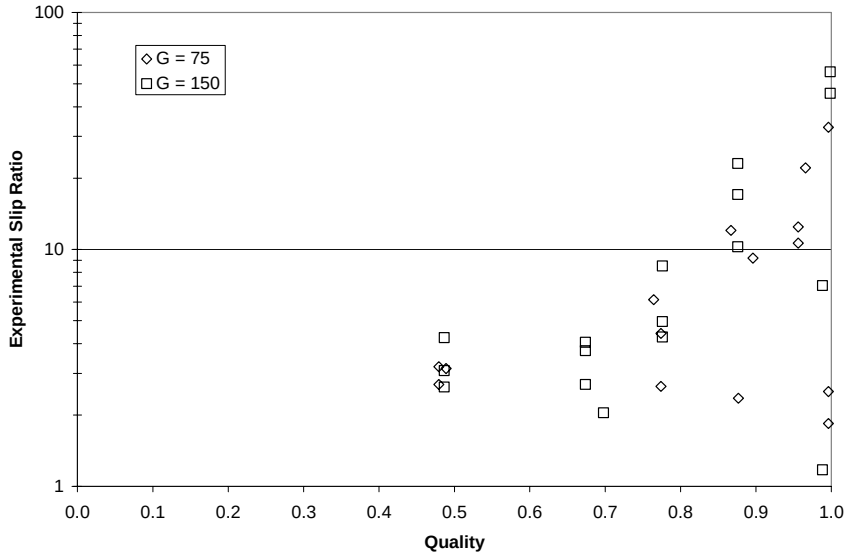

Figure 3.23. Experimental slip ratio on a logarithmic scale with respect to quality, separated by mass flux (kg/m^2s) for an R22/alkylbenzene mixture

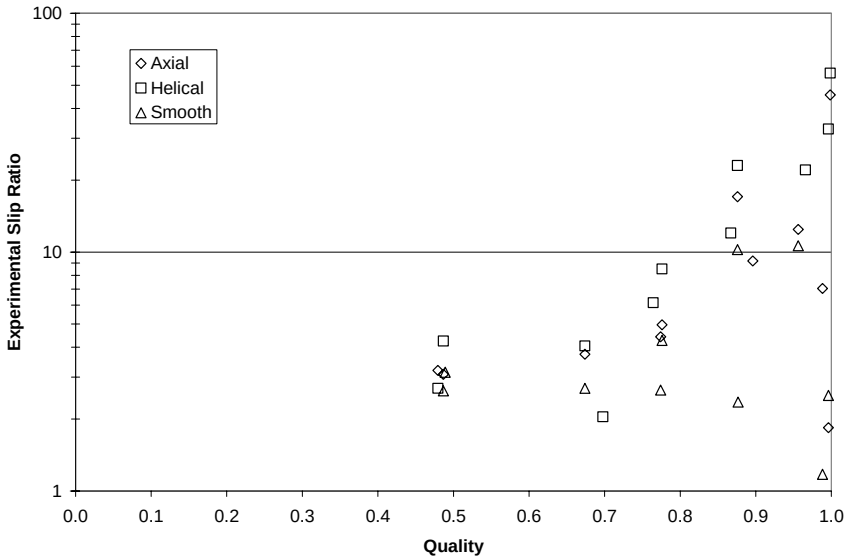

Figure 3.24. Experimental slip ratio on a logarithmic scale with respect to quality, separated by tube type for an R22/alkylbenzene mixture

3.3.3.4 Flow Visualization

As shown with the previous mixtures, a collection of flow visualization photographs is presented in Figure 3.25 for various mass fluxes and qualities. Though the number of pictures and various flow parameters is limited for this data set, it still provides a visible presence of oil during full operation. This presence appears at high mass fluxes and qualities, in Figures 3.25.*d* and 3.25.*e* as horizontal streaks, and can be seen as the majority of liquid in the liquid phase.

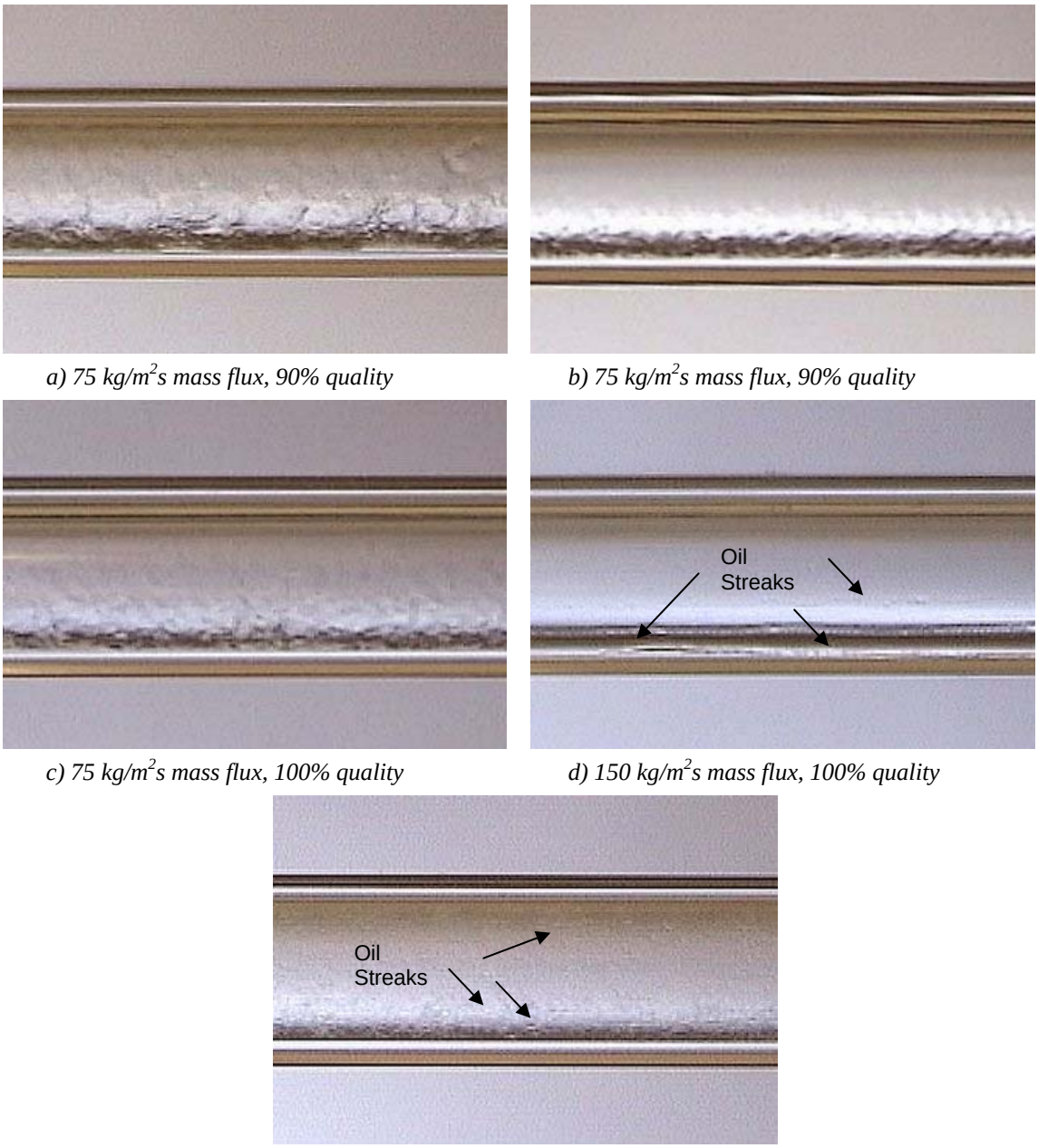

a) 75 kg/m^{2}s mass flux, 90% quality

b) 75 kg/m^{2}s mass flux, 90% quality

c) 75 kg/m^{2}s mass flux, 100% quality

d) 150 kg/m^{2}s mass flux, 100% quality

e) 300 kg/m^{2}s mass flux, 80% quality

Figure 3.25. Flow visualization photographs *(a)-(e)* of an R22/alkylbenzene mixture at various mass fluxes and qualities

3.3.4 R410A and Polyol Ester

The polyol ester lubricant used in this mixture has an average density of 965 kg/m^3, dynamic viscosity of 0.019 kg/m-s and kinematic viscosity of 1.97x10^{-5} m^2/s. Flow visualization results are not available for this mixture. The experimental apparatus operates in excess of 2000 kPa for this investigation, rendering use of the glass test section, sealed only with nylon ferrules, unfeasible.

3.3.4.1 Void Fraction

The ACRC, homogeneous and Zivi void fraction models are compared with experimental results for the R410A/POE mixture. This comparison is shown in Figure 3.26. Again, the homogeneous model shows the highest void fraction predictions and the ACRC model correlates well with experimental data. The experimental data separated by mass flux and tube type, respectively, follow in Figures 3.27 and 3.28.

Again, though slight, both mass flux and tube type are showing an influence on void fraction. Like the R134a/alkylbenzene and R22/alkylbenzene results, higher mass fluxes and the smooth test section give higher void fraction values.

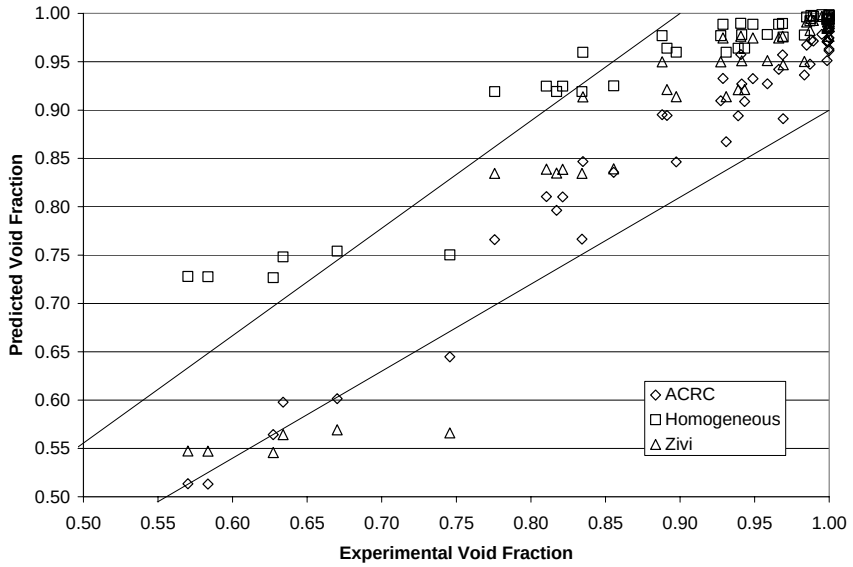

Figure 3.26. Comparison of void fraction models to experimental void fraction for an R410A/POE mixture with error lines of ±10%

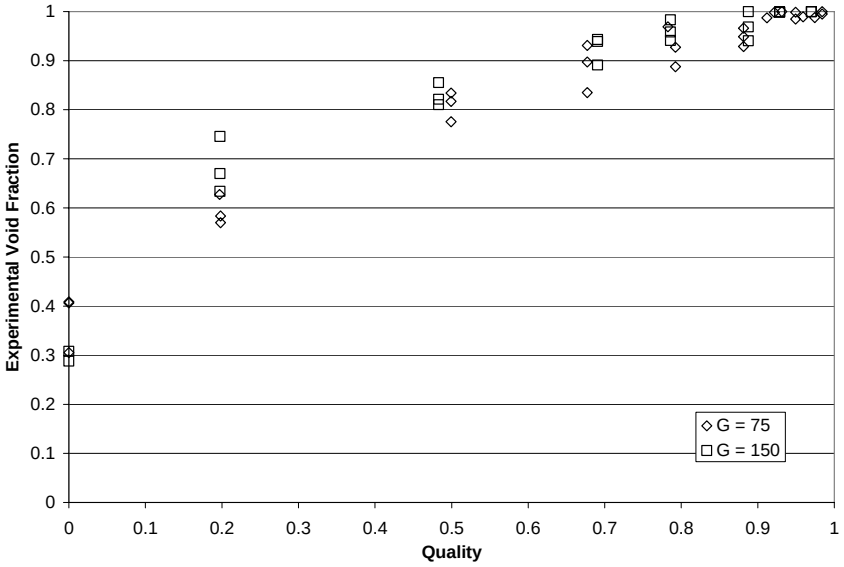

Figure 3.27. Experimental void fraction separated by mass flux (kg/m^2s) for an R410A/POE mixture

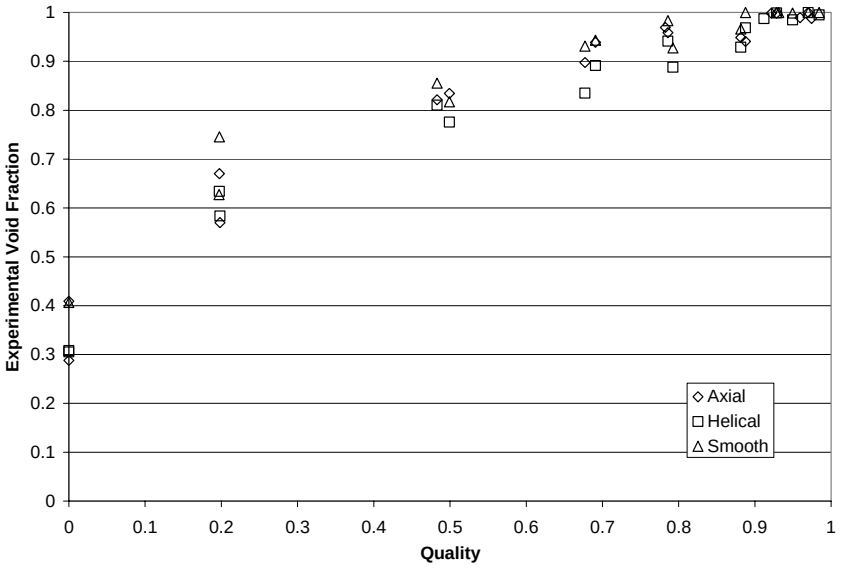

Figure 3.28. Experimental void fraction separated by tube type for an R410A/POE mixture

3.3.4.2 Oil Holdup

Figure 3.29 shows experimental oil holdup in grams per meter of the R410A/POE mixture separated by mass flux, and Figure 3.30 separates the data by tube type. Here mass flux has much less influence on oil holdup, while enhanced tubes still show higher oil holdup than smooth tubes.

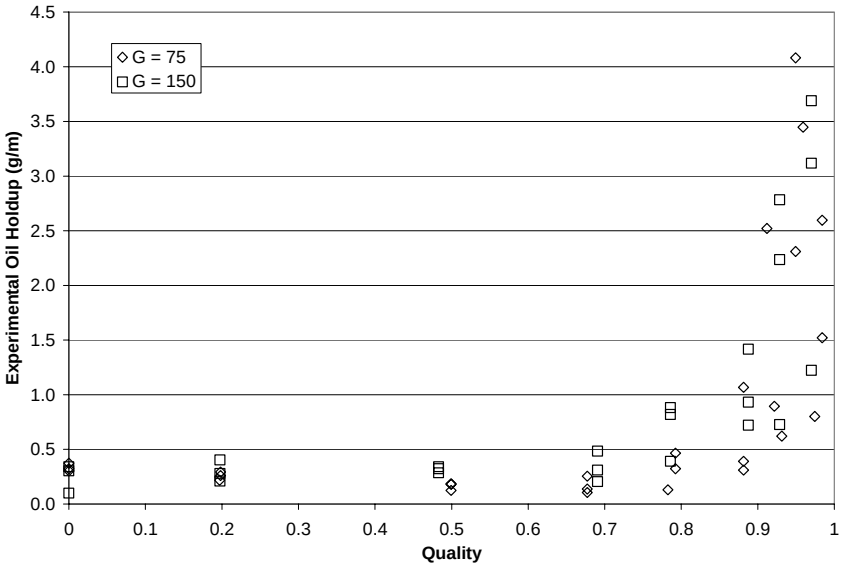

Figure 3.29. Experimental oil holdup for an R410A/POE mixture separated by mass flux (kg/m^2s)

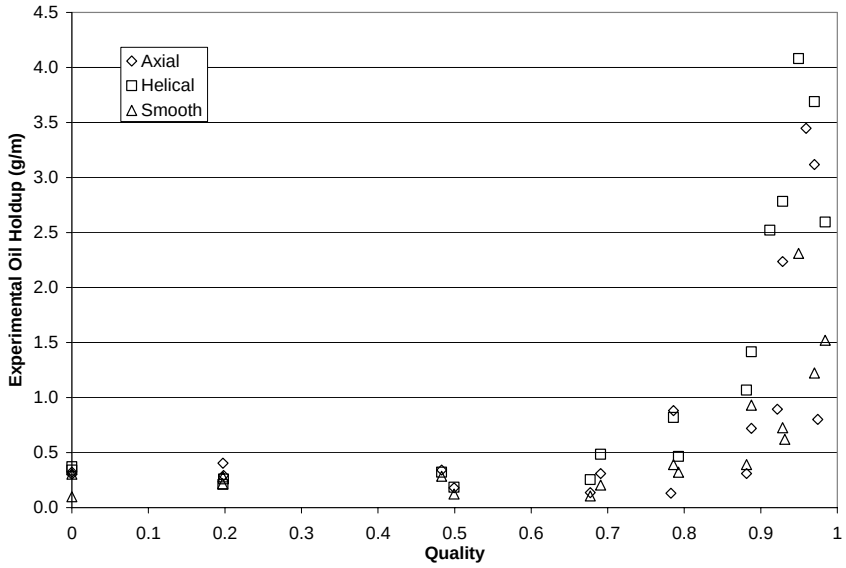

Figure 3.30. Experimental oil holdup for an R410A/POE mixture separated by tube type

3.3.4.3 Slip Ratio

Experimental slip ratio values are shown in Figures 3.31 and 3.32, separated by mass flux and tube type, respectively, for the R410A/POE mixture. Again increased mass flux shows a slight increase in slip ratio at high qualities, and enhanced tube types show an increase in slip ratio particularly at high qualities.

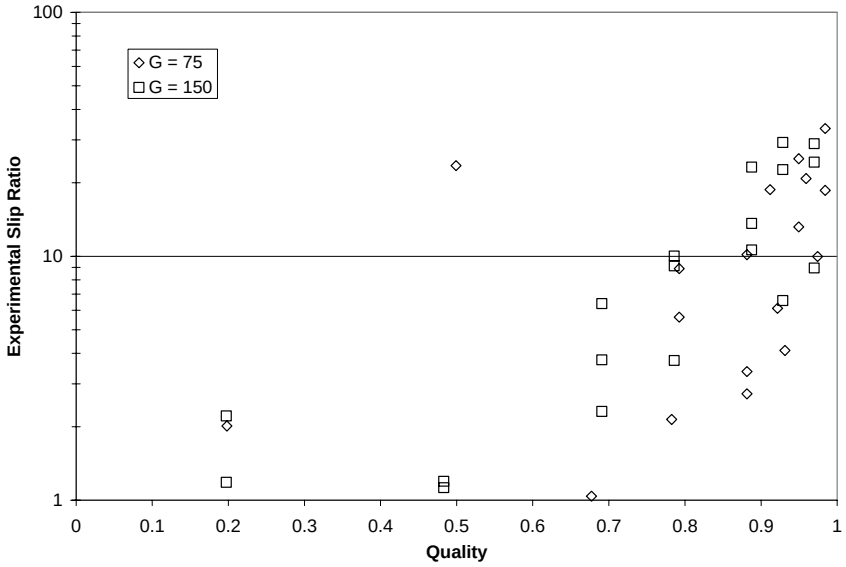

Figure 3.31. Experimental slip ratio on a logarithmic scale with respect to quality, separated by mass flux (kg/m^2s) for an R410A/POE mixture

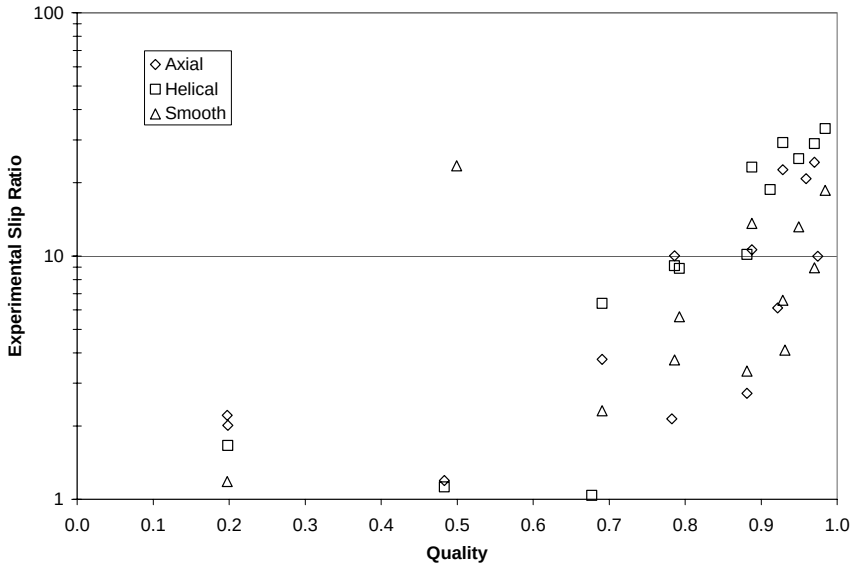

Figure 3.32. Experimental slip ratio on a logarithmic scale with respect to quality, separated by tube type for an R410A/POE mixture

3.4 Conclusions

3.4.1 Void Fraction

For all refrigerant-oil mixtures detailed in this chapter, a comparison is made between experimental void fraction values and those determined using the homogeneous, ACRC and Zivi models. All assessments show the closest correlation between experimental and the ACRC model, confirming the validity of its use in the rest of this investigation.

Recall, for the R134a/POE mixture void fraction was found to be slightly influenced by tube type with the smooth test section showing a higher value. However, mass flux was not found to be an influential factor in the high quality range.

The R134a/PAG results do not show a clear mass flux effect, however this can be attributed to the lack of data points at lower qualities where these effects are expected. Again, the smooth test section is showing higher void fraction values than the enhanced tubes.

Unlike the two previous mixtures, the R134a/alkylbenzene mixture does show a clear mass flux influence on void fraction due to testing lower qualities in addition to a tube type influence. Higher mass fluxes and the smooth test section give higher void fractions. Both the R22/alkylbenzene and R410A/POE mixtures follow suit, but to a lesser magnitude. The effect of mass flux and tube type is visible, but not considerably.

The general conclusion is that mass flux and tube type may both have an effect on void fraction. The effect of mass flux is less pronounced than that of tube type, but higher mass fluxes tend to show higher void fraction. Although for some of the refrigerant-oil mixtures the effect of tube type on void fraction is small, the effect is evident in all cases providing the conclusion that tube type does have an effect on void fraction with the smooth test section giving higher values. The one case where these effects are obvious is with the R134a/alkylbenzene mixture, an immiscible combination. Here, the oil failing to dissolve in the refrigerant is causing it to have a more influential

function. Therefore, the mass flux and tube type, each of which contributes to the flow of the oil, have a more significant impact on void fraction.

3.4.2 Oil Holdup

The most significant results found during the oil holdup investigation of the R134a/POE mixture include the parabolic trend and influences of mass flux and tube type. The oil holdup decreases from zero quality primarily due to a stretching of the liquid layer by the vapor's increased velocity. At mid-range qualities the holdup begins to increase when the viscosity of the oil starts dominating the behavior of the liquid fraction's flow. Lower mass fluxes are shown to give higher holdup values, particularly at the mid-range qualities, and the enhanced test sections are shown to increase the holdup as well. Tube type is shown to influence oil holdup principally at high qualities.

The results for the remaining mixtures vary. All combinations show the parabolic trend with low holdup at mid-range qualities and an increase at high qualities. The R134a/PAG and R134a/alkylbenzene mixtures show an influence of both mass flux and tube type, whereas the R22/alkylbenzene and R410A/POE mixtures only show the tube type influence clearly, and only at high qualities.

Like the void fraction results, not all refrigerant-oil mixtures show a clear oil holdup dependence on mass flux, however an effect cannot be ruled out for all cases. Similarly, the effect of tube type is clear for all data sets with the enhanced test sections, particularly the helical section, increasing the holdup results.

3.4.3 Slip Ratio

Slip ratio results are found to be affected minimally by mass flux and tube type in the study of the R134a/POE mixture. A lower mass flux shows a higher slip ratio, as do the enhanced test sections. These effects are indistinguishable below about 40 percent quality, and as expected, the slip ratio results increase with increasing quality.

The effect of mass flux on the remaining mixtures is less clear. For the R134a/PAG and R134a/alkylbenzene mixtures, mass flux does not show a significant trend. For the R22/alkylbenzene and R410A/POE mixtures it looks as though a higher mass flux results in a higher slip ratio, but only at high qualities. This directly contradicts the results found for the R134a/POE mixture.

The effect of tube type throughout the examinations is consistent. For all refrigerant-oil combinations an increase in slip ratio is observed for the enhanced test sections, particularly at high qualities. Like the oil holdup results, the helical test section followed by the axial has the most influence.

3.4.4 Flow Visualization

The R134a/PAG mixture video indicates the presence of the lubricant most clearly at high qualities and low mass fluxes with large and circumferential disturbances to the liquid layer, rather than the small and random disturbances of pure refrigerant. Essentially, the oil is altering the properties of the liquid layer and slightly laminarizes the flow. The presence is also visible, though, at high mass fluxes and 100% quality where a liquid layer remains. The R134a/alkylbenzene video shows the presence of oil in the same manner, but also as horizontal streaks where the surface wetting capabilities of the oil may have shifted and the lubricant fails to behave as a liquid film. Finally, the R22/alkylbenzene mixture did show repeated instances of visible oil. These instances are few due

to lack of video, but apparent in various forms. Again the non-wetting behavior creates horizontal oil streaks, but at high qualities and mass fluxes the presence of a liquid layer at 100% quality also indicates oil.

3.5 List of References

[1] Seeton, C. personal communication, ACRC, 2004

[2] Takaishi, Y., and K. Oguchi, "Measurements of Vapor Pressures of R-22/oil Solutions," *Proceedings of the XVIIIth International Congress of Refrigeration*, Vienna, Vol. B, pp. 217-222, 1987.

[3] Thome, J.R. and D. Phil, "A Comprehensive Thermodynamic Approach to Modeling Refrigerant-Lubricating Oil Mixtures," *International Journal of Heating, Ventilating, Air-Conditioning and Refrigerating Research*, Vol. 1, no. 2, pp. 110-125, 1995.

[4] Zivi, S.M. "Estimation of Steady-State Steam Void-Fraction by Means of the Principle of Minimum Entropy Production," *Transactions ASME, Journal of Heat Transfer*, Series C, Vol. 86, pp. 247-252, 1964.

Chapter 4. Oil Holdup Modeling and Analysis

4.1 Introduction

The R134a/POE data collected and reported in Chapter 2 is the basis for an empirical oil holdup model derived from a conservation of mass analysis. This model uses the calculated value of oil in the test section at the measured flowing oil concentration (assuming liquid fills the tube) to predict the amount of oil held up at a given quality and void fraction. This model uses the tube's liquid volume fraction to determine the oil holdup, which can be assumed a reasonable model for the lower qualities where oil effects do not significantly contribute to the flow field.

For the higher qualities it is expected that the viscous oil film will have a significant effect on the flow conditions and therefore increase the oil holdup in that range. A second prediction model is presented, formulated using the Blasius turbulent flow formula for predicting the interfacial shear stress between liquid and vapor phases. Both of these models are detailed and compared to each refrigerant-oil mixture.

4.2 Modeling

4.2.1 Liquid Volume Fraction Model Derivation

The derivation of the liquid volume fraction model begins with the conservation of mass.

$$\dot{m}_{ox} = \rho_{ox} A_{ox} V_{lx} = \rho_l A_l V_l c_o = \text{constant} \tag{4.1}$$

where $\dot{m}_{ox}$ is the oil flow rate, ρ_o is oil density, A_{ox} is the oil cross sectional area, V_{lx} is the liquid phase velocity, ρ_l is the liquid density for zero quality, $A_l = A_{tot}$ is the total tube cross sectional area for zero quality, V_l is the liquid mixture velocity for zero quality and c_o is the oil concentration. Here, $\rho_l A_l V_l$ is equal to $\dot{m}_{tot}$, the total mass flow rate of refrigerant and oil. This assumes that the liquid density is the linear average of refrigerant and oil liquid densities.

The oil mass per unit length is given as

$$\frac{m_{ox}}{L} = \rho_o A_{ox} \tag{4.2}$$

From Equation 4.1,

$$A_{ox} = \frac{\dot{m}_{tot}\, c_o}{\rho_o V_{lx}} \tag{4.3}$$

Substituting this into Equation 4.2 gives

$$\frac{m_{ox}}{L} = \frac{\dot{m}_{tot}\, c_o}{V_{lx}} \tag{4.4}$$

Also,

$$\dot{m}_{lx} = \rho_{lx} A_{lx} V_{lx} \tag{4.5}$$

By substituting for V_{lx}, Equation 4.4 can be reduced to

$$\frac{m_{ox}}{L} = \frac{\rho_{lx} A_{lx} \dot{m}_{tot}\, c_o}{\dot{m}_{lx}} \tag{4.6}$$

Because the ratio of $\dot{m}_{lx}$ to $\dot{m}_{tot}$ is equal to (1 - x_o) and the ratio of A_{lx} to A_{tot} is (1 - α),

$$\frac{m_{ox}}{L} = \frac{\rho_{lx}(1-\alpha) c_o A_{tot}}{(1-x_o)}, \tag{4.7}$$

where ρ_{lx} is the liquid phase density, A_{lx} is the refrigerant liquid phase cross sectional area and x_o is oil-based quality. However, the oil quality can be given by

$$x_o = x(1-c_o), \tag{4.8}$$

which gives

$$\frac{m_{ox}}{L} = \frac{\rho_{lx}(1-\alpha) c_o A_{tot}}{1-[x(1-c_o)]} \tag{4.9}$$

Finally, defining the oil holdup per unit length in the liquid feed line as

$$\frac{m_{ox}}{L} = \rho_{lx} c_o A_{tot} \tag{4.10}$$

allows for the oil mass per unit length to be written as

$$\frac{m_{ox}}{L} = \left(\frac{m_o}{L}\right)\frac{(1-\alpha)}{1-[x(1-c_o)]} \tag{4.11}$$

The model gives the oil holdup per unit length as

$$\frac{m_{ox}}{L} = \frac{m_o}{L}\left(\frac{1-\alpha}{1-x}\right), \tag{4.12}$$

assuming the oil concentration is small. The void fraction value used in this model is the ACRC void fraction as detailed in Chapter 2, but using the mixture density defined by Equation 3.4 and the following liquid mixture viscosity rather than pure refrigerant properties.

$$\mu_m = w_{oil}\mu_o + (1-w_{oil})\mu_l \tag{4.13}$$

Here, w_{oil} is the oil mass fraction, μ_o is the oil viscosity and μ_l is the liquid refrigerant viscosity.

4.2.2 Viscous Film Model Derivation

The viscous film model assumes an interfacial shear between the refrigerant liquid and vapor phases, and uses the Blasius formula for turbulent flow in smooth tubes as a basis. Figure 4.1 below illustrates flow in a pipe, where vapor travels through the center of the pipe (diameter D) with velocity V_v, and oil with thickness h travels along the inner diameter of the pipe with an interface velocity V_i. The oil film is assumed to have a linear profile, and along the length L of the pipe there occurs a pressure drop ΔP.

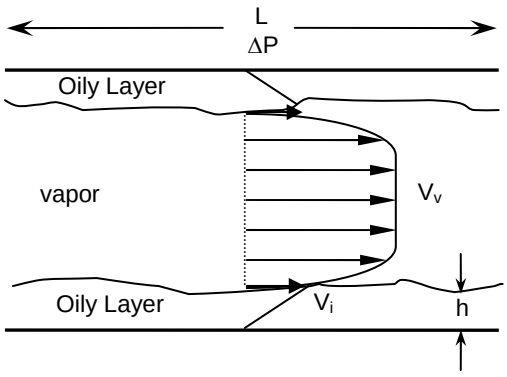

Figure 4.1. Two phase flow in a pipe including the presence of oil with film thickness h

The pressure drop in a pipe is defined as

$$\Delta P = f\,\frac{L}{D}\frac{1}{2}\rho V^2, \tag{4.14}$$

where the friction factor *f* is defined by Blasius as

$$f = 0.316\,\mathrm{Re}_D^{-0.25} \tag{4.15}$$

Accounting for the oil film thickness, phase velocities and substituting the Reynolds number gives the following relationship.

$$0.316\left[\frac{\left(V_v - V_i\right)\left(D-h\right)}{v_l}\right]^{-0.25} = \frac{2\Delta P\left(D-2h\right)}{\rho\left(V_v - V_l\right)^2 L} \tag{4.16}$$

Solving this relationship for pressure drop and simplifying gives

$$\Delta P = 0.158\left(\frac{\rho_v^{0.75} V_v^{1.75} L \mu_v^{0.25}}{D^{1.25}}\right) \tag{4.17}$$

Furthermore, the force balance of shear stress and pressure is

$$F = \left(\Delta P\right) A_{cs} = \tau_w A_s \tag{4.18}$$

$$\Delta P\left(\pi\frac{D^2}{4}\right) = \tau_w\left(\pi D L\right), \tag{4.19}$$

where the wall shear stress, assuming the wall film is laminar flow with a linear velocity profile, is

$$\tau_w = \mu_l\left(\frac{V_i}{h}\right) \tag{4.20}$$

Solving Equation 4.19 for ΔP using the wall shear stress results in

$$\Delta P = \left(\frac{4L\mu_l}{D}\right)\left(\frac{V_i}{h}\right) \tag{4.21}$$

Equating Equations 4.17 and 4.21 and solving for the quantity *hD* gives

$$\left(hD\right) = \frac{4\mu_l V_i D^{1.25}}{\left(0.158\right)\rho_v^{0.75} V_v^{1.75} \mu_v^{0.25}} \tag{4.22}$$

This quantity is important because the liquid mass per length of tube (including refrigerant and oil) can be defined as

$$\frac{m_l}{L} = \rho_l \pi D h \tag{4.23}$$

The mass flow rates of the liquid and vapor, accounting for the varying area with film thickness, are given by,

$$\dot{m}_l = \rho_l A_l V_l = \rho_l \pi \left(Dh - h^2 \right) \left(\frac{V_i}{2} \right) \tag{4.24}$$

$$\dot{m}_v = \rho_v A_v V_v = \rho_v \left[\frac{\pi \left(D - 2h \right)^2}{4} \right] V_v \tag{4.25}$$

but can also be defined in terms of mass flux and quality as follows.

$$\dot{m}_l = \left(1 - x \right) G A_l \tag{4.26}$$

$$\dot{m}_v = x G A_v \tag{4.27}$$

Equating the liquid and vapor mass flow rates and solving for the respective velocities gives the velocities in terms of mass flux and quality. Substituting these relationships into Equation 4.22 and simplifying produces

$$\left(hD \right) = \left(\frac{\rho_v}{\rho_l} \right) \left(\frac{2}{0.158} \right) \left(\frac{4 D^{1.25} \mu_l}{\mu_v^{0.25}} \right) \left(\frac{\left(1 - x \right)}{x^{1.75} G^{0.75}} \right) \tag{4.28}$$

Now, the liquid mass holdup from Equation 4.23 is given by

$$\frac{m_l}{L} = \pi \left(\frac{4}{0.316} \right) \left(\frac{\rho_l \rho_v 4 D^{1.25} v_l \left(1 - x \right)}{\mu_v^{0.25} x^{1.75} G^{0.75}} \right) \tag{4.29}$$

Finally, the oil holdup per length of tube in kg/m is defined as

$$\frac{m_{oil}}{L} = \left(\frac{m_l}{L} \right) \left(\frac{\dot{C}_o}{1 - x} \right), \tag{4.30}$$

where $\dot{x}$ is the vapor mass flow rate to total mass flow rate and $\dot{C}_o$ is the oil mass flow rate to the total mass flow rate.

4.2.3 Model Coalescence

The liquid volume fraction model is a good representation of the holdup in the low to mid-range quality spectrum where oil effects are minimal. It does not, however, account for viscous films, making it an incorrect model for the high quality range. In fact, the increase in oil holdup prediction at the high qualities for this model is due to a mathematical artifact rather than the physics of the flow. Referring to Equation 4.12, as the quality nears about 80%, the quality goes to one more quickly than void fraction goes to one, giving the model the appearance of following the correct increasing holdup trends. Data for the R134a/polyol ester mixture is shown in Figure 4.2 with only the liquid volume fraction model to illustrate this behavior. Conversely, the viscous film model is a physically correct representation of the high quality range, but explodes as quality goes to zero, again because of a mathematical artifact (refer to Equation 4.29).

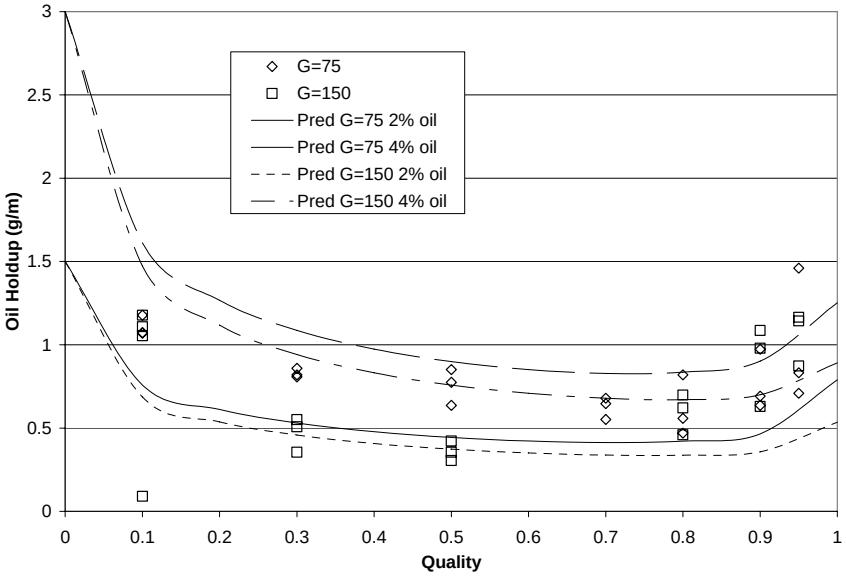

Figure 4.2. Liquid volume fraction prediction model compared with R134a/POE data, separated by mass flux (kg/m^2s) and oil concentration

The minimum holdup predicted by the liquid volume fraction model is consistently around 70% for various mass fluxes and oil concentration. Therefore, this quality is the assumed transition point between the liquid volume fraction model and the viscous film model.

Figure 4.3 shows the two models for a mass flux of 75 kg/m^2s and 5% oil concentration for the R134a/polyalkylene glycol mixture. The viscous film model shows the correct trend, but predicts holdup values an order of magnitude too large. One physical explanation for this behavior is the assumption of smooth tubes in order to use the Blasius formula. If enhanced tubes are considered, the friction factor would increase and the model would result in lower prediction values.

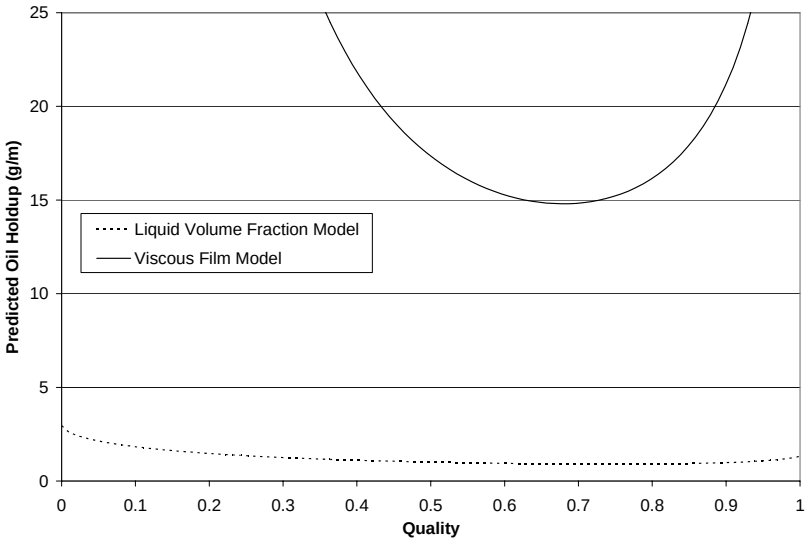

Figure 4.3. Oil holdup prediction models, not scaled, for an R134a/PAG mixture at a mass flux of 75 kg/m^2s and 5% oil concentration by mass

In order to merge the two models a multiplying factor, $\mathcal{M}$, is applied to the original viscous film model predictions. This multiplier is found by taking the ratio of the liquid volume fraction model to the viscous film model at 70% quality. The multiplier is a function of mass flux, G, and differs with the refrigerant, oil and oil concentration, c_o, being tested. The multipliers used for this investigation ranged from 0.62 to 1.0 and the functions are tabulated below. These functions are calculated using model predictions for one and five percent oil concentrations, and are used for predictions within this range.

The resulting models for the R134a/polyalkylene glycol mixture using the multiplier are shown in Figure 4.4. For the remainder of this study, the liquid volume fraction model will be utilized for qualities less than 70%, the viscous film model will be utilized for qualities greater than 70%, and the combination of the two will be referred to as a single oil holdup prediction model.

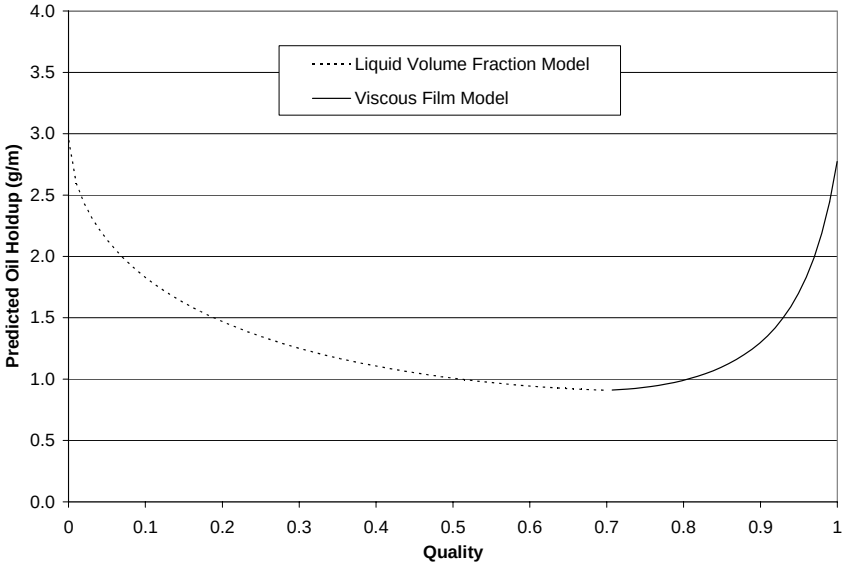

Figure 4.4. Oil holdup prediction model, a coalescence of the liquid volume fraction model and viscous film model, for an R134a/PAG mixture at a mass flux of 75 kg/m^{2}s and 5% oil concentration by mass

Table 4.1. Viscous film model multiplier as a function of mass flux and oil concentration for various refrigerant-oil mixtures and oil concentrations

Refrigerant/Oil	$\mathcal{M}$
R134a/POE	$(-0.006c_o + 0.0035)G - 0.1211c_o + 0.7589$
R134a/PAG	$(-0.0002c_o + 0.0012)G - 0.0427c_o + 0.2598$
R134a/alkylbenzene	$(-0.0003c_o + 0.0019)G - 0.0665c_o + 0.4111$
R22/alkylbenzene	$(-0.0003c_o + 0.0017)G - 0.0652c_o + 0.4015$
R410A/POE	$(-0.0005c_o + 0.0028)G - 0.1265c_o + 0.7802$

4.3 Results

4.3.1 R134a and Polyol Ester

A comparison of the combined model to the R134a/POE data is shown in Figures 4.5 and 4.6 (results figures are given at the end of the chapter). All of the data shown for this mixture have a measured oil concentration between 2% and 4%.

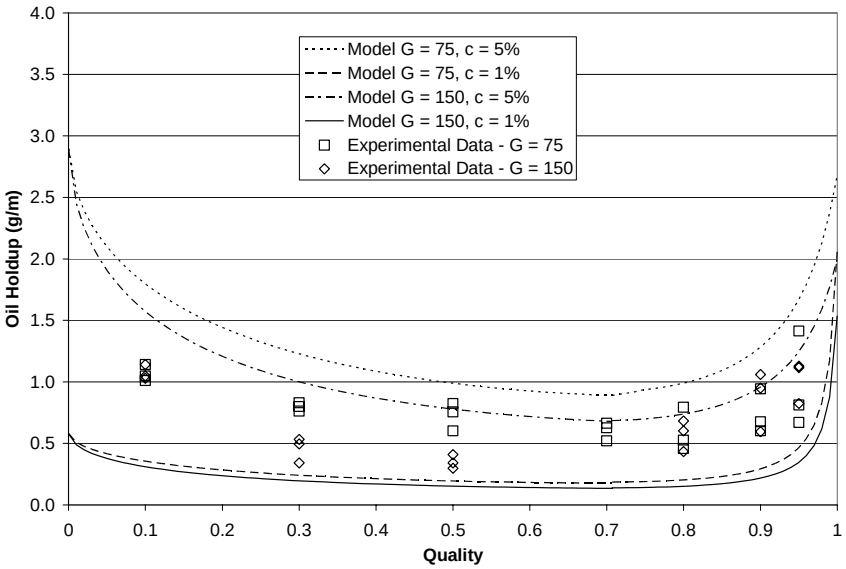

Figure 4.5. Experimental data for the R134a/POE mixture, separated by mass flux (kg/m^2s) in comparison to the holdup model

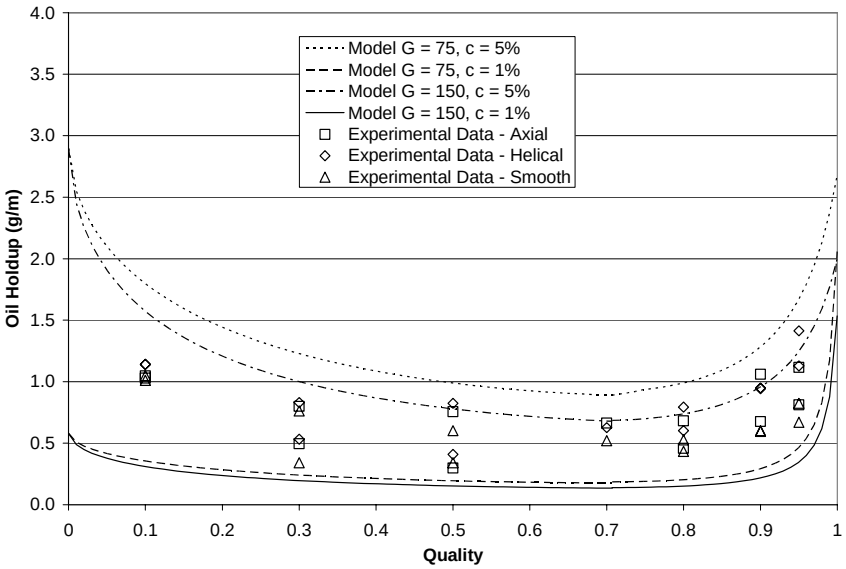

Figure 4.6. Experimental data for the R134a/POE mixture, separated by tube type in comparison to the holdup model

4.3.2 R134a and Polyalkylene Glycol

Experimental data for the R134a/PAG mixture is plotted against the holdup model in Figures 4.7 and 4.8. Note that the points that fall an extreme distance over or under the predictions are the points with measured oil

concentrations up to 15% or below 1%. Figures 4.9 and 4.10 constrain the data presented to those with measured oil concentrations between 1% and 5% to correspond to the models shown.

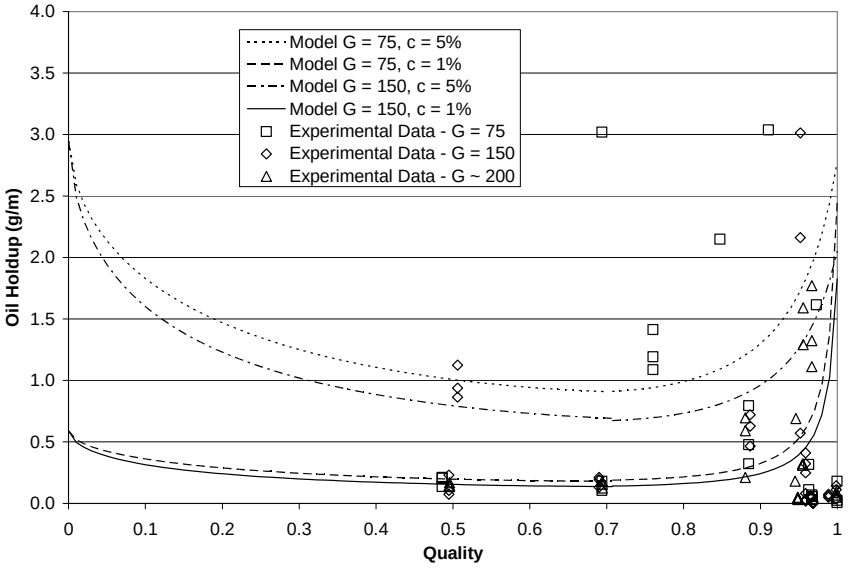

Figure 4.7. Experimental data for the R134a/PAG mixture, separated by mass flux (kg/m^2s) in comparison to the holdup model

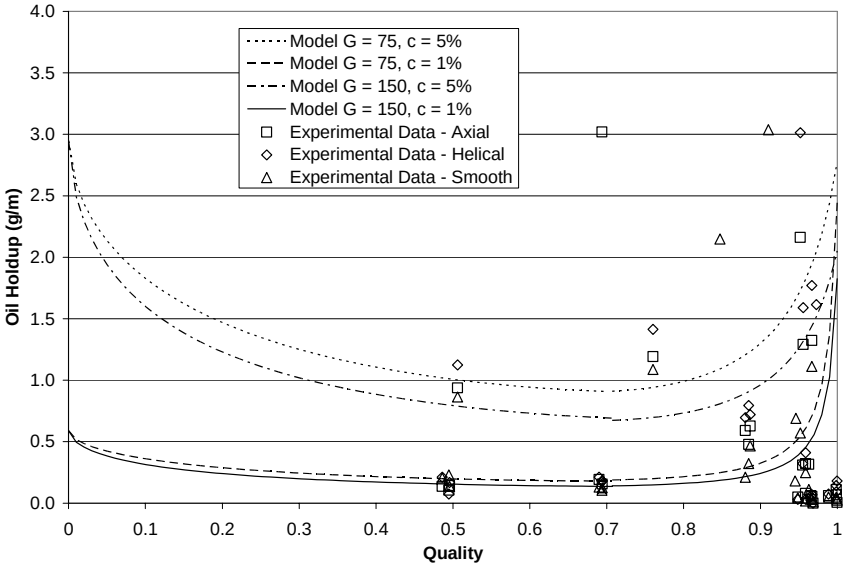

Figure 4.8. Experimental data for the R134a/PAG mixture, separated by tube type in comparison to the holdup model

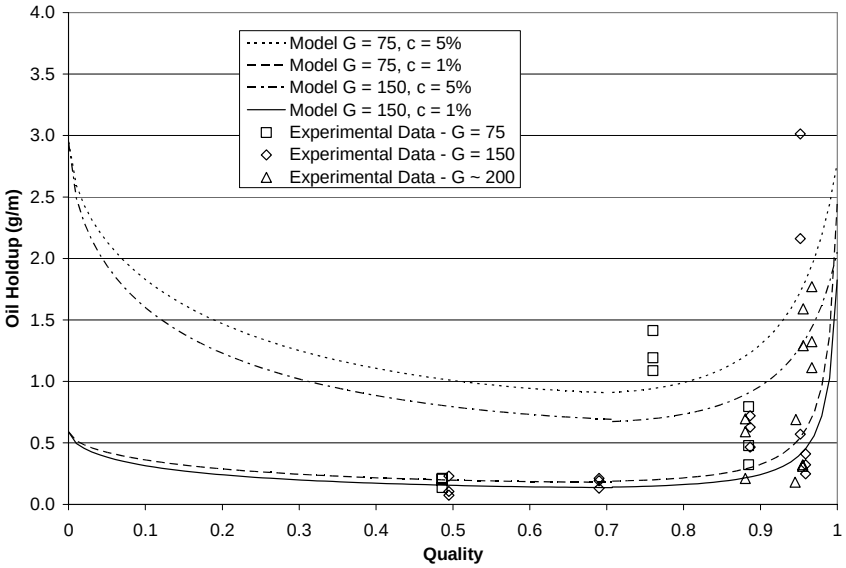

Figure 4.9. Experimental data between 1% and 5% oil concentration for the R134a/PAG mixture, separated by mass flux (kg/m^2s) in comparison to the holdup model

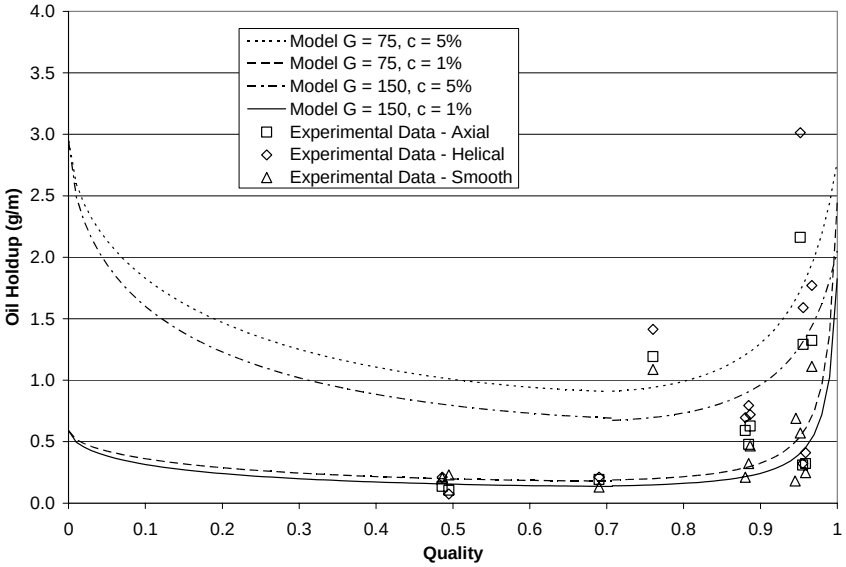

Figure 4.10. Experimental data between 1% and 5% oil concentration for the R134a/PAG mixture, separated by tube type in comparison to the holdup model

4.3.3 R134a and Alkylbenzene

Experimental results for the R134a/alkylbenzene mixture are plotted with the holdup model in Figures 4.11 and 4.12. All collected data is presented in these figures. To correspond to the models shown, Figures 4.13 and 4.14 present only R134a/alkylbenzene data with measured oil concentrations between 1% and 5%.

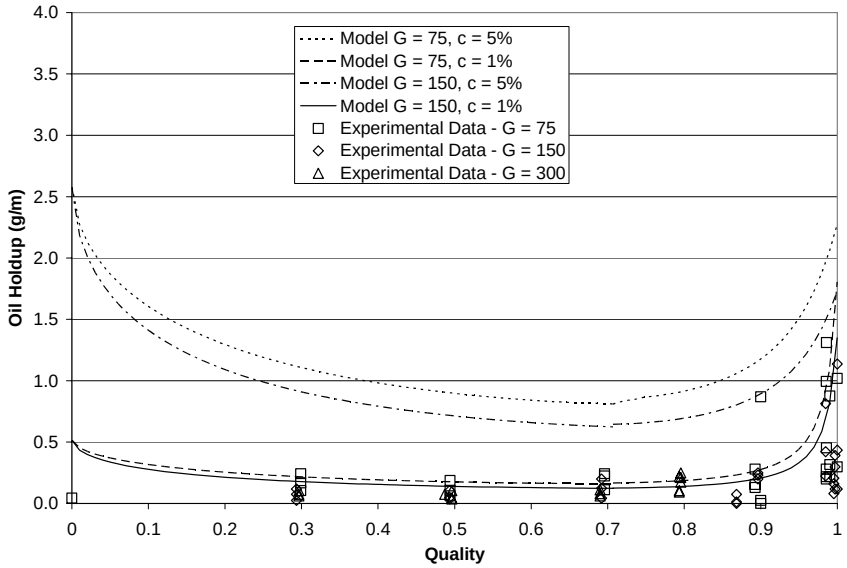

Figure 4.11. Experimental data for the R134a/alkylbenzene mixture, separated by mass flux (kg/m^{2}s) in comparison to the holdup model

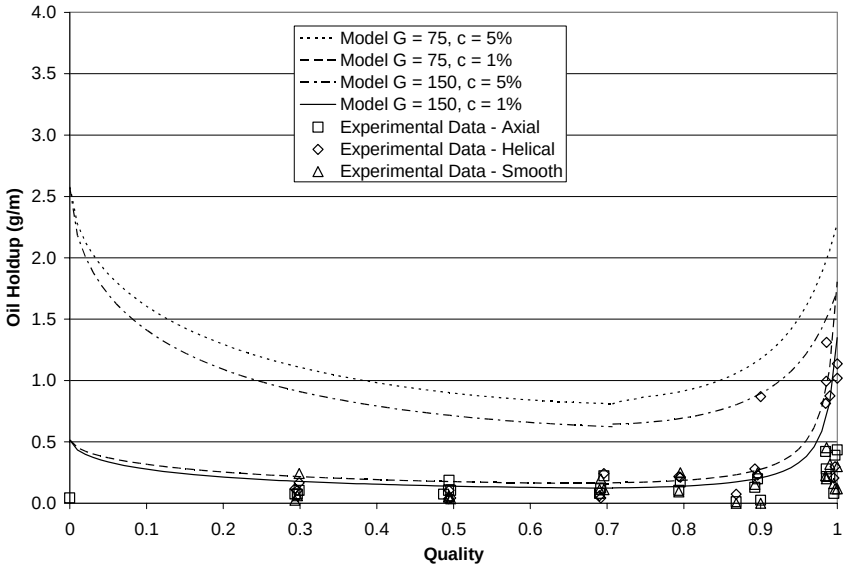

Figure 4.12. Experimental data for the R134a/alkylbenzene mixture, separated by tube type in comparison to the holdup model

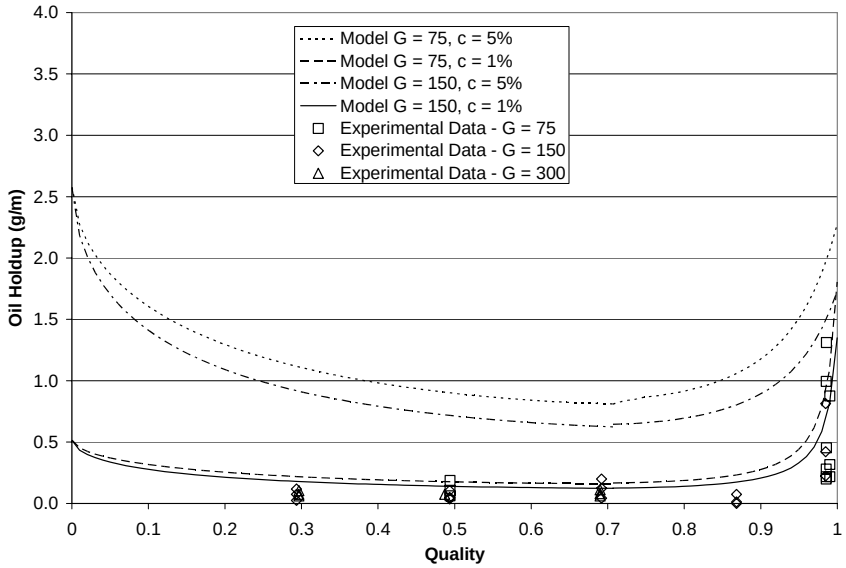

Figure 4.13. Experimental data between 1% and 5% oil concentration for the R134a/alkylbenzene mixture, separated by mass flux (kg/m^{2}s) in comparison to the holdup model

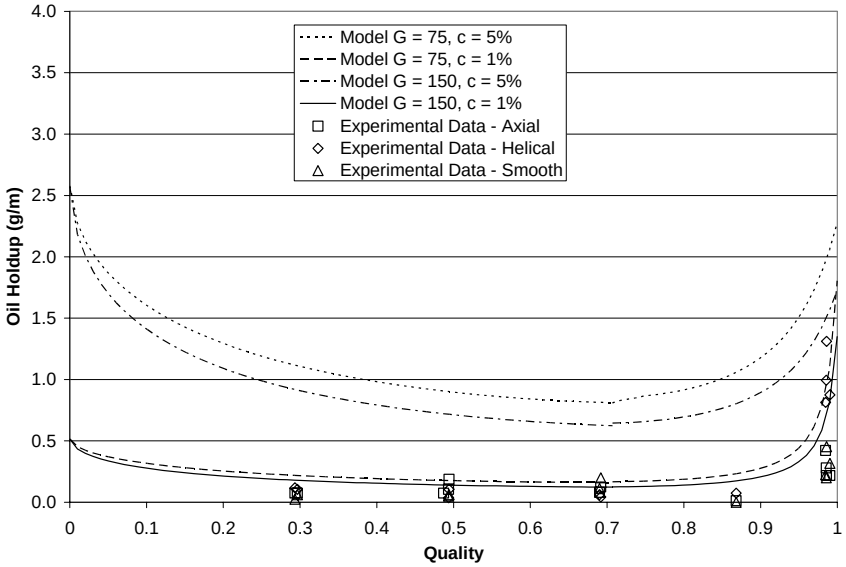

Figure 4.14. Experimental data between 1% and 5% oil concentration for the R134a/alkylbenzene mixture, separated by tube type in comparison to the holdup model

4.3.4 R22 and Alkylbenzene

All experimental results for the R22/alkylbenzene mixture are plotted with the holdup model in Figures 4.15 and 4.16. Figures 4.17 and 4.18 show only those data with measured oil concentrations between 1% and 5%.

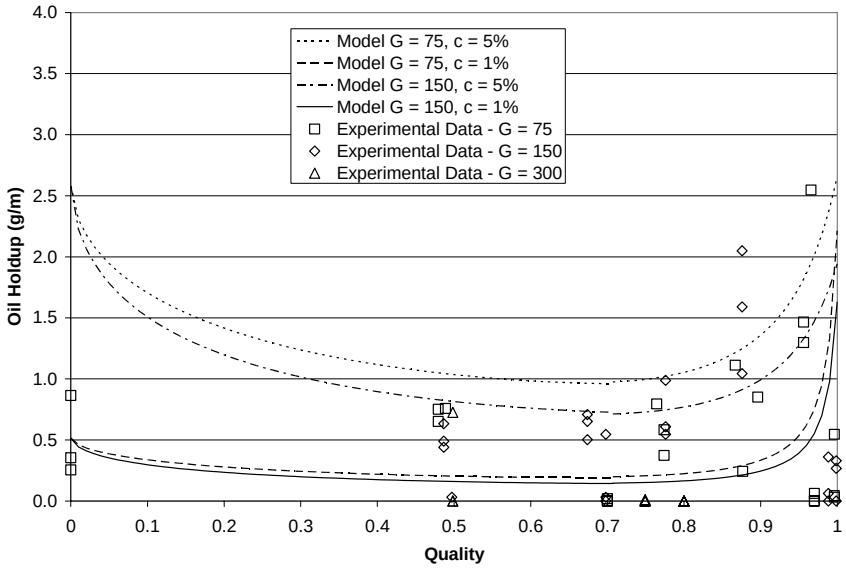

Figure 4.15. Experimental data for the R22/alkylbenzene mixture, separated by mass flux (kg/m^{2}s) in comparison to the holdup model

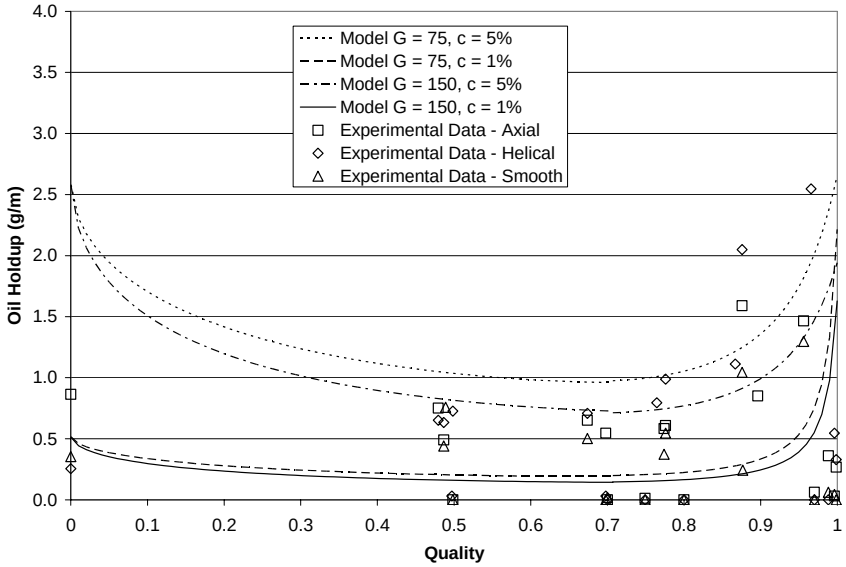

Figure 4.16. Experimental data for the R22/alkylbenzene mixture, separated by tube type in comparison to the holdup model

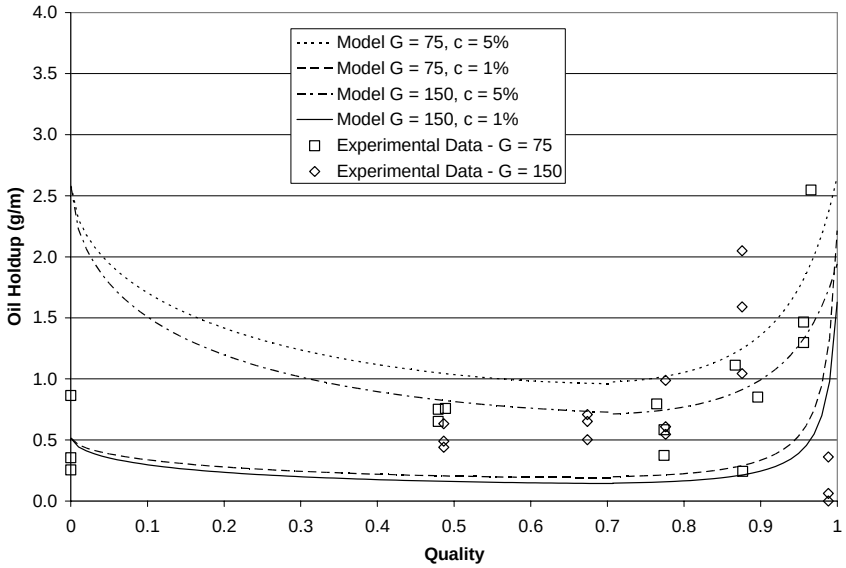

Figure 4.17. Experimental data between 1% and 5% oil concentration for the R22/alkylbenzene mixture, separated by mass flux (kg/m^{2}s) in comparison to the holdup model

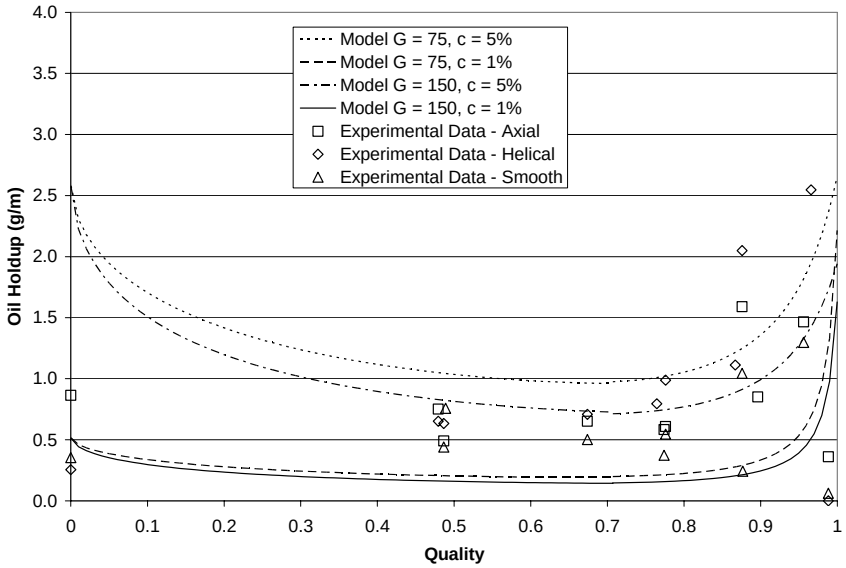

Figure 4.18. Experimental data between 1% and 5% oil concentration for the R22/alkylbenzene mixture, separated by tube type in comparison to the holdup model

4.3.5 R410A and Polyol Ester

All experimental data for the R410A/POE mixture are plotted with the holdup model in Figures 4.19 and 4.20. Figures 4.21 and 4.22 show only those data with measured oil concentrations between 1% and 5%.

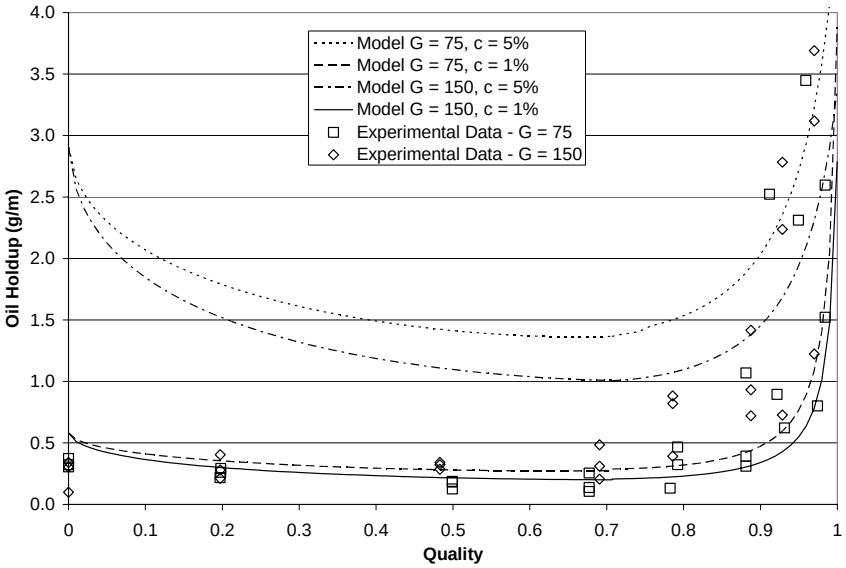

Figure 4.19. Experimental data for the R410A/POE mixture, separated by mass flux (kg/m^2s) in comparison to the holdup model

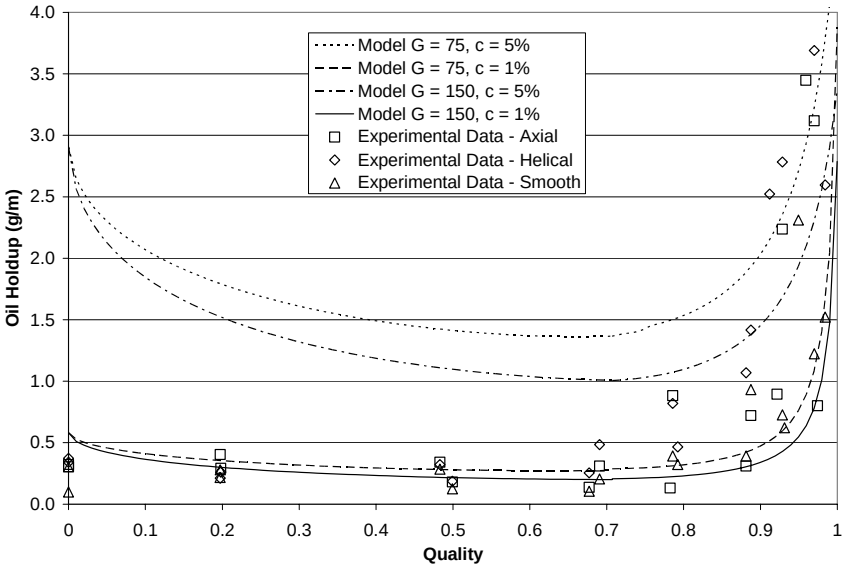

Figure 4.20. Experimental data for the R410A/POE mixture, separated by tube type in comparison to the holdup model

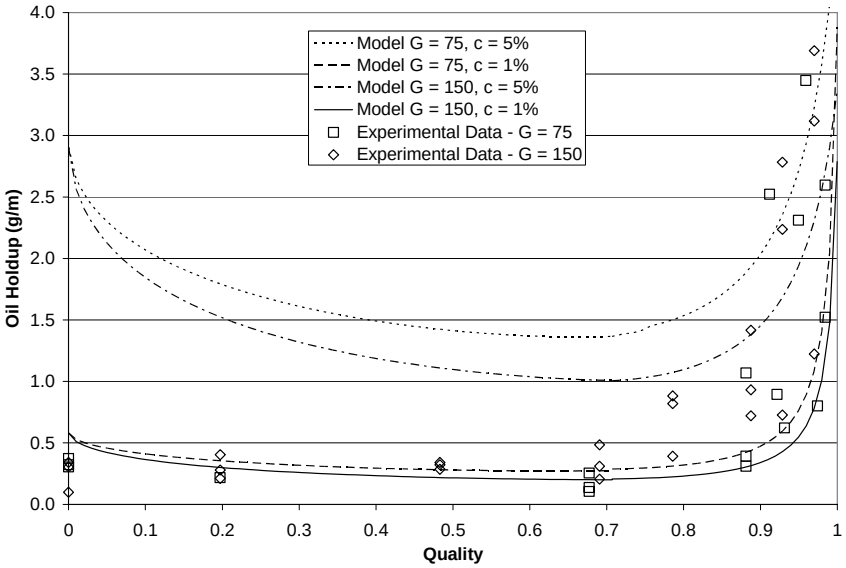

Figure 4.21. Experimental data between 1% and 5% oil concentration for the R410A/POE mixture, separated by mass flux (kg/m^{2}s) in comparison to the holdup model

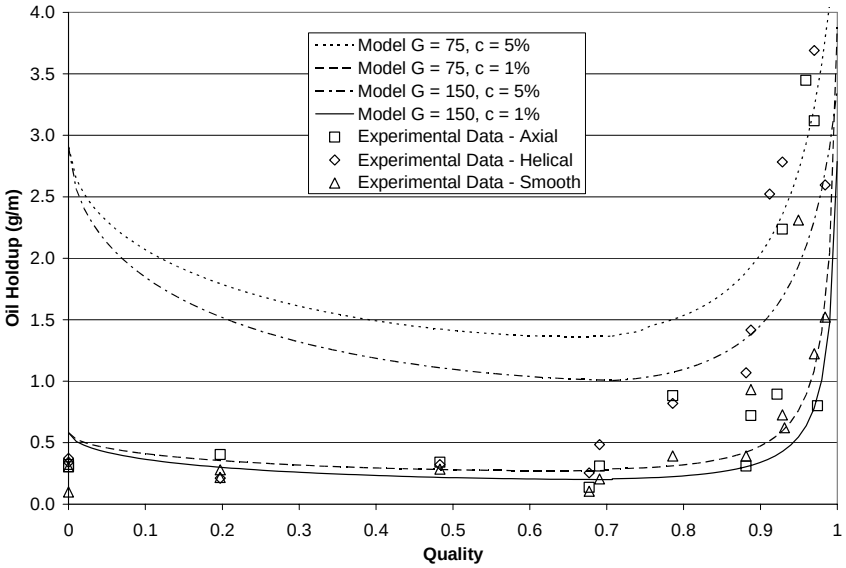

Figure 4.22. Experimental data between 1% and 5% oil concentration for the R410A/POE mixture, separated by tube type in comparison to the holdup model

4.4 Conclusions

As can be seen from the previous section, not only does the data for all refrigerant-oil mixtures follow the same oil holdup trends, but the model, composed of a liquid volume fraction region and a viscous film region, predicts holdup well in each case. The most deviation following the truncation of data points outside the oil concentration range of the shown model predictions occurs in the R134a/alkylbenzene data set. The most reasonable explanation for this behavior is due to alkylbenzene oil being immiscible in R134a refrigerant, where mixture properties are not accurately predictable at all flow conditions.

Additionally, the model and the experimental data, with the exception of the R134a/alkylbenzene mixture, are at a magnitude in the high quality range where groove effects seem to be primarily "hiding" the oil between the fins. The volume of the grooves in the enhanced test sections, along with the various oil densities, gives a base holdup of 2.0-2.5 g/m for oil occupying this space. The immiscible mixture experimental results show lower holdup because the oil and refrigerant do not dissolve together and the oil is less dense than the refrigerant causing it to float more and have less opportunity to build up between the fins.

Chapter 5. Concluding Remarks

5.1 Experimental Results

5.1.1 R134a and Polyol Ester

5.1.1.1 Void Fraction

The void fraction results, as expected, increase with increasing quality. Mass flux does not seem to have an influence on void fraction, whereas results show a slight dependence on tube type. An increase in void fraction is visible with the smooth test section. Oil concentrations also do not influence void fraction results. The only results that do not agree with previous work are those of void fraction separated by mass flux. Graham [1] and Kopke [2] found higher mass fluxes producing higher void fractions.

The void fraction results calculated using the procedure described in Chapter 1 are compared to the ACRC void fraction model using pure refrigerant properties and three sets of mixture properties detailed in the literature review. These results show agreement to within ±10% for all tube types and all oil concentrations. This implies, for the current study, that correction for the liquid void fraction due to the addition of oil provides little improvement to the model. It also indicates oil to have insignificant influence on refrigerant charge prediction.

5.1.1.2 Oil Holdup

Evident from the oil holdup data is the sensitivity of holdup to quality, mass flux, tube type and oil concentration. The following trends are observed:

1) At mid-range qualities, the oil holdup reaches a minimum. Stretching of the liquid layer by the vapor's increased velocity is the primary effect causing the reduction of oil holdup.
2) As higher qualities are reached, oil holdup increases as the viscosity of the oil begins to dominate the liquid fraction's flow. Significant effects are observed as quality moves beyond 90%, indicating the beginning of oil logging.
3) Some effects due to mass flux are observed with lower mass fluxes (75 kg/m^2s) displaying higher levels of oil holdup
4) Minimal effects of tube surface (smooth versus enhanced) on oil holdup are observed for adiabatic conditions from low to mid-range qualities.
5) Surface structure causes higher oil holdup and oil logging as high quality ranges are reached.
6) At low qualities, the oil in the refrigerant tends toward the limit of zero quality in which the amount of oil is determined by the "flow concentration" of oil in the system.

5.1.1.3 Slip Ratio

Slip ratio results also show an expected increase with increasing quality. Mass flux and tube type are found to have a minimal influence on slip ratio, but an influence none the less. This effect, however, is indistinguishable below about 40% quality. Lower mass fluxes and enhanced tubes show higher slip ratio values. Intuitively this makes sense because lower mass fluxes have a lower shear between the liquid and vapor phases, resulting in more slip and a higher slip ratio. Finally, oil concentration is seen to have no effect on slip ratio results.

5.1.1.4 Flow Visualization

At low mass fluxes and qualities oil can be seen moving on the flow visualization test section, while not affecting the flow conditions. At higher mass fluxes and qualities, when annular behavior is present, oil is not visible and does not exhibit any visible influence on the flow conditions, which progresses through common flow patterns.

5.1.2 Remaining Refrigerant-Oil Mixtures

5.1.2.1 Void Fraction

For all remaining refrigerant-oil mixtures, a comparison is made between experimental void fraction values and those determined using the homogeneous, ACRC and Zivi models. All assessments show the closest correlation between experimental and the ACRC model, confirming the validity of its use in this investigation.

Recall, for the R134a/POE mixture void fraction was found to be slightly influenced by tube type with the smooth test section showing a higher values. However, mass flux was not found to be an influential factor in the high quality range.

The R134a/PAG results do not show a clear mass flux effect, however this can be attributed to the lack of data points at lower qualities where these effects are expected. Again, the smooth test section is showing higher void fraction values than the enhanced tubes.

Unlike the two previous mixtures, the R134a/alkylbenzene mixture does show a clear mass flux influence on void fraction, as well as a tube type influence. Higher mass fluxes and the smooth test section give higher void fraction. Both the R22/alkylbenzene and R410A/POE mixtures follow suit, but to a lesser magnitude. The effect of mass flux and tube type is visible, but not considerably.

The general conclusion is that mass flux and tube type may both have an effect on void fraction. The effect of mass flux is less pronounced than that of tube type, but higher mass fluxes tend to show higher void fraction. Although for some of the refrigerant-oil mixtures the effect of tube type on void fraction is small, the effect is evident in all cases providing the conclusion that tube type does have an effect on void fraction with the smooth test section giving higher values. The one case where these effects are obvious is with the R134a/alkylbenzene mixture, an immiscible combination. Here, the oil failing to dissolve in the refrigerant is causing it to have a more influential function. Therefore, the mass flux and tube type, which each contribute to the flow of the oil, have a more significant impact on void fraction.

5.1.2.2 Oil Holdup

The most significant results found during the oil holdup investigation of the R134a/POE mixture include the parabolic trend and influences of mass flux and tube type. The oil holdup decreases from zero quality primarily due to a stretching of the liquid layer by the vapor's increased velocity. At mid-range qualities the holdup begins to increase when the viscosity of the oil starts dominating the behavior of the liquid fraction's flow. Lower mass fluxes are shown to give higher holdup values, particularly at the mid-range qualities, and the enhanced test sections are shown to increase the holdup as well. Tube type is shown to influence oil holdup principally at high qualities.

The results for the remaining mixtures vary. All combinations show the parabolic trend with low holdup at mid-range qualities and an increase at high qualities. The R134a/PAG and R134a/alkylbenzene mixtures show an influence of both mass flux and tube type, where the R22/alkylbenzene and R410A/POE mixtures only show the tube type influence clearly, and only at high qualities.

Like the void fraction results, not all refrigerant-oil mixtures show a clear oil holdup dependence on mass flux, however an effect cannot be ruled out for all cases. Similarly, the effect of tube type is clear for all data sets with the enhanced test sections, particularly the helical section, increasing the holdup results.

5.1.2.3 Slip Ratio

Slip ratio results are found to be affected minimally by mass flux and tube type in the study of the R134a/POE mixture. A lower mass flux shows a higher slip ratio, as do the enhanced test sections. These effects are indistinguishable below about 40 percent quality, and as expected, the slip ratio results increase with increasing quality.

The effect of mass flux on the remaining mixtures is less clear. For the R134a/PAG and R134a/alkylbenzene mixtures, mass flux does not show a significant trend. For the R22/alkylbenzene and R410A/POE mixtures it looks as though a higher mass flux results in a higher slip ratio, but only at high qualities. This directly contradicts the results found for the R134a/POE mixture.

The effect of tube type throughout the examinations is consistent. For all refrigerant-oil combinations an increase in slip ratio is observed for the enhanced test sections, particularly at high qualities. Like the oil holdup results, the helical test section followed by the axial has the most influence.

5.1.2.4 Flow Visualization

Though oil effects in the R134a/POE mixture are not evident, the presence of oil is visible for the remaining mixtures. The R134a/PAG mixture video indicates the presence of the lubricant most clearly at high qualities and low mass fluxes with large and circumferential disturbances to the liquid layer, rather than the small and random disturbances of pure refrigerant. Essentially, the oil is altering the properties of the liquid layer and slightly laminarizes the flow. The presence is also visible, though, at high mass fluxes and 100% quality where a liquid layer remains. The R134a/alkylbenzene video shows the presence of oil in the same manner, but also as horizontal streaks where the surface wetting capabilities of the oil may have shifted and the lubricant fails to behave as a liquid film. Finally, the R22/alkylbenzene mixture did show repeated instances of visible oil. These instances are few due to lack of video, but apparent in various forms. Again the non-wetting behavior creates horizontal oil streaks, but at high qualities and mass fluxes the presence of a liquid layer at 100% quality also indicates oil.

5.2 Modeling

Not only does the data for all refrigerant-oil mixtures follow the same oil holdup trends, but the model, composed of a liquid volume fraction region and a viscous film region, predicts holdup well in each case. The most deviation following the truncation of data points outside the oil concentration range of the shown model predictions occurs in the R134a/alkylbenzene data set. The most reasonable explanation for this behavior is due to alkylbenzene oil being immiscible in R134a refrigerant, where mixture properties are not accurately predictable at all flow conditions.

Additionally, the model and the experimental data, with the exception of the R134a/alkylbenzene mixture, are at a magnitude in the high quality range where groove effects seem to be primarily “hiding” the oil between the fins. The volume of the grooves in the enhanced test sections, along with the various oil densities, gives a base holdup of 2.0-2.5 g/m for oil occupying this space. The immiscible mixture experimental results show lower holdup because the oil and refrigerant do not dissolve together and the oil is less dense than the refrigerant causing it to float more and have less opportunity to build up between the fins.

5.3 Future Research Needs

With proper data collection procedures defined and a solid foundation of mixture data acquired at adiabatic conditions, continuing research can focus on various effects on systems at condensation and evaporation conditions. In addition to effects on void fraction, oil holdup, slip ratio and flow visualization, the effects of oil on heat transfer and pressure drop using the new procedure can be investigated and compared to previous research, which uses predetermined oil concentration charge (not necessarily the concentration in a given section of the system) or only the concentration measurement from the liquid feed line.

Furthermore, the data collected for condensation and evaporation conditions can be compared to the model developed in this investigation and modified as is necessary to apply to practical systems in industry.

5.4 List of References

[1] Graham, D.M. T.A. Newell and J.C. Chato, "Experimental Investigation of Void Fraction During Refrigerant Condensation," *ACRC TR-135* (also MS thesis by D.M. Graham), Air Conditioning and Refrigeration Center, University of Illinois, Urbana-Champaign IL, 1997.

[2] Kopke, H.R., T.A. Newell, and J.C. Chato, "Experimental Investigation of Void Fraction during Refrigerant Mixtures in Horizontal Tubes," *ACRC TR-142* (also MS thesis by H.R. Kopke), Air Conditioning and Refrigeration Center, University of Illinois, Urbana-Champaign, 1998.

Appendix A

A.1 R134a and Polyol Ester

The experimental void fraction results, computed as described in Chapter 1, are also compared to results using the ACRC model with various refrigerant-oil mixture properties. Methods for determining the mixture properties included in this comparison are a linear method used by Reid, the Baustian model and the Cawte model, all of which are detailed in the literature review of Chapter 2. These property values are then used to determine the Lockhart-Martinelli parameter. Additionally, the experimental results are compared to results using pure refrigerant properties. Results for the enhanced test sections are shown in Figures A.1.1 and A.1.2, respectively, with error lines of ±10%.

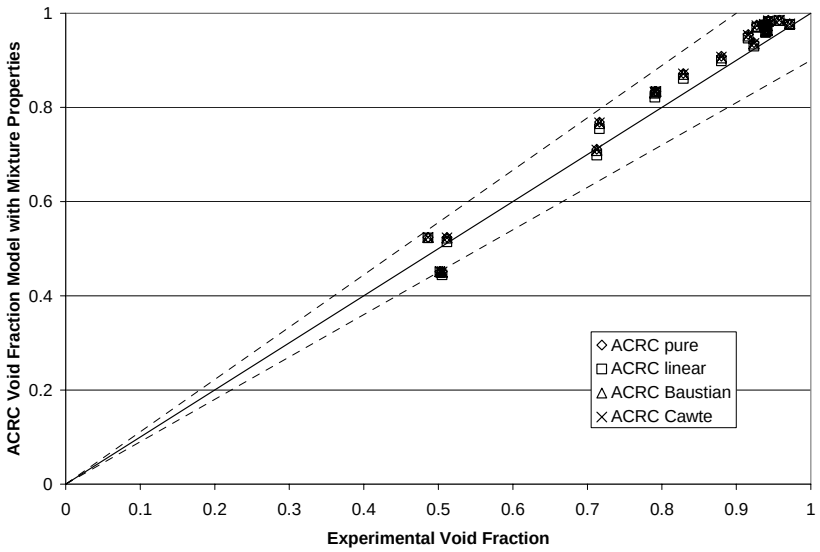

Figure A.1.1. Experimental void fraction data for the axial test section plotted versus void fraction determined using refrigerant-oil mixture properties in the ACRC model

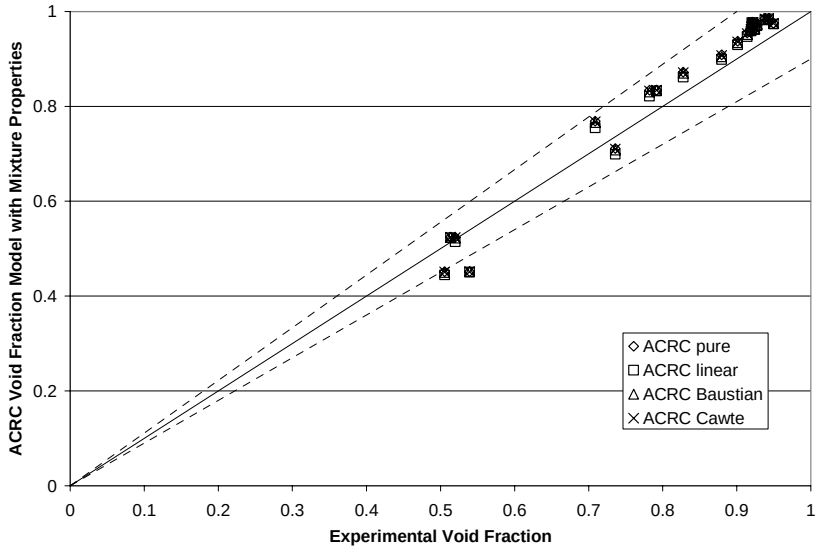

Figure A.1.2. Experimental void fraction data for the helical test section plotted versus void fraction determined using refrigerant-oil mixture properties in the ACRC model

Table A.1.1. Oil holdup and void fraction error and uncertainty for the R134a/POE experimental data

Oil Holdup, g (± 0.052g)	Percent Error	Experimental Void Fraction	Uncertainty ±	Percent Error
0.66	7.9	0.835	0.0117	1.41
0.48	10.8	0.834	0.0117	1.41
0.55	9.5	0.839	0.0117	1.40
0.86	6.0	0.718	0.0165	2.30
0.8	6.5	0.725	0.0161	2.21
0.55	9.5	0.766	0.0136	1.78
1.66	3.1	0.530	0.0320	6.05
1.84	2.8	0.540	0.0311	5.76
1.69	3.1	0.567	0.0287	5.06
1.28	4.1	0.915	0.0139	1.52
0.85	6.1	0.944	0.0156	1.65
0.74	7.0	0.932	0.0148	1.59
0.84	6.2	0.915	0.0139	1.52
1.01	5.1	0.890	0.0128	1.44
1.07	4.9	0.891	0.0128	1.44
1.22	4.3	0.804	0.0122	1.52
1.33	3.9	0.796	0.0124	1.56
0.97	5.4	0.842	0.0117	1.40
1.29	4.0	0.727	0.0159	2.19
1.34	3.9	0.750	0.0145	1.93
1.23	4.2	0.762	0.0139	1.82
1.69	3.1	0.524	0.0326	6.22
1.84	2.8	0.525	0.0324	6.17
1.63	3.2	0.580	0.0276	4.76
1.71	3.0	0.946	0.0157	1.66
1.53	3.4	0.944	0.0156	1.65
0.96	5.4	0.963	0.0169	1.75
1.1	4.7	0.928	0.0146	1.58
0.97	5.4	0.925	0.0144	1.56
0.7	7.4	0.954	0.0163	1.70
2.28	2.3	0.945	0.0157	1.66
1.31	4.0	0.952	0.0161	1.69
1.08	4.8	0.971	0.0174	1.79
1.52	3.4	0.936	0.0151	1.61
1.09	4.8	0.951	0.0161	1.69
0.97	5.4	0.949	0.0159	1.68
1.82	2.9	0.958	0.0165	1.72
1.8	2.9	0.963	0.0168	1.75

Appendix B

B.1 R134a and Polyol Ester Results

Table B.1.1. R134a and polyol ester results for the axial test section

Mass Flux, G (kg/m^2s)	Quality, x	Oil Concentration (%)	Void Fraction	Oil Holdup (g/m)
75	0.10	2.988	0.505	1.05
75	0.10	0.188	0.502	0.09
75	0.30	3.002	0.713	0.80
75	0.50	3.258	0.791	0.76
75	0.50	0.114	0.792	0.00
75	0.70	3.523	0.88	0.66
75	0.80	3.042	0.924	0.46
75	0.90	2.763	0.939	0.68
75	0.90	0.188	0.942	0.02
75	0.95	2.763	0.937	0.81
75	0.95	0.188	0.972	0.00
150	0.10	2.062	0.512	1.03
150	0.10	0.112	0.486	0.04
150	0.30	2.186	0.716	0.50
150	0.50	1.648	0.829	0.30
150	0.80	2.789	0.916	0.68
150	0.90	3.063	0.927	1.06
150	0.90	0.16	0.941	0.00
150	0.95	2.749	0.943	1.12
150	0.95	0.16	0.958	0.00

Table B.1.2. R134a and polyol ester results for the helical test section

Mass Flux, G (kg/m^2s)	Quality, x	Oil Concentration (%)	Void Fraction	Oil Holdup (g/m)
75	0.10	2.988	0.506	1.14
75	0.10	0.188	0.539	0.04
75	0.30	3.002	0.736	0.83
75	0.50	3.258	0.782	0.83
75	0.50	0.114	0.792	0.00
75	0.70	3.523	0.880	0.63
75	0.80	3.042	0.901	0.80
75	0.90	2.763	0.919	0.94
75	0.90	0.188	0.924	0.02
75	0.95	2.763	0.920	1.42
75	0.95	0.188	0.922	0.07
150	0.10	2.062	0.520	1.14
150	0.10	0.112	0.514	0.05
150	0.30	2.186	0.709	0.53
150	0.50	1.648	0.828	0.41
150	0.80	2.789	0.914	0.60
150	0.90	3.063	0.927	0.95
150	0.90	0.160	0.949	0.03
150	0.95	2.749	0.938	1.13
150	0.95	0.160	0.943	0.06

Table B.1.3. R134a and polyol ester results for the smooth test section

Mass Flux, G (kg/m^2s)	Quality, x	Oil Concentration (%)	Void Fraction	Oil Holdup (g/m)
75	0.10	2.988	0.563	1.01
75	0.10	0.188	0.559	0.02
75	0.30	3.002	0.749	0.76
75	0.50	3.258	0.831	0.60
75	0.50	0.114	0.839	0.00
75	0.70	3.523	0.906	0.52
75	0.80	3.042	0.935	0.53
75	0.90	2.763	0.939	0.60
75	0.90	0.188	0.975	0.00
75	0.95	2.763	0.959	0.67
75	0.95	0.188	0.971	0.01
150	0.10	2.062	0.548	1.05
150	0.10	0.112	0.561	0.09
150	0.30	2.186	0.760	0.34
150	0.50	1.648	0.833	0.34
150	0.80	2.789	0.947	0.43
150	0.90	3.063	0.953	0.60
150	0.90	0.160	0.970	0.00
150	0.95	2.749	0.963	0.83
150	0.95	0.160	0.967	0.02

B.2 R134a and Polyalkylene Glycol Results

Table B.2.1. R134a and polyalkylene glycol results for the axial test section

Mass Flux, G (kg/m^2s)	Quality, x	Oil Concentration (%)	Void Fraction	Oil Holdup (g/m)
73	0.91	8.23	0.976	4.37
75	1.00	0.00	0.996	0.01
75	0.88	1.69	0.940	0.48
75	0.97	0.32	0.959	0.06
75	0.69	0.88	0.906	3.02
75	0.49	2.70	0.791	0.14
75	0.85	13.24	0.974	4.21
76	0.96	0.74	0.951	0.32
76	0.76	4.74	0.912	1.19
150	0.95	4.60	0.986	2.16
150	0.96	0.13	0.948	0.08
150	0.69	1.39	0.872	0.19
150	1.00	0.14	0.961	0.11
150	0.49	1.05	0.827	0.11
150	0.51	8.78	0.850	0.94
150	0.97	0.44	0.954	0.06
150	0.96	1.15	0.943	0.32
151	0.89	1.45	0.943	0.63
151	0.99	0.15	0.958	0.06
153	0.97	0.17	0.959	0.00
185	0.96	4.25	0.960	1.29
188	0.97	3.21	0.969	1.32
200	0.69	0.81	0.849	0.16
201	0.50	0.88	0.817	0.14
207	0.88	2.14	0.941	0.59
207	0.95	1.53	0.967	0.31
259	1.00	0.12	0.977	0.07
261	0.95	0.14	0.956	0.05

Table B.2.2. R134a and polyalkylene glycol results for the helical test section

Mass Flux, G (kg/m^2s)	Quality, x	Oil Concentration (%)	Void Fraction	Oil Holdup (g/m)
75	0.88	1.69	0.914	0.80
75	0.49	2.70	0.748	0.21
75	0.69	0.88	0.872	0.18
75	0.85	13.24	0.974	4.69
75	0.97	0.74	0.983	1.61
75	0.97	0.32	0.952	0.07
76	0.91	8.23	0.964	4.69
76	1.00	0.00	0.934	0.18
77	0.76	4.74	0.893	1.41
149	0.95	4.60	0.979	3.01
150	0.51	8.78	0.837	1.12
150	0.69	1.39	0.862	0.21
150	0.49	1.05	0.832	0.07
150	0.89	1.45	0.936	0.72
150	0.97	0.44	0.935	0.06
150	0.99	0.15	0.961	0.07
150	0.96	1.15	0.936	0.41
150	1.00	0.14	0.966	0.14
151	0.96	0.13	0.959	0.03
151	0.97	0.17	0.923	0.00
185	0.96	4.25	0.969	1.59
188	0.97	3.21	0.964	1.77
200	0.50	0.88	0.826	0.17
200	0.69	0.81	0.894	0.18
204	0.95	1.53	0.956	0.32
207	0.88	2.14	0.939	0.70
256	1.00	0.12	0.969	0.09
261	0.95	0.14	0.956	0.03

Table B.2.3. R134a and polyalkylene glycol results for the smooth test section

Mass Flux, G (kg/m^2s)	Quality, x	Oil Concentration (%)	Void Fraction	Oil Holdup (g/m)
73	0.49	2.70	0.780	0.20
75	1.00	0.00	0.996	0.02
75	0.69	0.88	0.907	0.11
75	0.91	8.23	0.985	3.04
75	0.85	13.24	0.980	2.15
75	0.88	1.69	0.952	0.32
75	0.97	0.32	0.975	0.03
76	0.76	4.74	0.929	1.09
76	0.96	0.74	0.928	0.11
150	0.69	1.39	0.911	0.13
150	0.49	1.05	0.855	0.23
150	0.89	1.45	0.954	0.47
150	1.00	0.14	0.972	0.04
150	0.96	1.15	0.975	0.25
150	0.99	0.15	0.971	0.05
150	0.97	0.44	0.970	0.04
150	0.97	0.17	0.950	0.01
151	0.51	8.78	0.877	0.86
151	0.96	0.13	0.974	0.02
151	0.95	4.60	0.989	0.57
181	0.95	4.25	0.968	0.69
184	0.97	3.21	0.972	1.11
200	0.69	0.81	0.914	0.12
200	0.50	0.88	0.859	0.14
203	0.88	2.14	0.949	0.21
211	0.95	1.53	0.981	0.18
254	0.95	0.14	0.951	0.04
254	1.00	0.12	0.978	0.05

B.3 R134a and Alkylbenzene Results

Table B.3.1. R134a and alkylbenzene results for the axial test section

Mass Flux, G (kg/m^2s)	Quality, x	Oil Concentration (%)	Void Fraction	Oil Holdup (g/m)
72	0.00	0.00	1.000	0.04
73	0.99	1.38	0.998	0.22
75	0.70	0.59	0.884	0.22
75	0.99	1.43	0.952	0.28
75	0.99	0.96	1.000	0.22
75	0.90	0.00	0.961	0.02
75	0.30	0.37	0.638	0.11
76	0.89	0.81	0.958	0.13
76	0.49	1.16	0.780	0.19
149	0.87	3.41	0.995	0.01
150	1.00	0.00	1.000	0.43
150	0.29	2.15	0.695	0.07
150	0.69	1.15	0.928	0.12
150	0.49	1.26	0.805	0.11
150	1.00	0.45	0.950	0.08
150	0.98	1.50	0.991	0.42
151	1.00	0.30	0.999	0.39
151	0.90	0.42	0.999	0.20
300	0.49	2.51	0.722	0.07
300	0.30	1.11	0.758	0.07
300	0.80	0.57	0.975	0.17
300	0.79	0.81	1.000	0.11
300	0.69	1.38	0.885	0.08
301	0.50	0.74	0.854	0.11

Table B.3.2. R134a and alkylbenzene results for the helical test section

Mass Flux, G (kg/m^2s)	Quality, x	Oil Concentration (%)	Void Fraction	Oil Holdup (g/m)
73	1.00	0.00	0.979	1.02
74	0.99	1.43	0.973	0.99
75	0.99	1.38	0.970	1.31
75	0.90	0.00	0.954	0.87
75	0.99	0.96	0.979	0.88
75	0.89	0.81	0.963	0.28
75	0.49	1.16	0.759	0.11
75	0.70	0.59	0.840	0.24
76	0.30	0.37	0.666	0.17
148	1.00	0.00	0.978	1.14
149	0.29	2.15	0.709	0.12
150	0.69	1.15	0.920	0.04
150	0.49	1.26	0.842	0.04
150	1.00	0.45	1.000	0.20
150	0.98	1.50	0.984	0.81
151	0.90	0.42	0.997	0.23
151	0.87	3.41	0.986	0.07
151	1.00	0.30	1.000	0.30
299	0.69	1.38	0.824	0.06
300	0.50	0.74	0.865	0.04
300	0.30	1.11	0.748	0.11
301	0.80	0.57	0.966	0.21
302	0.79	0.81	0.995	0.22

Table B.3.3. R134a and alkylbenzene results for the smooth test section

Mass Flux, G (kg/m^2s)	Quality, x	Oil Concentration (%)	Void Fraction	Oil Holdup (g/m)
73	1.00	0.00	1.000	0.30
74	0.49	1.16	0.817	0.06
74	0.70	0.59	0.924	0.11
74	0.99	0.96	0.998	0.32
75	0.90	0.00	0.959	0.00
75	0.99	1.43	0.976	0.20
75	0.89	0.81	0.965	0.16
75	0.30	0.37	0.707	0.24
77	0.99	1.38	0.991	0.45
149	0.69	1.15	0.934	0.20
149	0.29	2.15	0.764	0.02
150	0.49	1.26	0.877	0.05
150	1.00	0.30	1.000	0.12
150	0.98	1.50	1.000	0.22
150	0.87	3.41	0.999	0.00
150	1.00	0.45	1.000	0.16
150	1.00	0.00	1.000	0.12
151	0.90	0.42	1.000	0.25
298	0.50	0.74	0.915	0.04
298	0.79	0.81	0.980	0.09
300	0.30	1.11	0.802	0.06
301	0.69	1.38	0.979	0.11
301	0.80	0.57	1.000	0.25

B.4 R22 and Alkylbenzene Results

Table B.4.1. R22 and alkylbenzene results for the axial test section

Mass Flux, G (kg/m^2s)	Quality, x	Oil Concentration (%)	Void Fraction	Oil Holdup (g/m)
73	0.96	3.31	0.939	1.47
74	0.90	2.53	0.934	0.85
75	0.48	3.96	0.728	0.75
75	0.00	1.95	0.004	0.86
75	0.97	0.00	0.601	0.06
75	1.00	0.38	1.000	0.03
75	0.70	0.00	0.928	0.00
75	0.77	3.14	0.915	0.58
149	0.67	3.60	0.905	0.65
149	0.70	0.30	1.000	0.55
150	0.99	1.16	1.000	0.36
150	1.00	0.14	1.000	0.27
150	0.88	2.61	0.946	1.59
151	0.49	2.62	0.860	0.49
151	0.78	2.91	0.932	0.61
298	0.80	0.00	0.982	0.00
300	0.50	0.30	0.829	0.00
300	0.75	0.11	0.948	0.01

Table B.4.2. R22 and alkylbenzene results for the helical test section

Mass Flux, G (kg/m^2s)	Quality, x	Oil Concentration (%)	Void Fraction	Oil Holdup (g/m)
73	0.97	3.31	0.921	2.55
75	1.00	0.38	0.980	0.55
75	0.48	3.96	0.776	0.65
75	0.97	0.00	0.832	0.00
75	0.00	1.95	0.001	0.25
75	0.70	0.00	0.910	0.00
76	0.76	3.14	0.873	0.80
77	0.87	2.53	0.922	1.11
149	0.70	0.30	0.932	0.03
150	1.00	0.14	1.000	0.33
150	0.88	2.61	0.939	2.05
150	0.78	2.91	0.932	0.99
150	0.99	1.16	1.000	0.00
150	0.67	3.60	0.895	0.71
151	0.50	0.59	0.813	0.03
151	0.49	2.62	0.818	0.63
298	0.80	0.00	1.000	0.00
300	0.50	0.30	0.712	0.73
300	0.75	0.11	0.899	0.00

Table B.4.3. R22 and alkylbenzene results for the smooth test section

Mass Flux, G (kg/m^2s)	Quality, x	Oil Concentration (%)	Void Fraction	Oil Holdup (g/m)
75	0.49	3.96	0.768	0.76
75	0.88	2.53	0.982	0.24
75	1.00	0.38	1.000	0.04
75	0.00	1.95	0.018	0.35
75	0.96	3.31	0.965	1.30
75	0.97	0.00	0.932	0.00
75	0.70	0.00	0.958	0.02
76	0.77	3.14	0.946	0.37
149	0.49	2.62	0.883	0.44
149	0.70	0.30	0.966	0.00
150	1.00	0.14	1.000	0.00
150	0.99	1.16	1.000	0.06
150	0.78	2.91	0.963	0.55
150	0.67	3.60	0.934	0.50
150	0.88	2.61	0.973	1.04
298	0.80	0.00	0.992	0.00
300	0.50	0.30	0.821	0.00
300	0.75	0.11	0.964	0.00

B.5 R410A and Polyol Ester Results

Table B.5.1. R410A and polyol ester results for the axial test section

Mass Flux, G (kg/m^2s)	Quality, x	Oil Concentration (%)	Void Fraction	Oil Holdup (g/m)
74	0.96	4.09	0.989	3.45
75	0.68	3.26	0.898	0.14
75	0.88	2.07	0.949	0.31
75	0.20	0.90	0.570	0.29
75	0.97	1.58	0.988	0.80
75	0.00	1.49	0.409	0.32
76	0.92	2.99	0.999	0.89
76	0.78	0.95	0.969	0.13
76	0.50	0.15	0.834	0.18
150	0.48	3.39	0.821	0.34
150	0.89	1.37	0.941	0.72
150	0.00	1.70	0.288	0.30
150	0.97	3.00	1.000	3.12
150	0.20	1.32	0.670	0.40
150	0.93	2.26	0.999	2.24
151	0.69	1.32	0.939	0.31
151	0.79	1.76	0.959	0.88

Table B.5.2. R410A and polyol ester results for the helical test section

Mass Flux, G (kg/m^2s)	Quality, x	Oil Concentration (%)	Void Fraction	Oil Holdup (g/m)
74	0.95	4.09	0.985	4.08
75	0.98	1.58	0.995	2.60
75	0.00	1.49	0.305	0.37
75	0.20	0.90	0.584	0.26
75	0.68	3.26	0.835	0.25
75	0.88	2.07	0.929	1.07
75	0.50	0.15	0.776	0.19
76	0.79	0.95	0.888	0.47
76	0.91	2.99	0.987	2.52
150	0.97	3.00	1.000	3.69
150	0.00	1.70	0.308	0.34
150	0.89	1.37	0.969	1.42
150	0.79	1.76	0.941	0.82
150	0.93	2.26	0.999	2.78
150	0.48	3.39	0.810	0.32
151	0.20	1.32	0.634	0.21
151	0.69	1.32	0.891	0.48

Table B.5.3. R410A and polyol ester results for the smooth test section

Mass Flux, G (kg/m^2s)	Quality, x	Oil Concentration (%)	Void Fraction	Oil Holdup (g/m)
74	0.95	4.09	0.999	2.31
74	0.00	1.70	0.407	0.30
75	0.93	2.99	1.000	0.62
75	0.98	1.58	1.000	1.52
75	0.68	3.26	0.931	0.11
75	0.50	0.15	0.817	0.12
75	0.88	2.07	0.966	0.39
75	0.20	1.49	0.627	0.22
76	0.79	0.95	0.927	0.32
150	0.79	1.76	0.983	0.39
150	0.89	1.37	1.000	0.93
150	0.93	2.26	1.000	0.73
150	0.48	3.39	0.856	0.29
150	0.00	1.34	0.000	0.10
150	0.97	3.00	1.000	1.22
150	0.20	1.32	0.746	0.28
150	0.69	1.32	0.943	0.20